UNIVERSIDADE FEDERAL DE MINAS GERAIS

ESCOLA DE ENGENHARIA

DEPARTAMENTO DE ENGENHARIA NUCLEAR

POSTGRADUATE IN NUCLEAR SCIENCE AND TECHNIQUES

FELIPE MARTINS GOMES PEREIRA

A THORIUM-FUEL PIN NEUTRONIC ANALYSIS USING DIFFERENT NUCLEAR CODES

Belo Horizonte – MG
2019

FELIPE MARTINS GOMES PEREIRA

A THORIUM-FUEL PIN NEUTRONIC ANALYSIS USING DIFFERENT NUCLEAR CODES

Dissertation submitted to the *Departamento de Engenharia Nuclear da Universidade Federal de Minas Gerais* in partial fulfillment of the requirements for the degree of Master of Science in Nuclear Science and Techniques.

Concentration Area: Nuclear and Energy Engineering

Advisor: Prof.ª Dr.ª Cláubia Pereira Bezerra Lima
Co-advisor: Prof. Dr. Carlos Eduardo Velasquez Cabrera

Belo Horizonte – MG
2019

Pereira, Felipe Martins Gomes.
P436t A thorium-fuel pin neutronic analysis using different nuclear codes [recurso eletrônico] / Felipe Martins Gomes Pereira. - 2019.
1 recurso online (93 f. : il., color.) : pdf.

Orientadora: Claubia Pereira Bezerra Lima.
Coorientador: Carlos Eduardo Velasquez Cabrera.

Dissertação (mestrado) - Universidade Federal de Minas Gerais, Escola de Engenharia.

Anexos: f. 63-93.

Bibliografia: f. 60-62.
Exigências do sistema: Adobe Acrobat Reader.

1. Engenharia nuclear - Teses. 2. Combustíveis nucleares - Teses. 3. Verificação (Lógica) - Teses. I. Lima, Claubia Pereira Bezerra. II. Cabrera, Carlos Eduardo Velasquez. III. Universidade Federal de Minas Gerais. Escola de Engenharia. IV. Título.

CDU: 621.039(043)

Ficha catalográfica: Biblioteca Profº Mário Werneck, Escola de Engenharia da UFMG

UNIVERSIDADE FEDERAL DE MINAS GERAIS

PROGRAMA DE PÓS-GRADUAÇÃO EM CIÊNCIAS E TÉCNICAS NUCLEARES

PCTN

FOLHA DE APROVAÇÃO

A THORIUM-FUEL PIN NEUTRONIC ANALYSIS USING DIFFERENT NUCLEAR CODES

FELIPE MARTINS GOMES PEREIRA

Dissertação submetida à Banca Examinadora designada pelo Colegiado do Programa de Pós-Graduação em CIÊNCIAS E TÉCNICAS NUCLEARES, como requisito parcial para obtenção do grau de Mestre em CIÊNCIAS E TÉCNICAS NUCLEARES, área de concentração ENGENHARIA NUCLEAR E DA ENERGIA.

Aprovada em 29 de maio de 2019, pela banca constituída pelos membros:

Profa. Cláubia Pereira Bezerra Lima - Orientadora
Departamento de Engenharia Nuclear - UFMG

Prof. Carlos Eduardo Velasquez Cabrera - Coorientador
Departamento de Engenharia Nuclear - UFMG

Dra. Graiciany de Paula Barros
CNEN/CDTN

Dr. Daniel de Almeida Magalhães Campolina
CNEN/CDTN

Dr. Alexandre David Caldeira
Instituto de Estudos Avançados - IEAv

Belo Horizonte, 29 de maio de 2019.

ACKNOWLEDGMENTS

First of all, I would like to thank my advisors, Claubia and Carlos, who during these years endured me and taught me a lot.

I thank my parents, brothers, and my girlfriend, who provided me with essential support from the beginning to the end of this journey.

Thanks also to my colleagues in the department who provided me essential assistance and my students that supported me.

I thank once more to Claubia, Carlos, Clarysson, Dôra, Antonella, Victor, Fabiano, Rochkhudson, Patricia, and Arno, who succeeded as teachers and tutors to transform a layperson in the nuclear physics field into an aspiring master and also thank to those who did the same indirectly.

Finally, thank the funding agencies, CNEN – Comissão Nacional de Energia Nuclear (Brazil), CAPES – Coordenação de Aperfeiçoamento de Pessoal de Nível Superior (Brazil), FAPEMIG – Fundação de Amparo à Pesquisa do Estado de Minas Gerais (MG/Brazil) and CNPq – Conselho Nacional de Desenvolvimento Científico e Tecnológico (Brazil) for the financial support for the research.

RESUMO

A utilização de diversos códigos nucleares para realização de cálculos de criticalidade, evolução do combustível e simulações de condições reais de trabalho já é um recurso difundido entre os pesquisadores de todo o mundo. Cada código nuclear, seja de transporte neutrônico ou para análise de evolução do combustível, tem suas características específicas. Assim sendo, esse trabalho tem como objetivo validar o modelo desenvolvido e os dados de seções de choque em diferentes temperaturas de trabalho gerados pelo Departamento de Engenharia Nuclear - DEN da Universidade Federal de Minas Gerais – UFMG usando o sistema de códigos NJOY99 e adotando um benchmark de vareta combustível abastecido com combustível baseado em tório realizado pelo MIT, INEEL e Czech Technical University usando diferentes códigos nucleares. A verificação consiste em comparar os resultados entre os códigos, usando a mesma metodologia do benchmark. Para realizar a validação, foram feitos cálculos de criticalidade e de evolução do combustível, utilizando os códigos MCNPX, MCNP5, Serpent, o sistema SCALE6.0 e Monteburns. Outrossim, uma extensão dos cálculos apresentados pelo benchmark é realizada e parâmetros de segurança de reatores nucleares são calculados para o modelo desenvolvido. Neste trabalho foram avaliados também, a fração de nêutrons atrasados efetiva, o coeficiente de temperatura do combustível e as taxas de produção e transmutação para cada código considerando situações de combustível fresco e queimado. Foram obtidas frações de nêutrons atrasados efetivas que decresciam de valor respondendo a variação da composição do combustível e k_∞ que iniciam a simulação com valores muito próximos e tem sua diferença aumentada ao longo da queima, ambos resultados são reflexos das taxas de produção e transmutação consideradas por cada código. Com isso, a ENDL utilizada implicitamente para os cálculos de queima mostra-se o fator determinante para as simulações mostra a influência. Ainda, conclusões são feitas sobre o procedimento de cálculo dos coeficientes de temperatura do combustível e também sobre a rotina de pré-processamento de alargamento Doppler do código Serpent. As conclusões são trazidas separadamente em cada capítulo, e o capítulo final apresenta discussões e conclusões que foram obtidas ao longo de todo o trabalho, além do apresentar ideias de trabalhos e perspectivas futuras relacionadas ao escopo deste trabalho.

PALAVRAS-CHAVE: Códigos nucleares. Verificação. Cálculos de criticalidade. Dados de seção de choque. k_∞. Fração efetiva de nêutrons atrasados. Coeficiente de temperatura do combustível. Parâmetros de segurança de reatores nucleares.

ABSTRACT

Several different nuclear codes have been used to perform depletion and criticality calculations, already widespread among worldwide researchers. The neutron transport and depletion codes have their particularities such as the number of energy groups and multigroup cross section data included for each code. Therefore, this work aims to validate the model and cross sections data generated at DEN/UFMG using NJOY99 system and adopting a thorium fuel pin benchmark performed by MIT, INEEL and Czech Technical University, and using different computational nuclear codes. The validation consists in comparing results from codes and reference using benchmark methodology in criticality and depletion situations. To perform criticality at steady state and depletion calculations are used MCNPX, MCNP5, Serpent, SCALE6.0 system, and Monteburns. Besides that, an extension of the benchmark calculations is performed and nuclear reactor safety parameters are calculated for developed model. In this work are evaluated quantities such as the effective delayed neutron fraction, fuel temperatures coefficients and production and consumption rates for each code considering fresh fuel and depletion situations. It is achieved effective delayed neutron fractions that decreased responding to changes in fuel composition and k_∞ that began simulation with lower differences than the ones obtained at burnup end, both results are a reflection of production and consumption rates considered by each code. Thus, the determining factor for the simulations is the ENDL used implicitly to depletion calculations. Besides that, conclusions are made about fuel temperature coefficient calculation and Serpent Doppler broadening preprocessor routine related to cross section data usage. The conclusions are presented in each chapter separately and accompanying their respective results. To sum up, the last chapter presents future perspectives discussions and overall conclusions and discussions from the obtained results.

KEYWORDS: Nuclear codes. Validation. Criticality calculation. Cross sections data. Depletion. k_∞. Effective delayed neutron fraction. Fuel temperature coefficient. Nuclear reactor safety parameters.

LIST OF FIGURES

LIST OF TABLES

LIST OF ABBREVIATIONS AND ACRONYMS

ADS - Accelerator Driven System

BOL - Beginning of Life

BWR - Boiling Water Reactor

CAPES - Coordenação de Aperfeiçoamento de Pessoal de Nível Superior

CNEN - Comissão Nacional de Energia Nuclear

CNPq - Conselho Nacional de Desenvolvimento Científico e Tecnológico

DEN - Departamento de Engenharia Nuclear

ENDF - Evaluated Nuclear Data File

ENDL - Evaluated Nuclear Data Library

EOL - End of Life

ENSDF - Evaluated Nuclear Structure Data File

FAPEMIG - Fundação de Amparo à Pesquisa do Estado de Minas Gerais

GENDF - Groupwise Evaluated Nuclear Data File

IAEA - International Atomic Energy Agency

ICENES - International Conference on Emerging Nuclear Energy Systems

INAC - International Nuclear Atlantic Conference

INEEL - Idaho National Engineering and Environmental Laboratory

JEFF - Joint Evaluation Fission and Fusion

JENDL - Japanese Evaluated Nuclear Data Library

MCNP5 - Monte Carlo N-Particle 5

MCNPX - Monte Carlo N-Particle eXtended

MIT - Massachusetts Institute of Technology

NEWT_CE - NEWT using continuous energy libraries

NEWT_238 - NEWT using 238-groups energy libraries

ORIGEN - Oak Ridge Isotope Generation and Depletion

ORNL - Oak Ridge National Laboratory

PENDF - Pointwise Evaluated Nuclear Data File

PWR - Pressurized Water Reactor

SCALE - Standardized Computer Analyses for Licensing Evaluations

SENCIR - Semana de Engenharia Nuclear e Ciências das Radiações

Serpent-DBR - Serpent with Doppler Broadening Routine

ThO_2-UO_2 - Thorium-Uranium Dioxide

UFMG - Universidade Federal de Minas Gerais

UO_2 - Uranium Dioxide

WT - Work Temperature

Zr-4 - Zircaloy-4

LIST OF SYMBOLS

2D - Two dimensional.

α_F - Fuel temperature coefficient

β_{eff} - Effective delayed neutron fraction

atoms/cm³ - Atoms per cubic centimeter

g/cm³ - Grams per cubic centimeter

GWd/MTHM - Gigawatts days per Metric Ton of Heavy Metal

K - Kelvin

k_{∞} – Infinity multiplication factor

k_{prompt} - Multiplication factor considering only prompt neutrons.

k_{total}- Multiplication factor considering delayed and prompt neutrons.

mm - Millimeter

MW/MTHM - Mega Watts per Metric Ton of Heavy Metal

pcm - Per cent mille

pcm/K - Per cent mille per Kelvin.

w/o - Weight fraction

SUMMARY

1. INTRODUCTION

Computational nuclear codes were developed for performing studies about the different types of reactors, geometries, and fuels. Therefore, they have been used for reproducing thermohydraulic and neutronic scenarios of a nuclear reactor over the years. The coupled processes or systems involving more than one simultaneously physical field are defined as Multiphysics.

The nuclear codes are capable of simulating behaviors, conditions, and even accidents that can occur to real nuclear reactors considering. In the academic environment and in nuclear power plants, the computational simulations have enormous importance, either to study behavior of materials or to analyze safety parameters. One may argue that there is not only one code to perform nuclear simulations, and indeed, there are dozens of codes that can achieve the same nuclear study, however, each one of the codes has their particularities such as energy groups or cross sections.

The cross section libraries are quantities that are directly related to the reaction probabilities per unit area. However, these probabilities are not constant and depends on many factors including: incident particles, target nuclides, energy, and temperature. Given the importance of cross section inside the nuclear simulation, this work aims to validate the model and cross section data generated by Departamento de Engenharia Nuclear - DEN in Universidade Federal de Minas Gerais - UFMG adopting a thorium pin benchmark [1] as the reference.

Furthermore, the same model and data are used to perform an extension of the benchmark calculation and evaluation of changes in nuclide inventory, especially for thorium and other nuclides that directly or indirectly impacts in k_∞. In addition, this study aims to be additional material in the literature in the context of computational simulations using different nuclear codes and cross sections evaluation.

Therefore, different nuclear codes are used to accomplish this work. The Monte Carlo N-Particle eXtended – MCNPX [2, 3], the Monteburns code [4], the Monte Carlo N-Particle 5 - MCNP5 [5], the ORIGEN2.1 [6], the Serpent 2.1.26 [7], and from the Standardized Computer Analyses for Licensing Evaluation 6 - SCALE6.0 [8] code system, the sequences CSAS [9] and

TRITON [10] are used. The CSAS and TRITON sequences use KENO-VI [11] and NEWT [12] modules to perform steady state problems and links these control modules to the ORIGEN-S [13] depletion module in time-dependent modules, respectively.

The SCALE code system developed in Oak Ridge National Laboratory. It is a verified and validated licensed code system composed of modules allowing user a variety of evaluations such as criticality safety, reactor physics, spent fuel characterization, radiation shielding, and sensitivity and uncertainty analysis. It performs the calculations from the collapsing of cross section libraries until deterministic cell calculation by means of NEWT, or of criticality, through the KENO-VI, and perform depletion using its several pre-prepared sequences, using ORIGEN-S, thus guarantees self-sufficiency to the user in cross section processing.

The NEWT module from SCALE6.0 system was selected to be used in this work aiming for the second part of this work. NEWT is capable of performing β_{eff} calculation and the results are used together with the β_{eff} calculated from stochastic codes to perform an evaluation, considering fresh fuel and depletion situations.

The MCNPX, MCNP5 codes are responsible for the neutron transport, based on geometry, materials, temperature, and incident neutron energy, obtaining the neutron flux through stochastics methods in the designed cells. To perform this, the codes use cross section data previously generated coupled with material distribution inside modeled cells, achieving neutronic parameters such as fluxes and multiplication factors. The MCNPX, by the CINDER subroutine, implemented implicitly, can do depletion evaluation, dealing both criticality and depletion evaluation.

Serpent has an implicit depletion code and deals both with neutron transport and fuel depletion. In addition to the objectives of this work, the Doppler broadening preprocessor routine is evaluated using different cross section data. Theoretically, the use of this routine would guarantee to the researcher the autonomy of dismissing processing codes such as NJOY code system [14] to generate the cross sections at desired temperatures.

The Monteburns code is used to link the neutron transport code MCNP5 to the ORIGEN2.1 code. The ORIGEN2.1 is responsible with the nuclide depletion, obtaining the previously achieved fluxes by neutron transport codes and manage the composition changes in nuclear fuel

during burnup considering all the possible reactions for each nuclide involved in the simulation. These codes also use the nuclides cross sections to perform the depletion. However, different from neutron transport codes that have cross section data that can easily be modified and treated, some nuclear depletion codes have already their own cross section data.

The thorium-based fuel pin benchmark was selected based on previous cross section studies and validations from the Departamento de Engenharia Nuclear - DEN at Universidade Federal de Minas Gerais - UFMG [15 - 17, 21 - 23].

The first study [15] describes a cross section analysis using a KRITZ benchmark modeled with the MCNP code using different ENDL. The second study [16] involves spiking thorium into reprocessed fuels in PWR systems considering homogeneous and micro-heterogeneous treatment, the same thorium fuel pin benchmark used in the study is adopted to perform this dissertation. The third study [17] presents an analysis of the behavior of thorium insertion spiked with reprocessed fuel considering different enrichments. The other works [21- 23] present a series of studies of the use of thorium and the different nuclear codes, each of these studies contributed to the progress of this dissertation.

To perform the benchmark study, cross sections were generated at work temperatures of 900 K, 621 K, and 583 K corresponding to the fuel, cladding and coolant materials respectively using NJOY code system [14] and the ENDF/B-VII.0 [18]. Besides that, four other cross section datasets were used, 300 K, 600 K, 900 K and 1200 K, available in Serpent package and based on ENDF/B-VII.0. The cross sections datasets are used only in MCNPX, MCNP5 and Serpent, since SCALE6.0 system has modules assigned for processing the ENDF independently from NJOY code system.

The ENDF/B-VII.0 is used based on the previous studies performed at DEN/UFMG using different ENDL to evaluate cross sections [15] and neutronic studies [16] using the adopted benchmark.

The quality of a nuclear code is a very subjective topic, since benchmark values can be obtained from computational simulations with specific conditions and data. Therefore, the different nuclear codes can produce divergent results depending on neutron transport and fuel depletion

data and calculations. Thus, the best results are considered to be the ones with lower absolute differences in relation to the thorium fuel pin benchmark reference.

It is important to notice that it is not proposed here to compare the nuclear codes that are going to be used. Thus, this work has no intention in classifying the best nuclear computational codes. Instead, one of the objectives of this work is to evaluate the influence of the fuel composition and the nuclear code used in the results of the computational simulations. Hence, to perform the analysis important nuclear safety parameters are going to be analyzed, some of which are: infinite multiplication factor - k_{∞}, effective delayed neutron fraction - β_{eff}, fuels isotopic composition and fuel temperature coefficient or Doppler coefficient - α_F.

In addition, state-of-art works are used as reference [19, 20] to establish methodologies of comparison with the selected benchmark. Although any of these works use the codes proposed to be used in this dissertation, the methodology is verified, and already published.

The chapters division of this work was implemented in a way that the next chapter contains general detailing from codes used in this work. Chapter three presents the benchmark description followed with the methodology performed to complete the validation considering criticality and depletion situation.

Therefore, chapter four comprehends the benchmark extension using the validated model and cross section generated at DEN using the NJOY package. In this chapter quantities such as effective delayed neutron fraction - β_{eff}, fuels isotopic composition and fuel temperature coefficient - α_F and production and consumption rates are calculated and evaluated taking into account fuel composition and considering both fresh fuel situation and fuel depletion over the burnup.

Chapter five exhibits a compilation of all analysis performed, discussions, results, and conclusions. After all ponderations about the work, some future perspectives and opportunities are discussed. Lastly, the appendix presents three works submitted to nuclear engineering conferences (INAC, SENCIR and ICENES) that contributed to the progress of this work [21 - 23].

2. NUCLEAR CODES DESCRIPTION

2.1. MCNPX

The MCNPX [2, 3] code stands as an enhancement of the previous versions of the Monte Carlo N-Particle codes such as MCNP4B and MCNP4C3 in support of the Accelerator Production of Tritium Project - APT. In this work, among the several MCNPX applications in nuclear engineering, nuclear criticality safety, consumption, activation, and burnup in the reactor are used.

MCNPX is a general-purpose Monte Carlo transport code that is capable of tracking particles with energies up to 150 MeV. The MCNPX is used to achieve criticality eigenvalues using pointwise cross sections in XSDIR format [24]. In addition, MCNPX uses the CINDER ’90 algorithm to perform depletion, implementing the capacity of activation and consumption to the code, implemented implicitly.

CINDER ’90 [25] was originally used for irradiation calculations. It can be used for regular reactor burnup to Accelerator Drive Systems - ADS or even accelerator activation. The code is used to calculate the inventory of isotopes in the described materials over time, based on initial material, isotopes production and consumption rates and neutron fluxes.

The CINDER ’90 uses multi-group cross section data. It has 63-group libraries that include decay, cross section, and fission products yield libraries. The data library describes over 3400 nuclides in the range $1 \leq Z \leq 103$. These data include decay constants, branching ratios, average decay energies, activation cross sections, fission product yields, and gamma production spectra. The data provided by CINDER ’90 was obtained from multiple sources, including some ENDL such as ENDF/B, Joint Evaluation Fission, and Fusion – JEFF [26] and Japanese Evaluated Nuclear Data Library – JENDL [27].

2.2. MCNP5

The Monte Carlo N-Particle Transport Code Version 5 is a general-purpose transport code that can track neutrons, photons, and electrons. It is capable of performing the eigenvalues

calculation for critical systems. MCNP5 [5] considers neutron energy regime from 10^{-11} MeV to 20 MeV for all isotopes and in addition, some isotopes have energies up to 150 MeV.

MCNP5 uses pointwise cross sections in the traditional ENDF6 format that can be prepared and generated using the NJOY code package. Since MCNP5 does not have a depletion algorithm within, the Monteburns automated coupling tool is used to link it with ORIGEN2.1 depletion code.

2.3. Monteburns

Monteburns [4] code is an automated tool used to link the neutron transport code MCNP5 with the radioactive decay and burnup code ORIGEN2.1. The Monteburns code is capable of producing a large number of neutronic parameters based on material and other code-specific variables, such as the k_{eff}, burnup, flux spectrum, one group cross sections, fission-to-capture ratio, masses at beginning and end of steps, radioactivity, heat decay and, inhalation and ingestion radiotoxicity.

Monteburns works transferring one-group fluxes and criticality results from MCNP5 to ORIGEN2.1, and then after burnup transfer the resulting material compositions from ORIGEN2.1 back to the MCNP5 in a repeated cyclic way.

ORIGEN2.1 [6] has a one group data library, dividing the nuclides into three segments, the activation products, actinides, and fission products, these add up to 1700 nuclides. In each of these segments there are three libraries that may be read, the decay data library that was based on Evaluated Nuclear Structure Data File – ENSDF at ORNL and also from ENDF/B-IV, the cross section and fission products yield library that was retrieved from ENDF/B-IV, and the photon yield library assembled based on ENSDF.

2.4. Serpent

Serpent [7] started as a simplified reactor physics code, although with the improvements it became a general-purpose Monte Carlo particle transport code. Since it started as a reactor

physics code, it has some exclusive features, such as pin modeling functions, Doppler-broadening preprocessor routine, and a nuclide inventory transmutation algorithm within.

The Doppler broadening preprocessor routine guarantees the capacity of adjusting the temperatures of the nuclide cross sections. However, the routine can only be used to adjust cross section to higher temperature values, e.g. 600 K cross sections can be adjusted to 900 K but not able to be adjusted to 300 K.

Serpent reads continuous energy cross section libraries likewise other neutron transport codes, although the cross section files organization is slightly different from traditional XSDIR format and is named XSDATA. To convert the XSDIR file to XSDATA, a utility script provided with Serpent package is used.

The burnup is performed using a collapsed one energy group and the data libraries are read in ENDF6 format. The decay libraries contain data for almost 4000 nuclide and meta-stable states. Energy-dependent fission yields are available for all main actinides all based on the ENDL ENDF/B-VII.0 [18].

2.5. SCALE6.0

The SCALE code system [8] was developed in United States at the Oak Ridge National Laboratory. It is a validated code system composed of several modules and used for different objectives such as criticality safety, reactor physics, spent fuel characterization, radiation shielding, and sensitivity and uncertainty analysis.

Among SCALE6.0 system modules, there are two main control modules that were used frequently in this work, the CSAS (Criticality Safety Analysis Sequence) [9] for criticality calculations and the TRITON (Transport Rigor Implemented with Time-dependent Operation for Neutronic depletion) [10] for transport and depletion calculations.

Both sequences prepare cross section data to be used for neutron transport code, which can be the Monte Carlo KENO-VI [11] transport code or the deterministic neutron transport NEWT [12] code. Both continuous energy and collapsed cross sections can be used for

performing criticality calculations with KENO-VI. The NEWT code only can use collapsed cross sections.

In this SCALE system version, the TRITON depletion sequence is used to perform fuel depletion with collapsed cross sections. When using TRITON, cross section processing modules and neutron transport code are called, and again, it can be KENO-VI or NEWT, and then TRITON perform the communication with depletion code ORIGEN-S.

KENO-VI is a Monte Carlo code for nuclear criticality safety analyses, and it is part of the SCALE code system. The code allows the user to perform the calculation choosing different types of energy groups and ENDL. Considering previous studies performed at DEN/UFMG using the same benchmark [16] and the cross sections used in others transport codes of this work, the ENDF/B-VII.0 continuous energy library and 238 collapsed energy groups are used in KENO-VI to perform calculations.

The NEWT is a deterministic code and considers two-dimensional (2D) geometry. Therefore, NEWT perform criticality calculations using collapsed energy groups. Based on the same studies performed at DEN/UFMG, the 238 collapsed groups presented best results [16]. Jointly with the k_{∞}, NEWT [12] is capable of calculating the effective delayed neutron factor and decay constant per precursor group.

The Oak Ridge Isotope Generation and Depletion – ORIGEN code was developed to compute the time-dependent isotopic concentrations during burnup for all nuclides that might be involved through nuclear irradiation, neutron activation or radioactive decay using three-group cross section libraries. The ORIGEN-S present in SCALE6.0 system is a modular version that has been already validated to perform nuclide depletion over time.

This depletion module can be linked both to KENO-VI or NEWT to perform the burnup using the TRITON module [10]. The nuclear data used by ORIGEN-S are mostly developed from the ENDF/B-VII.0 and JEFF3.1. These data include Nuclear decay data for 904 activation products, 174 actinides, and 1149 fission products, multigroup cross sections for 774 target nuclei, and also fission product yield for 30 actinides [13, 28].

2.6. NJOY

Each module from NJOY99 system has a different task to provide the ideal cross section processing and generating. Although this work is not intended to evaluate the processing of the cross sections, the NJOY99 modules used to processing the data used will be put on topics with brief descriptions of their functions and the parameters used to generate cross sections. The following section with modules descriptions is to demonstrate to the reader the rigor and complexity in the task of generating cross sections using dedicated codes such as NJOY system [14, 29].

To perform this study, the ENDF/B-VII.0 [18] cross section data provided by the Los Alamos National Laboratory are used in dedicated processing code NJOY system to generate a data set at work temperature to be used in this work. Besides that, four others already generated cross section data set from Serpent package were used in work, each of these data set was generated considering different temperatures 300, 600, 900, and 1200 K.

It must be noticed that due to an error in multigroup nuclear data generation using the ^{232}Th ENDF/B-VII.0 file [30], it was necessary to use other ENDL version. Since the benchmark authors use cross sections from ENDF/B-VI [31] for some nuclides, the data used to substitute ^{232}Th data is selected to be from ENDF/B-VI. Hence, for all other nuclides are used the ENDF/B-VII.0 evaluated libraries.

MODER converts the ENDF, Pointwise ENDF – PENDF, and Groupwise ENDF – GENDF tapes from blocked-binary mode to ASCII formatted mode and also oppositely. It is used to extract materials section from an ENDF in the ENDF/B format. In addition, it can handle the ENDF4 through ENDF6 formats, plus special purpose formats developed for NJOY system. MODER requires an entry for designate the data type followed by a sequence of tapes and material number to convert and save the data into respective tapes.

RECONR reconstructs pointwise cross sections from ENDF resonance parameters and nonlinear interpolation schemes. It writes files with all cross sections on a unionized grid, usable for linear interpolation to within a specified tolerance. RECONR requires data tape entries, values for the fractional reconstruction tolerance (0.001 and 0.003) and reconstruction

temperature used as default 0 K. Fractional reconstruction tolerance is used in order to refine the grid points added to tape to represent resonances.

BROADR applies the Doppler broadening effect to the PENDF. It uses as entry the same tapes and the fractional reconstruction tolerances required from RECORN. In addition, the number of temperatures, respective temperature values and maximum for broadening and thinning must be entry. For each nuclide a single temperature was selected for example 900 K, 621 K or 583 K depending on the material, and the maximum energy was set to 2 MeV.

HEATR generates and adds pointwise heat production cross sections and radiation damage energy production for specified reactions and to an existing PENDF file. The partial KERMAS values and temperatures of processing are required as entries. For this generation, seven different partial KERMAS were selected (MT302, MT303, MT304, MT318, MT402, MT443, and MT444) [32]. Temperature processing was set to default meaning all temperatures on input tape.

THERM generates and adds pointwise neutron scattering cross sections in thermal energy range to an existing PENDF file. It works with original ENDF/B-III thermal and ENDF-6 formats. THERM entries are to add thermal scattering data to PENDF file, it requires processing temperatures, a sequence of elastic and inelastic scattering treatments options, tolerance and maximum energy for thermal treatment, usually set to temperature divided by 300.

GROUPR computes the group-to-group scattering matrices, photon production matrices, and charged particles matrices from ENDL pointwise input. It can provide ratio quantities such as delayed neutron spectra, anisotropic thermal neutron scattering. GROUPR accounts the neutron group structure specification, processing temperatures, flux calculator parameters, files and sections to be generated.

PURR produces the unresolved resonances self-shielding probabilities tables that can be used by the Monte Carlo continuous energy transport codes. PURR requires numbers of bins and ladders to perform accurate cross section calculations and also processing temperature.

GASPR generates and adds gas production cross sections in the pointwise PENDF format. It is required that this module goes after BROADR. To perform GASPR execution only data tapes are required.

ACER prepares libraries in the traditional ACE format for the use in the Monte Carlo transport codes such as MCNP or Serpent. ACER requires the type of run option which can be thermal, fast, dosimetry, photo-atomic or photo-nuclear data. It needs the ACE output type, id suffix for cross section and processing temperatures.

MATSXR formats the cross sections, group-to-group matrices, self-shielding, and time dependence of the neutron, photon, and charged-particle data, to the MATXS material cross section format. This type of library can be used with the TRANSX code to produce effective cross sections for a wide variety of application codes. The module uses tape obtained from GROUPR execution; it requires a set of identifiers for a number of materials, particles, and groups.

3. MODEL VALIDATION

3.1. BENCHMARK DESCRIPTION

In order to study the use of thorium in PWRs, it is selected a thorium based fuel pin benchmark to perform the evaluation. It presents a validation study based on the thorium fuel pin followed by an extension of the calculations presented in the benchmark. Besides that, future studies intend to extrapolate fuel pin geometry and apply the same methodology to cores.

The selected benchmark was performed by the Massachusetts Institute of Technology – MIT, the Idaho National Engineering and Environmental Laboratory – INEEL, and the Czech Technical University. It represents a PWR fuel pin cell, extracted from a 17x17 pin assembly typical from a large Westinghouse PWRs. A ThO_2-UO_2 mixture substituted the traditional UO_2 fuel [1].

Figure 1 exhibits the benchmark fuel pin used as a reference. The fuel consists of 75 w/o Th, 25 w/o U on a heavy metal basis. The uranium is 19.5 w/o ^{235}U, and that results in an overall enrichment of 4.869 w/o ^{235}U in total heavy metal. The cladding is Zircaloy-4 - Zr-4, and the coolant and moderator material is regular light water. The defined Work Temperature – WT is 900 K for the fuel, 621 K for the cladding and 583 K for the coolant.

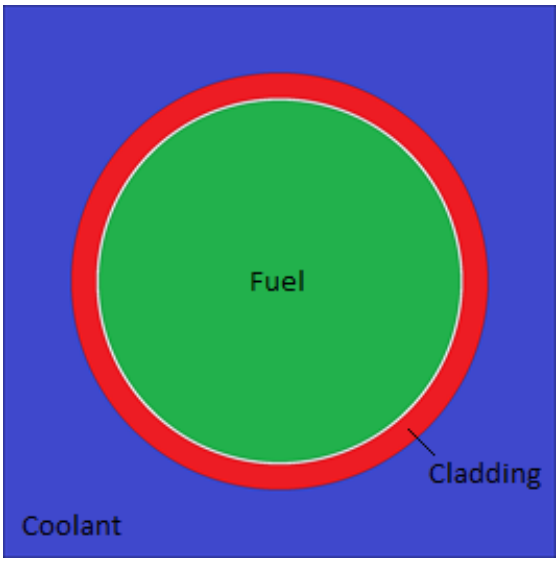

Figure 1 - Fuel pin extracted from typical Westinghouse PWRs [1]

The boundary conditions in simulated fuel pin are reflective, then considering that the neutron is reflected into the geometry after reaching the bounds of the geometry. The specific power utilized to perform the burnup on the fuel pin is 38.1347 MW/MTHM, and the total burnup is 72.189 GWd/MTHM. Thus, the burnup is completed in 1893 days, that is approximately 5.2 years. All the information about geometry, compositions and burnup parameters can be found in Tables 1 and 2 [1].

Table 1: Pin-cell model burnup parameters [1]

Parameter	**Full Power**
Power	38.1347 MW/MTHM
Total Burnup	72.189 GWd/MTHM
Fuel Temperature	900 K
Cladding Temperature	621 K
Coolant Temperature	583 K
Fuel Density	9.424 g/cm³
Cladding Density	6.505 g/cm³
Coolant Density	0.705 g/cm³
Fuel Pellet Radius	4.127 mm
Cladding Inner Radius	4.189 mm
Cladding Outer Radius	4.761 mm
Pin Pitch	12.626 mm
Burnup duration	1893 days

Table 2: Initial compositions at full power conditions [1]

	Nuclide	**Weight Percent (%)**
Fuel	^{232}Th	65.909
	^{234}U	0.0340
	^{235}U	4.2910
	^{238}U	17.740
	^{16}O	12.026
Cladding	Zr-4	100
Coolant	^{1}H	11.19
	^{16}O	88.81

The benchmark authors use two code packages (CASMO-4 [33] and MOCUP [34]) that combine the MCNP4B to accomplishing the neutron transport and ORIGEN2 to perform the fuel depletion. Overall, three different models were used in this benchmark, two were done by MIT using CASMO-4 and MOCUP, and the last result from INEEL using the MOCUP code.

The authors use the JEF-2.2 [26] and ENDF/B-VI [31] for CASMO-4 code, and the UTXS [35] cross section compilation for MOCUP.

The results refer to the k_∞ along the burnup of 72.189 GWd/MTHM. Besides that, the actinide isotopic composition is presented at the 60.749 GWd/MTHM. This particular burnup step represents the upper limit of discharge burnup if a 3-batch core refueling scheme is considered.

3.2. CRITICALITY

3.2.1. Methodology

The content presented in this section consists of a validation study using the described benchmark. Five different data sets based on ENDF/B-VII.0 are used in five different neutron transport code to perform criticality calculations. k_∞ are compared to the step 0 benchmark results.

The analysis performed to evaluate the data consists in calculating quantities such as mean value (1), standard deviation (2), and relative standard deviation (3) for benchmark data and comparing these to results obtained in this work, thus, validating the modelling.

$$\bar{s} = \frac{1}{n}\sum_{i=1}^{n} s_i \tag{1}$$

$$\sigma = \sqrt{\frac{\sum_1^n (s_i - \bar{s})^2}{n}} \tag{2}$$

$$\sigma_{\%} = \frac{\sigma}{\bar{s}} \tag{3}$$

In addition, following the methodology proposed in reference works using the same benchmark, the k_∞ fractional difference is calculated using the benchmark value (CASMO-4) and the results from this dissertation (4).

$$Frac.Diff. = \frac{(k - k_{CASMO4})}{k_{CASMO4}} \quad (4)$$

Five different data sets are used to perform the evaluation. The first cross sections data set is generated at DEN at work temperatures of 900 K, 621 K, and 583 K corresponding to the fuel, cladding and coolant materials, respectively using NJOY99 system for processing and the ENDF/B-VII.0 as ENDL. Besides that, four other cross section datasets are used at different temperatures, (300 K, 600 K, 900 K, and 1200 K) available in Serpent package and based on ENDF/B-VII.0. For this evaluation, the neutron transport codes used are: MCNPX, MCNP5, Serpent, KENO-VI, and NEWT.

The cross section generation at DEN/UFMG is performed using the NJOY99 code package following the methodology described in the previous section. The generated cross section data set is designated as Work Temperatures - WT for considering 900 K to fuel, 621K to the cladding and 583 K to coolant material. For academic reasons, each of other cross section data sets considers all materials to be at the same temperature, this is a far from real proposition, however, performing this provides evidences for further conclusions.

All data sets are employed in MCNPX, MCNP5 and Serpent, in addition, the 300 K, 600 K and 900 K are employed in Serpent using the Doppler broadening preprocessor routine setting the temperature to the work temperatures (tmp card). Since the Doppler broadening preprocessor routine is not able to set cross sections temperature to lower values, the 1200 K data set is not able to be used.

The 300 K cross sections are used and adjusted to 583 K, 621 K and 900 K considering coolant, cladding and fuel materials, respectively. The 600 K cross sections are used and adjusted to 621 K and 900 K considering cladding and fuel materials, respectively. The 900 K cross sections are used and for academic reasons adjusted to 900 K considering only the fuel.

These three cases which considers the Doppler broadening preprocessor routine differs from the ordinary 300 K, 600 K and 900 K Serpent cases just from the use of the routine. Therefore, differences in results are assigned to the use of it.

SCALE6.0 system CSAS sequence is used to perform criticality calculation, only the internally generated libraries were used due to difficulties in implementing external cross sections in SCALE6.0 system. Based on previous studies at DEN/UFMG using the same thorium fuel pin benchmark [16], the collapsed 238 energy groups presented the best multiplication factor results when compared to benchmark. Thus, KENO-VI used the continuous energy libraries and the 238 energy groups obtained from collapsing, both based on the ENDF/B-VII.0, while NEWT for being deterministic uses only the collapsed 238 energy groups library. All cases were performed using KENO-VI and NEWT neutron transport codes.

To describe each case, the name of the code with the respective temperature used are mentioned. For example, using the MCNPX code with the 300 K cross sections, then the result is MCNPX-300.

To refer to the Doppler broadening preprocessor routine, the acronym Serpent-DBR is used, and Serpent refers to no using the Doppler broadening preprocessor routine. The Doppler broadening preprocessor routine can only be used to adjust cross section temperatures to higher values. Therefore, 1200 K is not able to be adjusted to 900 K and thus is not used. KENO-VI_CE and KENO-VI_238 are used to address the continuous energy libraries and collapsed 238 energy groups.

Table 3 presents all the cases performed considering fresh fuel situation, including the cross sections temperatures and the neutron transport codes used. The “X” marked cells refers to simulated cases while the “-” cells are not able to accomplish.

Table 3: Simulated cases for criticality calculations and cross section validation

	MCNPX	***MCNP5***	***Serpent***	***Serpent DBR***	***NEWT***	***KENO-VI_CE***	***KENO-VI_238***
300K	X	X	X	X	-	-	-
600K	X	X	X	X	-	-	-
900K	X	X	X	X	-	-	-
1200K	X	X	X	-	-	-	-
NJOY-WT	X	X	X	-	X	X	X

Table 4 presents detailed information for each of the cases. In this step, the validation consists of comparing the initial k_∞ from each case and the benchmark results. The k_∞ mean value, k_∞ standard deviation and k_∞ relative standard deviation is calculated considering the results from all simulations and benchmark and are compared to the same quantities considering only the benchmark results.

Table 4: Cases descriptions

ENDL	**CODE**	**CROSS SECTION PROCESSING TEMPERATURES**	
ENDF/B-VII.0	MCNPX	300 K	MCNPX-300
		600 K	MCNPX-600
		900 K	MCNPX-900
		1200 K	MCNPX-1200
		WT	MCNPX-WT
	MCNP5	300 K	MCNP5-300
		600 K	MCNP5-600
		900 K	MCNP5-900
		1200 K	MCNP5-1200
		WT	MCNP5-WT
	Serpent	300 K	Serpent-300
		600 K	Serpent-600
		900 K	Serpent-900
		1200 K	Serpent-1200
		WT	Serpent-WT
		300 K	Serpent-DBR-300
		600 K	Serpent-DBR-600
		900 K	Serpent-DBR-900
	CSAS NEWT	WT	NEWT-WT
	CSAS KENO-VI	WT	KENO-VI_CE-WT
		WT	KENO-VI_238-WT

The stochastics simulations are performed with 2000 active cycles using 50000 histories. Therefore, the total number of neutrons in each simulation is 100 million. A large number of particles guarantee a low standard deviation. Therefore, it is desired a standard deviation lower than 10 pcm.

3.2.2. Results

To initiate the validation, Table 5 presents the results obtained for all performed cases in fresh fuel situation using different codes and their correspondent temperature. Except for NEWT result, each k_∞ is associated with a standard deviation from the stochastic method.

From results obtained, the maximum k_∞ value was 1.29136 using 300 K data and MCNPX code, the minimum k_∞ value was 1.22506 using 1200 K data and Serpent. To proceed with validation only results with absolute difference lower than 500 pcm in relation to the benchmark k_∞ mean value is considered.

Table 5: k_∞ results for fresh fuel situation

	k_∞	***STANDARD DEVIATION (pcm)***
MCNPX-300	1.29136	6
MCNPX-600	1.26480	6
MCNPX-900	1.23483	6
MCNPX-1200	1.22978	6
MCNPX-WT	1.23537	6
MCNP5-300	1.25153	6
MCNP5-600	1.24218	6
MCNP5-900	1.23476	6
MCNP5-1200	1.22857	6
MCNP5-WT	1.23539	6
Serpent-300	1.29379	4.2
Serpent-600	1.26342	4.4
Serpent-900	1.24194	4.6
Serpent-1200	1.22506	4.7
Serpent-WT	1.23796	4.6
Serpent-DBR-300	1.24469	4.6
Serpent-DBR-600	1.24475	4.6
Serpent-DBR-900	1.24504	4.5
NEWT-WT	1.23041	-
KENO-VI_CE-WT	1.24377	6.4
KENO-VI_238-WT	1.23571	5.4

Table 6 indicates three initial k_∞ results obtained from benchmark authors, the mean value is taken, and it is used as a reference value to further criticality analyses. The results from Table 7 with absolute differences of 500 pcm or less with respect to benchmark k_∞ mean value is taken to perform the validation.

Table 6: k_∞ results obtained from benchmark authors [1]

Benchmark	k_∞	k_∞ Mean value
MIT - CASMO-4	1.23782	1.23161
MIT - MOCUP	1.23354	
INEEL - MOCUP	1.22347	

Table 7 presents the selected cases to proceed with the validation jointly to the k_∞ absolute difference ($|k_{\infty\ Result} - k_{\infty\ Reference}|$). The analysis performed to evaluate the data consists in calculating quantities such as mean value, standard deviation, and relative standard deviation for benchmark data and comparing these to results obtained in this work.

Benchmark data is addressed as "before" and the results are addressed as "updated". This type of analysis is used when validations are performed, analyzing then statistical quantities and their changes when adding the results obtained from simulations.

Table 7: k_∞ results with less than 500 pcm from k_∞ mean value from benchmark authors

Simulated cases	k_∞	Absolute differences
MCNPX-900	1.23483	322
MCNPX-1200	1.22978	183
MCNPX-WT	1.23537	376
MCNP5-900	1.23476	315
MCNP5-1200	1.22857	304
MCNP5-WT	1.23539	378
CSAS NEWT-WT	1.23041	120
CSAS KENO-VI_238-WT	1.23571	410

The results from the analysis are presented in Table 8. The results addressed as BEFORE considers only benchmark results. The results referred to as UPDATED contemplate the results obtained in this work. It is observed a decrease in multiplication factor standard deviation and multiplication factor relative standard deviation, the lower differences that the ones found by the MIT-INEEL validate the modeling and cross section processing performed at DEN.

Table 8: Analysis using the selected data and benchmark results

Country	**Institute**	**Code**	**Library**	**k_∞**
USA	MIT	CASMO-4	ENDF/B-VI	1.23782
USA	MIT	MOCUP	UTXS	1.23354
USA	INEEL	MOCUP	UTXS	1.22347
BRAZIL	DEN	MCNPX	ENDF/B-VII.0 900 K	1.23483
BRAZIL	DEN	MCNPX	ENDF/B-VII.0 1200 K	1.22978
BRAZIL	DEN	MCNPX	ENDF/B-VII.0 WT	1.23537
BRAZIL	DEN	MCNP5	ENDF/B-VII.0 900 K	1.23476
BRAZIL	DEN	MCNP5	ENDF/B-VII.0 1200 K	1.22857
BRAZIL	DEN	MCNP5	ENDF/B-VII.0 WT	1.23539
BRAZIL	DEN	CSAS - NEWT	ENDF/B-VII.0 WT	1.23041
BRAZIL	DEN	CSAS – KENO -VI_238	ENDF/B-VII.0 WT	1.23571
Multiplication Factor Mean Value			Before	1.23161
			Updated	1.23269
Multiplication Factor Standard Deviation			Before	0.00602
			Updated	0.00399
Multiplication Factor Relative Standard Deviation			Before	0.49%
			Updated	0.32%

Following the methodology proposed in reference works, the initial k_∞ fractional differences are presented in Table 9. The values represent the percentage differences in relation to the benchmark value (CASMO4) including the results from the reference works and the Table 7 k_∞ results. The HELIOS [36] fractional differences are presented as an additional source of comparison, the results presented are in agreement with both benchmark and reference works values.

Table 9: k_∞ fractional differences from benchmark, references and dissertation results

CASMO4 (Benchmark) – 1.23782	k_∞ Fractional Difference (%)
MIT-MOCUP	-0.346
INEEL-MOCUP	-1.159
MCNPX-900	-0.242
MCNPX-1200	-0.650
MCNPX-WT	-0.198
MCNP5-900	-0.247
MCNP5-1200	-0.747
MCNP5-WT	-0.196
CSAS NEWT-WT	-0.599
CSAS KENO-VI_238-WT	-0.170
HELIOS 35RE4	-0.993
HELIOS 35RE4	-0.137
HELIOS 190RE4	-0.204
HELIOS 190RE6	0.227

As an additional result, Table 10 presents Serpent results for 300 K, 600 K, and 900 K, when the Serpent Doppler broadening preprocessor uses the routine or not. The Doppler broadening preprocessor routine can only be used to adjust cross section temperatures to higher values, therefore if adjusted at 900 K, the code is not able to use higher temperatures cross sections such as 1200 K.

Although none of the Serpent-DBR cases are considered in the evaluation, the routine can be used to approach the results to the reference value. It is simple to use a tool to approximate the processing temperature of cross sections, however, depending on the cross section used the results may worsen.

Table 10: Serpent criticality results

	k_∞	**Absolute Difference**
Serpent-300	1.29379	6218
Serpent-600	1.26342	3181
Serpent-900	1.24194	1033
Serpent-DBR-300	1.24469	1308
Serpent-DBR-600	1.24475	1314
Serpent-DBR-900	1.24504	1343

3.3. DEPLETION

3.3.1. Methodology

Since fuel depletion runs require much more time when compared to criticality cases, only the best result from the cross section data set were selected to continue the validation. Thus, the thorium-based fuel pin benchmark with 72.189 GWd/MTHM burnup is performed using the WT cross sections generated using NJOY code system for MCNPX, Monteburns (MCNP5 linked to ORIGEN2.1) and Serpent. For SCALE6.0 system, the depletion sequence TRITON is used with the work temperature (WT).

Table 11 presents detailed information about the neutron transport and depletion codes that are used to perform the depletion. Each code has particularities such as a different number of energy groups and cross section data libraries. The 238 collapsed groups in NEWT and KENO-VI are

used based on previous studies performed at DEN/UFMG that presented the nearest results in relation to the reference value among other possibilities of choice [16].

Table 11: Neutron transport and depletion codes descriptions

Neutron Transport Code	Energy Groups	ENDL	Depletion Code	Energy Groups	ENDL
MCNPX	Continuous	ENDF/B-VII.0	CINDER '90	63	ENDF/B - JEFF - JENDL
MCNP5	Continuous	ENDF/B-VII.0	ORIGEN2.1	1	ENSDF - ENDF/B-IV
Serpent	Continuous	ENDF/B-VII.0	Serpent	1	ENDF/B-VII.0
NEWT	238 groups	ENDF/B-VII.0	ORIGEN-S	3	ENDF/B-VII.0 and JEFF3.1
KENO-VI	238 groups	ENDF/B-VII.0			

This section aims to continue the validation considering fuel depletion using the same analysis performed in the last section using the k_∞ during burnup. In addition, an analysis of the fractional difference in isotopes concentrations is performed at the 60.749 GWd/MTHM. The number of nuclides followed from decay chains along depletion is chosen to be the largest possible number of nuclides for most codes.

In MCNPX this feature consists in selecting the Tier3 option in burnup card. In Serpent setting the inventory with 201, 202, 204, and 208 designations allow the code to follow all actinides, fission products, decay products below thorium in the natural actinide decay series, and noble gases in fission product range that have data in ENDF/B-VII.0. In SCALE6.0 system depletion sequence, TRITON, this parameter corresponds to Addnux3. In Monteburns the nuclides followed are selected according to the nuclides at Tier3.

Table 12 presents all followed nuclides including the Tier3 setting from MCNPX and the Addnux3 from KENO-VI and NEWT.

Table 12: Followed nuclides using the Tier3 and Addnux3 parameters

Tier3	Addnux3
^{69}Ga ^{71}Ga ^{70}Ge ^{72}Ge ^{73}Ge ^{74}Ge ^{76}Ge ^{74}As ^{75}As ^{74}Se ^{76}Se ^{77}Se ^{78}Se ^{79}Se ^{80}Se ^{82}Se ^{79}Br ^{81}Br ^{78}Kr ^{80}Kr ^{82}Kr ^{83}Kr ^{84}Kr ^{85}Kr ^{86}Kr ^{85}Rb ^{86}Rb ^{87}Rb ^{84}Sr ^{86}Sr ^{87}Sr ^{88}Sr ^{89}Sr ^{90}Sr ^{89}Y ^{90}Y ^{91}Y ^{90}Zr ^{91}Zr ^{92}Zr ^{93}Zr ^{94}Zr ^{95}Zr ^{96}Zr ^{93}Nb ^{94}Nb ^{95}Nb ^{92}Mo ^{94}Mo ^{95}Mo ^{96}Mo ^{97}Mo ^{98}Mo ^{99}Mo ^{100}Mo ^{99}Tc ^{96}Ru ^{98}Ru ^{99}Ru ^{100}Ru ^{101}Ru ^{102}Ru ^{103}Ru ^{104}Ru ^{105}Ru ^{106}Ru ^{103}Rh ^{105}Rh ^{102}Pd ^{104}Pd ^{105}Pd ^{106}Pd ^{107}Pd ^{108}Pd ^{110}Pd ^{107}Ag ^{109}Ag ^{111}Ag ^{106}Cd ^{108}Cd ^{110}Cd ^{111}Cd ^{112}Cd ^{113}Cd ^{114}Cd ^{116}Cd ^{113}In ^{115}In ^{112}Sn ^{113}Sn ^{114}Sn ^{115}Sn ^{116}Sn ^{117}Sn ^{118}Sn ^{119}Sn ^{120}Sn ^{122}Sn ^{123}Sn ^{124}Sn ^{125}Sn ^{126}Sn ^{121}Sb ^{123}Sb ^{124}Sb ^{125}Sb ^{126}Sb ^{120}Te ^{122}Te ^{123}Te ^{124}Te ^{125}Te ^{126}Te ^{128}Te ^{130}Te ^{132}Te ^{127}I ^{129}I ^{130}I ^{131}I ^{135}I ^{123}Xe ^{124}Xe ^{126}Xe ^{128}Xe ^{129}Xe ^{130}Xe ^{131}Xe ^{132}Xe ^{133}Xe ^{134}Xe ^{135}Xe ^{136}Xe ^{133}Cs ^{134}Cs ^{135}Cs ^{136}Cs ^{137}Cs ^{130}Ba ^{132}Ba ^{133}Ba ^{134}Ba ^{135}Ba ^{136}Ba ^{137}Ba ^{138}Ba ^{140}Ba ^{138}La ^{139}La ^{140}La ^{133}Ce ^{138}Ce ^{139}Ce ^{140}Ce ^{141}Ce ^{142}Ce ^{143}Ce ^{144}Ce ^{141}Pr ^{142}Pr ^{143}Pr ^{142}Nd ^{143}Nd ^{144}Nd ^{145}Nd ^{146}Nd ^{147}Nd ^{148}Nd ^{150}Nd ^{147}Pm ^{148}Pm ^{149}Pm ^{151}Pm ^{144}Sm ^{147}Sm ^{148}Sm ^{149}Sm ^{150}Sm ^{151}Sm ^{152}Sm ^{153}Sm ^{154}Sm ^{151}Eu ^{152}Eu ^{153}Eu ^{154}Eu ^{155}Eu ^{156}Eu ^{157}Eu ^{152}Gd ^{153}Gd ^{154}Gd ^{155}Gd ^{156}Gd ^{157}Gd ^{158}Gd ^{160}Gd ^{159}Tb ^{160}Tb ^{156}Dy ^{158}Dy ^{160}Dy ^{161}Dy ^{162}Dy ^{163}Dy ^{164}Dy ^{165}Ho ^{162}Er ^{164}Er ^{166}Er ^{167}Er ^{168}Er ^{170}Er	^{72}Ge ^{73}Ge ^{74}Ge ^{76}Ge ^{75}As ^{79}Br ^{76}Se ^{77}Se ^{78}Se ^{80}Se ^{82}Se ^{81}Br ^{80}Kr ^{82}Kr ^{84}Kr ^{85}Kr ^{86}Kr ^{85}Rb ^{86}Rb ^{87}Rb ^{84}Sr ^{86}Sr ^{87}Sr ^{88}Sr ^{89}Sr ^{90}Sr ^{89}Y ^{90}Y ^{91}Y ^{90}Zr ^{91}Zr ^{92}Zr ^{93}Zr ^{95}Zr ^{96}Zr ^{92}Mo ^{94}Mo ^{96}Mo ^{97}Mo ^{98}Mo ^{99}Mo ^{100}Mo ^{94}Nb ^{95}Nb ^{96}Ru ^{98}Ru ^{99}Ru ^{100}Ru ^{101}Ru ^{102}Ru ^{103}Ru ^{104}Ru ^{105}Ru ^{102}Pd ^{104}Pd ^{105}Pd ^{106}Pd ^{107}Pd ^{108}Pd ^{110}Pd ^{107}Ag ^{111}Ag ^{106}Cd ^{108}Cd ^{110}Cd ^{111}Cd ^{112}Cd ^{113}Cd ^{114}Cd ^{115m}Cd ^{116}Cd ^{113}In ^{115}In ^{112}Sn ^{114}Sn ^{115}Sn ^{127m}Te ^{128}Te ^{129m}Te ^{130}Te ^{132}Te ^{127}I ^{129}I ^{130}I ^{131}I ^{124}Xe ^{126}Xe ^{128}Xe ^{129}Xe ^{130}Xe ^{132}Xe ^{133}Xe ^{134}Xe ^{136}Xe ^{134}Ba ^{135}Ba ^{136}Ba ^{137}Ba ^{138}Ba ^{140}Ba ^{136}Cs ^{139}La ^{141}Pr ^{142}Pr ^{140}La ^{142}Nd ^{144}Nd ^{150}Nd ^{140}Ce ^{141}Ce ^{142}Ce ^{143}Ce ^{151}Pm ^{144}Sm ^{148}Sm ^{153}Sm ^{154}Sm ^{152}Eu ^{156}Eu ^{157}Eu ^{159}Tb ^{160}Tb ^{160}Dy ^{161}Dy ^{162}Dy ^{163}Dy ^{164}Dy ^{161}Ho ^{166}Er ^{167}Er ^{175}Lu ^{176}Lu ^{181}Ta ^{182}W ^{183}W ^{184}W ^{186}W ^{185}Re ^{187}Re ^{197}Au ^{231}Pa ^{233}Pa ^{230}Th ^{232}Th ^{232}U ^{233}U ^{116}Sn ^{117}Sn ^{118}Sn ^{119}Sn ^{120}Sn ^{122}Sn ^{123}Sn ^{124}Sn ^{125}Sn ^{121}Sb ^{123}Sb ^{124}Sb ^{125}Sb ^{126}Sb ^{120}Te ^{122}Te ^{123}Te ^{124}Te ^{125}Te ^{126}Te

According to Table 1, the total burnup considered is 72.189 GWd/MTHM and the specific power is 38.1347 MW/MTHM. Thus, the total operation time is 1893 days, equivalent to approximately 5.2 years. All burnup simulations are divides into 20 steps matching the benchmark burnup steps.

Besides that, all stochastics simulations use 1000 active cycles with 5000 histories, thus the total amount of neutrons per burnup step is 5 million. The particles number is relatively low compared to criticality analysis due to the computer time required to perform burnup simulations.

To proceed with the validation, the k_∞ during burnup are evaluated under the same analysis performed in criticality section. In addition, the actinide isotopic composition at

60.749 GWd/MTHM is also evaluated using the same analysis performed by benchmark authors.

3.3.2. Results

Considering that fuel depletion simulation requires much more time when compared to criticality cases, it is chosen that only the data set which provided majority of the results closer to the results of the benchmark k_∞ mean value (Table 7) proceed to depletion validation. This data set corresponds to WT cross sections generated in DEN using the NJOY system.

To illustrate the time taken from simulations. criticality calculations lasted from 2 to 6 hours depending on neutron transport code, meanwhile, fuel depletion using MCNPX took 7 days to complete calculations.

Table 13 presents the values for the k_∞ using all codes including the benchmark results along the burnup. The burnup steps match the division performed by the benchmark authors. k_∞ maximum and minimum results were respectively, 1.23797 and 1.23165 at step zero burnup and 0.89571 and 0.87993 at 72.189 GWd/MTHM. Since each code performs depletion using different ENDFs, it is expected a crescent deviation over burnup.

Table 13: k_∞ results along the 72.189GWd/MTHM burnup

BURNUP	MIT CASMO4	MIT MOCUP	INEEL MOCUP	MCNPX	Monteburns	Serpent	TRITON - KENO-VI & ORIGEN S	TRITON - NEWT & ORIGEN S
0	1.23782	1.23354	1.22347	1.23645	1.23515	1.23797	1.23689	1.23165
0.114	1.20071	1.19708	1.18051	1.19779	1.19898	1.20082	1.19895	1.19403
5.835	1.14828	1.14466	1.13563	1.14711	1.14768	1.15026	1.14619	1.14180
10.411	1.12108	1.11662	1.11325	1.12212	1.12328	1.12509	1.12055	1.11607
19.563	1.07245	1.07154	1.06648	1.07778	1.07842	1.08001	1.07340	1.06948
31.004	1.02014	1.02168	1.01906	1.03063	1.02660	1.02939	1.02202	1.01866
40.156	0.98190	0.98453	0.98514	0.99443	0.99073	0.99254	0.98391	0.98097
49.308	0.94636	0.95383	0.95035	0.96068	0.95517	0.95846	0.94939	0.94761
51.596	0.93817	0.94477	0.94063	0.95202	0.94750	0.95041	0.94109	0.93940
60.749	0.90701	0.91851	0.91447	0.92569	0.91782	0.92124	0.91141	0.91076
72.189	0.87348	0.88449	0.87942	0.89571	0.88718	0.88960	0.87993	0.88707

In addition to Table 13 results the k_∞ fractional differences are calculated and presented in Table 14. The values refer to benchmark values (CASMO4), other reference works (MIT-MOCUP, INEEL-MOCUP, HELIOS) and the results from this work. Similar to the k_∞ fractional differences calculated in last section (Table 9), the results obtained are in agreement with adopted comparisons. The maximum absolute k_∞ fractional difference obtained is 2.545% for MCNPX at 72.189 GWd/MTHM.

Table 14: k_∞ fractional differences along the 72.189GWd/MTHM burnup

BURNUP	**1**	**2**	**3**	**4**	**5**	**6**	**7**	**8**	**9**	**10**	**11**	**12**
0	1.23782	-0.346	-1.159	-0.111	-0.216	0.012	-0.075	-0.498	-0.993	-0.137	-0.204	0.227
0.114	1.20071	-0.302	-1.682	-0.243	-0.144	0.009	-0.147	-0.556	-0.986	-0.129	-0.201	0.232
5.835	1.14828	-0.315	-1.102	-0.102	-0.052	0.172	-0.182	-0.564	-0.874	-0.073	-0.167	0.236
10.411	1.12108	-0.398	-0.698	0.093	0.196	0.358	-0.047	-0.447	-0.744	-0.009	-0.078	0.294
19.563	1.07245	-0.085	-0.557	0.497	0.557	0.705	0.089	-0.277	-0.519	0.061	0.128	0.417
31.004	1.02014	0.151	-0.106	1.028	0.633	0.907	0.184	-0.145	-0.372	-0.011	0.254	0.425
40.156	0.98190	0.268	0.330	1.276	0.899	1.084	0.205	-0.095	-0.311	-0.139	0.310	0.373
49.308	0.94636	0.789	0.422	1.513	0.931	1.279	0.320	0.132	-0.220	-0.248	0.379	0.319
51.596	0.93817	0.703	0.262	1.476	0.994	1.305	0.311	0.131	-0.167	-0.242	0.418	0.334
60.749	0.90701	1.268	0.822	2.060	1.192	1.569	0.485	0.413	-0.234	-0.499	0.308	0.096
72.189	0.87348	1.260	0.680	2.545	1.568	1.845	0.738	1.556	-0.330	-0.783	0.180	-0.151

[1] - MIT CASMO4 – benchmark values
[2] - MIT MOCUP
[3] - INEEL MOCUP
[4] - MCNPX
[5] - Monteburns
[6] - Serpent
[7] - TRITON-KENO-VI & ORIGEN S
[8] - TRITON-NEWT & ORIGEN S
[9] - HELIOS 35RE4
[10] - HELIOS 35RE6
[11] - HELIOS 190RE4
[12] - HELIOS 190RE6

Figure 2 presents the k_∞ above along the burnup. The validation is performed analyzing the same quantities from the previous section. The analysis is performed for each of the burnup step.

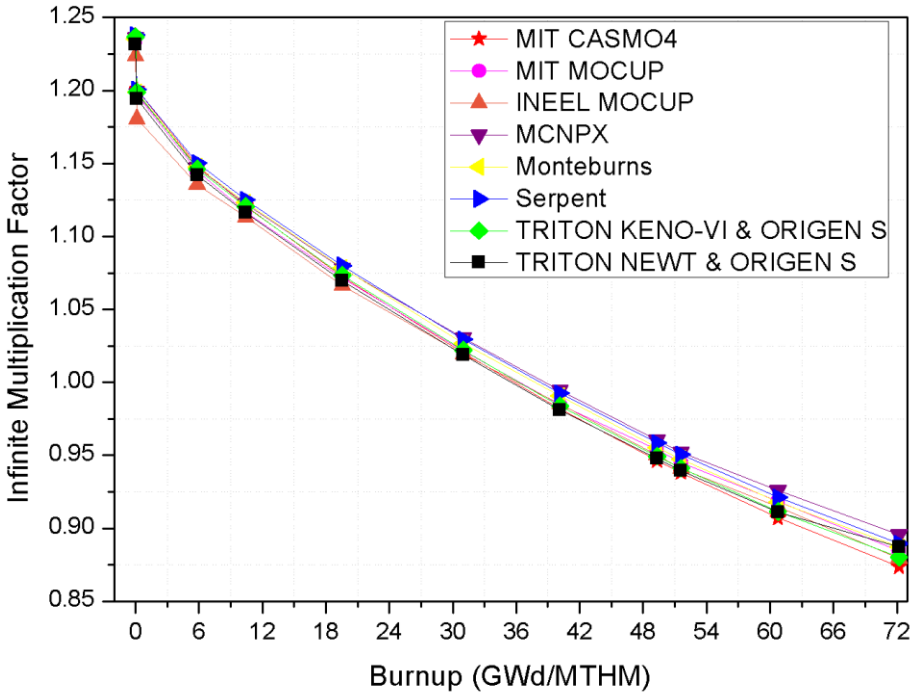

Figure 2: k_∞ over burnup

Table 15 presents benchmark k_∞ along burnup. Quantities such as mean value, standard deviation and relative standard deviation are also displayed in Table 13. Maximum and minimum relative standard deviations are respectively presented in step one (0.74%) and step five (0.11%).

Table 15: k_∞ benchmark data along the 72.189GWd/MTHM burnup [1]

BURNUP	MIT CASMO4	MIT MOCUP	INEEL MOCUP	MEAN	STANDARD DEVIATION	RELATIVE STANDARD DEVIATION (%)
0	1.23782	1.23354	1.22347	1.23161	0.00601	0.49
0.114	1.20071	1.19708	1.18051	1.19276	0.00879	0.74
5.835	1.14828	1.14466	1.13563	1.14285	0.00531	0.47
10.411	1.12108	1.11662	1.11325	1.11698	0.00320	0.29
19.563	1.07245	1.07154	1.06648	1.07015	0.00262	0.25
31.004	1.02014	1.02168	1.01906	1.02029	0.00107	0.11
40.156	0.98190	0.98453	0.98514	0.98385	0.00140	0.14
49.308	0.94636	0.95383	0.95035	0.95018	0.00305	0.32
51.596	0.93817	0.94477	0.94063	0.94119	0.00272	0.29
60.749	0.90701	0.91851	0.91447	0.91333	0.00476	0.52
72.189	0.87348	0.88449	0.87942	0.87913	0.00449	0.51

Table 16 presents the analysis performed using the same methodology applied in criticality section. Different from Table 15 which considers only the benchmark data, the mean value, standard deviation, and relative standard deviation in Table 16 are calculated considering both results from depletion validation and the benchmark data. Maximum and minimum relative standard deviations occur respectively at step ten (0.73%) and step three (0.34%).

Comparing relative standard deviations from Tables 15 and 16, it is observed that maximum values reduced by 0.01% using data from this study. In addition, analyzing step by step the maximum decrease and increase in relative standard deviation values are observed in step one reducing from 0.74% to 0.52% and in step six increasing from 0.14% to 0.48%.

Table 16: k_∞ results plus benchmark data along the 72.189 GWd/MTHM burnup

BURNUP	MCNPX	MONTE BURNS	Serpent	TRITON - KENO-VI & ORIGEN S	TRITON - NEWT & ORIGEN S	MEAN	STANDARD DEVIATION	RELATIVE STANDARD DEVIATION (%)
0	1.23645	1.23515	1.23797	1.23689	1.23165	1.23411	0.00450	0.37
0.114	1.19779	1.19898	1.20082	1.19895	1.19403	1.19610	0.00623	0.52
5.835	1.14711	1.14768	1.15026	1.14619	1.14180	1.14520	0.00432	0.38
10.411	1.12212	1.12328	1.12509	1.12055	1.11607	1.11975	0.00378	0.34
19.563	1.07778	1.07842	1.08001	1.07340	1.06948	1.07369	0.00440	0.41
31.004	1.03063	1.02660	1.02939	1.02202	1.01866	1.02352	0.00440	0.43
40.156	0.99443	0.99073	0.99254	0.98391	0.98097	0.9867	0.00475	0.48
49.308	0.96068	0.95517	0.95846	0.94939	0.94761	0.95273	0.00483	0.51
51.596	0.95202	0.9475	0.95041	0.94109	0.93940	0.94425	0.00491	0.52
60.749	0.92569	0.91782	0.92124	0.91141	0.91076	0.91586	0.00572	0.63
72.189	0.89571	0.88718	0.88960	0.87993	0.88707	0.88461	0.00645	0.73

Table 17 presents the fractional difference in actinide isotope concentration. The results are a continuation of the data presented in benchmark including the results from this validation. The isotope concentration fractional difference (5) is calculated in relation to the MIT CASMO-4 case following benchmark authors methodology. The fractional difference in relation to the CASMO-4 isotopic concentration is calculated using the following equation, where N refers to nuclide atomic density.

$$Frac.Diff. = \frac{(N - N_{CASMO4})}{N_{CASMO4}} \quad (5)$$

Table 17: Fractional difference in isotope concentration at 60.749 GWd/MTHM

	MIT CASMO4	**MIT MOCUP**	**INEEL MOCUP**	**MCNPX**	**MONTE BURNS**	**Serpent**	**TRITON - KENO-VI & ORIGEN S**	**TRITON - NEWT & ORIGEN S**
^{232}Th	1.5377E+22	-0.003	-0.003	-0.003	-0.003	-0.002	-0.003	-0.003
^{231}Pa	1.7044E+18	0.048	0.018	-0.035	-0.065	-0.034	-0.089	-0.103
^{233}U	2.7420E+20	0.040	0.044	0.034	0.053	0.046	0.046	0.056
^{235}U	1.7810E+20	-0.021	-0.033	-0.023	-0.049	-0.042	-0.028	-0.010
^{238}U	3.8842E+21	0.004	0.003	0.004	0.003	0.005	0.002	0.001
^{239}Pu	5.3709E+19	-0.071	-0.050	-0.057	-0.024	-0.047	-0.100	-0.069
^{241}Pu	1.9071E+19	-0.024	-0.041	-0.080	-0.039	-0.061	-0.015	0.018

The results above compare the results from atomic density for some nuclides at 60.749 GWd/MTHTM with the available for CASMO-4 benchmark. Negative results imply in underestimation of these densities and positive values overestimation of these densities in relation to CASMO-4 values.

Isotope concentrations calculated in this work agrees with benchmark calculated values except for ^{241}Pu in TRITON using NEWT & ORIGEN-S. The values displayed in Table 17 represent the percentual deviation with respect to MIT CASMO4 case, thus maximum positive and negative deviations from it are respectively 0.056% for TRITON using NEWT & ORIGEN-S and -0.1% for TRITON using KENO-VI & ORIGEN-S.

Although TRITON-NEWT & ORIGEN-S presents an inversion of behavior for ^{241}Pu and the greatest absolute values for the ^{233}U and ^{232}Th, it also presented the closer results to the reference for ^{235}U and ^{238}U.

3.4. CONCLUSIONS

3.4.1. Criticality

Considering all data sets and codes used, 21 cases were performed. From all results obtained, the cases selected were the ones with less than 500 pcm from the benchmark initial k_∞ mean value. Following this criterion, eight from 21 cases proceed to evaluation. None of the cases from 300 K or 600 K cross sections, advanced to the evaluation. From the eight selected cases, two were performed using 900 K cross sections, other two using 1200 K cross sections and four using the WT cross sections generated using NJOY system.

The analysis performed intend to validate the model and data generated at DEN - UFMG. The analysis contains quantities such as mean value, standard deviation and relative standard deviation that are used to measure the proximity of benchmark results.

Using the selected data to perform the evaluation, the mean k_∞ value passed from 1.23161 to 1.23269, the k_∞ standard deviation and k_∞ relative standard deviation went from 0.00602 to 0.00399 and 0.49% to 0.32%, respectively. Therefore, considering the fresh fuel situation, the results led to lowering in standard deviation and relative standard deviation, implying that the model and data used to perform the evaluation agrees with benchmark results.

Besides that, the results present information about the Doppler broadening preprocessor routine from Serpent code. Hence, for this specific simulation and using the benchmark adopted and the selected cross section data, the results (Table 10) showed that the use of the routine can be useful depending on the data or model to be simulated. Using the 300 K cross section, results exhibited an approximation of 4910 pcm in relation to the benchmark reference value. In the other hand, when using the 900 K cross sections an increase of 300 pcm were obtained in results.

3.4.2. Depletion

In depletion evaluation, only the WT cross sections were used due to time requirement to complete each simulation. Thus, the five different coupled codes are used to perform calculations. Hence, results from all codes are used in the evaluation. To accomplish the

analysis quantities such as mean values, standard deviations and relative standard deviations are calculated in each step of burnup for the benchmark. Therefore, the same calculations are performed using the results obtained from simulations using the five different coupled codes and also the benchmark. The calculated quantities are compared aiming to validate the data obtained.

The analyses are identical to the one performed in criticality section, quantities such as mean value, standard deviation and relative standard deviation are used to measure the proximity to benchmark results.

The initial k_∞ analysis presented close results to the ones from the previous section with 0.08% of difference or in terms of absolute difference 142 pcm. The k_∞ mean value, k_∞ standard deviation and k_∞ relative standard deviation results passed from 1.23161 to 1.23412, 0.00602 to 0.00451 and 0.49% to 0.37% respectively.

The same evaluation is performed in every burnup step, the decreasing standard deviation and the relative standard deviation is observed for the first three steps. Besides that, the final k_∞ presented more divergent results where the k_∞ mean value, k_∞ standard deviation and k_∞ relative standard deviation results passed from 0.87913 to 0.88461, 0.00450 to 0.00646 and 0.51% to 0.73% respectively.

The results are explained due to the different cross sections used by each depletion code. The differences in the cross sections lead to differences in fuel composition in each burnup step. The divergences in fuel composition in each code lead to divergences in k_∞.

Although the results from depletion ending were more divergent than the beginning, quantities remained reasonable, the increase in k_∞ standard deviation was 196 pcm and in k_∞ relative standard deviation was 0.22%, maintaining below 1%.

In addition, the fractional differences in isotope concentration are calculated and analyzed. It is observed that greatest divergences are presented by plutonium isotopes, followed by fissile uranium nuclides. Therefore, the modelled system agrees with benchmark behavior and results, in addition it contributes to the conclusion that the average energy per fission and nuclide plus capture differs from code to code.

4. EFFECTIVE DELAYED NEUTRON FRACTION AND DOPPLER COEFFICIENT ANALYSIS

4.1. INTRODUCTION

In the previous chapter, a validation study was presented considering a thorium-based fuel pin benchmark. Moreover, the validation used five different combinations of neutron transport and fuel depletion codes and used ENDF/B-VII.0.

The codes used to perform this chapter evaluation are the same from the previous chapter, MCNPX, MCNP5, Serpent, CSAS - KENO-VI (Continuous Energy and 238 energy groups), and CSAS – NEWT for steady state calculations, and MCNPX, Monteburns (MCNP5 linked to ORIGEN2.1), Serpent, TRITON (KENO-VI & ORIGEN-S) and TRITON (NEWT & ORIGEN-S) for fuel depletion. Besides that, cross sections used are all based on ENDF/B-VII.0 and generated at DEN using the NJOY99 code system.

In summary, the study was divided into steady state calculation and fuel depletion, it consisted of analyzing parameters such as k_∞ and isotopic composition over burnup and comparing them with benchmark results. Unfortunately, the adopted benchmark does not provide results beyond those already compared on last chapter.

Intending to use the vast amount of data obtained from steady state and fuel depletion calculations, an extension of the previous analysis is performed in this chapter. Therefore, using neutron transport capabilities of performing a simulation with only prompt neutrons the effective delayed neutron fraction - β_{eff} [37], which represents the fraction of delayed neutrons among total neutrons is calculated. In addition, using the NJOY99 code package cross section data are generated aiming to calculate fuel temperature coefficient - α_F [38].

NEWT is capable of presenting the β_{eff} results for each criticality or depletion simulation. This capability provides a comparison value for the other stochastic codes which do not directly provide the β_{eff}.

Effective delayed neutron fractions are calculated in steady state and in fuel depletion along with the ten steps division matching the benchmark previously adopted. All calculations are performed using the WT cross sections generated using NJOY99 code system at work temperatures of 900 K, 621 K, and 583 K corresponding to the fuel, cladding and coolant materials respectively.

Since to calculate fuel temperature coefficient are required different temperatures generated cross sections, two additional cross section data set are generated using the NJOY code system – 870 K and 600 K. Therefore, using the three datasets generated using NJOY99 system, two different fuel temperature coefficients are calculated, the first on considering the 870-900 K and 600-900 K variations.

4.2. CRITICALITY

4.2.1. Methodology

Using the verified model, an extension of the calculations of the benchmark is performed. The effective delayed neutron fraction - β_{eff} and the fuel temperature coefficient - α_F are calculated using the described geometry and the same parameters from the last chapter Figure 1 and Table 1 and Table 2.

To accomplish the calculation, the same neutron transport codes are used working with the WT cross sections. To provide the β_{eff} values each stochastic simulation is executed two times. The first execution considers only prompt neutrons - k_{prompt}, the second execution used both delayed and prompt neutrons - k_{total}.

To perform the evaluation each Monte Carlo simulation is performed with 2000 active cycles using 50000 histories. Therefore, the total number of neutrons in each criticality simulation is 100 million.

The KENO-VI from SCALE6.0 system “pnu parameter” does not work properly but that is already fixed in SCALE6.2 system version. NEWT does not need to perform the simulation

execution twice to provide the β_{eff} [37]. For all other codes, the β_{eff} results are calculated according to the following equation (6).

$$\beta_{eff} = 1 - \frac{k_{prompt}}{k_{total}} \tag{6}$$

To achieve the standard deviation from effective delayed neutron fractions, is performed the differentiation in relation to each of the quantities of the equation five, such procedure is a common validated method to achieve the uncertainty about a physical quantity.

$$\sigma_{\beta_{eff}} = \sqrt{\left(1 - \frac{1}{k_{total}}\right)^2 \left(\sigma_{k_{prompt}}\right)^2 + \left(1 - \frac{k_{prompt}}{{k_{total}}^2}\right)^2 \left(\sigma_{k_{total}}\right)^2} \tag{7}$$

Analogously to β_{eff}, the α_F values have to be calculated from the k_∞ results. To accomplish the fuel temperature coefficient evaluation three different temperatures are considered, 600, 870, and 900 K. Thus, two different α_F are calculated; the first value refers to 870 K to 900 K variation, and the second value refers to 600 K to 900 K variation.

For each different temperature, cross sections were generated using NJOY system and the same methodology described in chapter 2. The 30 K variation presented in first α_F value can be imperceptible to some of the codes, thus the results might end up within the code standard deviation. Therefore, the 300 K variation is performed to ensure that this condition does not occur.

To assure that the observed difference is caused only by the fuel, the cladding and moderator cross sections are always maintained the same [38]. Based on the k_∞ and absolute temperature difference, the α_F is calculated according to the following equation (8).

$$\alpha_F = \frac{\Delta\rho}{\Delta T} = \frac{k_{T1} - k_{T2}}{k_{T1} \times k_{T2}} \times \frac{1}{\Delta T} \tag{8}$$

4.2.2. Results

To initiate the β_{eff} analysis, Table 18 presents the calculated values for the effective delayed neutron fractions using each capable code of performing this calculation and the WT cross sections generated using the NJOY99 system. The KENO-VI from SCALE6.0 system have a malfunction in prompt neutrons parameter and is not able to provide the β_{eff}, however, this is already corrected in version SCALE6.2 system [39].

Table 18: β_{eff} results and standard deviations

	β_{eff}	**STANDARD DEVIATION**
MCNPX-WT	0.00667	0.00027
MCNP5-WT	0.00677	0.00027
Serpent-WT	0.00658	0.00027
NEWT-WT	0.00693	-

The criticality evaluation considers a fresh fuel situation, which the fuel matrix has not yet undergone modifications due to depletion. Thus, the only fissile nuclide present in fuel composition is ^{235}U. Therefore, is expected that the effective delayed neutron fraction assumes values near to the one provided by the literature for the ^{235}U effective delayed neutron fraction.

As a way of comparing the β_{eff} results, Table 19 presents the published nuclides characteristic β_{eff} values from the International Atomic Energy Agency – IAEA [40, 41]. Therefore, except for NEWT β_{eff}, results are within the IAEA published values for ^{235}U considering the standard deviation range. NEWT greater β_{eff} value is explained observing Table 17 from depletion results, from the codes used in this work NEWT is the one which considers less ^{235}U fission and more ^{238}U reactions.

Table 19: IAEA βeff published data [39, 40]

NUCLIDES	β_{eff}	STANDARD DEVIATION
^{232}Th	0.02032	0.00079
^{233}U	0.00268	0.00013
^{235}U	0.00665	0.00021
^{238}U	0.01650	0.00086
^{239}Pu	0.00225	0.00011
^{241}Pu	0.00543	0.00028

Two different fuel temperatures coefficients - α_F are calculated using different cross section data. The first α_F is calculated using the 870 K and 900 K cross sections. The second α_F is calculated using the 600 K and 900 K cross sections.

The 30 K difference in first α_F calculation lead stochastics codes to result in superimposed values due to standard deviation, thus, incongruous. Using 300 K difference this problem no longer persists and valid results are obtained.

It must be noticed that 300 K variations in fuel temperature are far from real in nuclear reactors behavior, and this temperature variation value was selected in an arbitrary way. A study that can be performed in future works consists in decreasing fuel temperature variation and calculating the α_F values for each case, until reaching inconsistent results due to low temperature variation, consecrating a minimum temperature difference between cross section data used.

Table 20 and 21 presents the results from the first and second calculated α_F respectively. The primary validation analysis consists of signal verification in α_F results. Table 18 results presented four inconsistent values resulted from superimposed results due to the standard deviation in some neutron transport code.

Table 20: Calculated α_F values for each code (900 K – 870 K)

900 K – 870 K	**FUEL TEMPERATURE COEFFICIENT (pcm/K)**
MCNPX	0.42
MCNP5	0.63
Serpent	0.09
NEWT	-3.31
KENO-VI_CE	0
KENO-VI_238	-3.37

The α_F results are shown in Table 21, since temperature difference in cross sections was ten times higher, 300 K instead of 30 K, none from stochastic codes resulted in superimposed values, thus, 900 K k_∞ results were lower than 600 K, resulting in negative α_F results.

Table 21: Calculated α_F values for each code (900K – 600K)

900 K – 600 K	**FUEL TEMPERATURE COEFFICIENT (pcm/K)**
MCNPX	-4.88
MCNP5	-5.14
Serpent	-6.35
NEWT	-1.26
KENO-VI_CE	-6.99
KENO-VI_238	-2.55

Although no work has been found using this same exact fuel composition, relevant studies using different enrichments for uranium dioxide [42] and a Th-MOX core [43] considering different core arrangement are used as reference. The results from these values range from -1.37 pcm to -7.92 pcm.

4.3. DEPLETION

4.3.1. Methodology

The composition dependence presented by the effective delayed neutron fraction makes it and interesting for analyzing. Thus, in depletion benchmark extension calculation, the first neutronic parameter to be analyzed is the β_{eff} during the fuel depletion.

To perform the β_{eff} the methodology presented in the last section is also applied. Executing each depletion simulation twice, using the k_{prompt} and k_{total} according to equation 6.

The evaluation performed in this section differs from the validation performed in the previous chapter. Since the benchmark model is already validated the data is presented and are analyzed in the results section.

In addition, some actinide and fission products isotope concentrations and masses are displayed along the burnup. Using this evaluation, it is possible to provide information about production and consumption rates for each code. These results are used to provide information about the treatment performed by each code according to each nuclide.

In each Monte Carlo simulation, 1000 active cycles and 5000 histories were used. The total operation time is 1893 days, divided into 20 steps matching the benchmark burnup steps described in chapter 2.

4.3.2. Results

To perform depletion extension evaluation, the β_{eff} is calculated in each burnup step. The same methodology used in previous sections is applied. Therefore, considering the composition dependence of β_{eff}, different results are obtained since the beginning through the end of the burnup.

Table 22, presents the Beginning of Life – BOL and End of Life – EOL β_{eff} values for each code simulated and Table 16 is used as a reference for comparing results. Due to malfunction, KENO-VI is not able to perform the β_{eff} calculations,

Results from effective delayed fraction at BOL and EOL reasonably differ due to the relative low number of particles to perform the evaluation. Fuel depletion evaluations were performed 5000 neutron histories using 1000 active cycles per burnup step, totalizing hundred million neutrons at last burnup step, however, steady state simulations used the same number of neutron histories in a single calculation.

Table 22: Initial and final β_{eff} results for the 72.189 GWd/MTHM burnup

MCNPX		**Monteburns**		**Serpent**		**TRITON - NEWT & ORIGEN-S**	
BOL	EOL	BOL	EOL	BOL	EOL	BOL	EOL
0.00790	0.00308	0.00581	0.00410	0.00667	0.00378	0.00693	0.00388

Figure 3 presents all β_{eff} calculated values for all simulated codes and for each burnup step, it also presents the confidence interval using the standard deviation as parameter. The decreasing value consists of changes in initial composition due to thorium transmutation into ^{233}U, fissions from ^{235}U, and plutonium build-up. Besides that, stochastic codes results oscillated around NEWT effective delayed neutron fraction, demonstrating confidence in the results.

Stochastics methods provide confidence within a standard deviation range, producing and confidence interval for these results. Although the calculations are performed to minimize these uncertainties, they still exist.

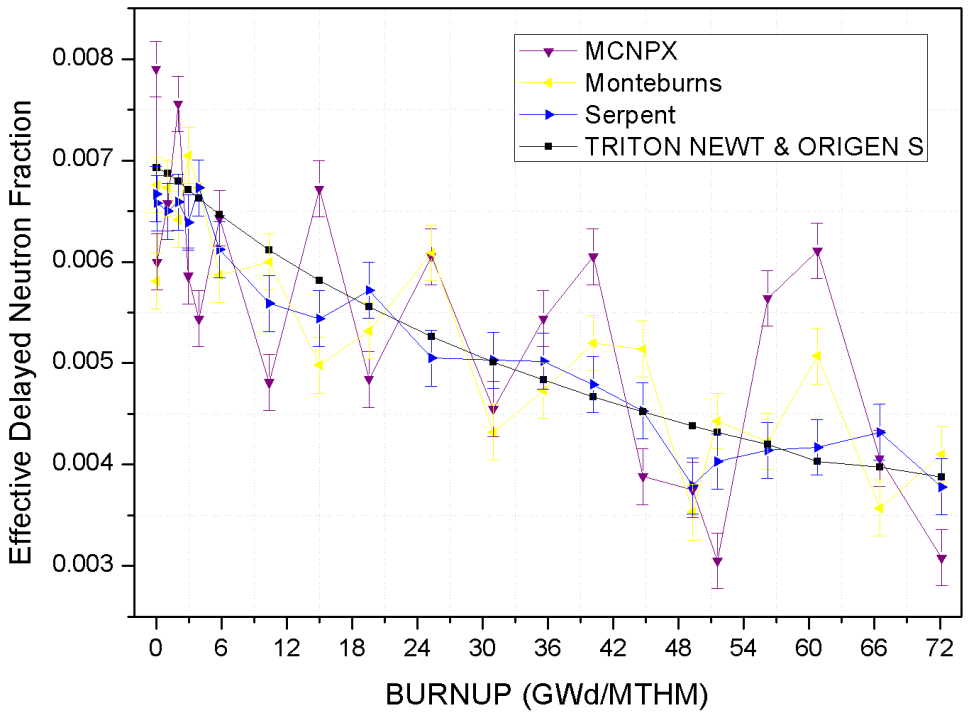

Figure 3: Effective delayed neutron fraction along burnup

In addition to β_{eff} evaluation, the next set of figures presents the masses of some nuclides throughout the burnup. The nuclides include the major actinides, thorium, and fission products nuclides that most influence the k_{∞}.

In previous chapter, the isotopic composition was compared to the adopted benchmark and it presented the percentage variations in relation to the MIT CASMO4 case. On the other hand, the evaluation presented in the following pages demonstrates mass changes in each step over burnup.

Figures 4 to 16 describe the masses variations throughout the 72.189 GWd/MTHM. The nuclides that are selected to participate in the mass evaluation along the burnup are the ones considered to, directly and indirectly, influence in multiplication factor value of a critical system. The nuclide set is composed by ^{232}Th, ^{231}Pa, ^{233}U, ^{235}U, ^{238}U, ^{239}Pu, ^{241}Pu, ^{135}I, ^{135}Xe, ^{149}Pm, ^{149}Sm, ^{155}Eu, and ^{157}Gd.

These are the nuclides that most influence in multiplication factor due to their high absorption cross sections. Part of these nuclides contributes to the raise of the multiplication factor due to be fissile, other part of these nuclides act poisoning the fuel pin, therefore, lowering the multiplication factor value, the last part of the nuclides results from fission and have half-lives lower than one day, decaying into poisoning nuclides.

These nuclides were selected according to three main considerations. The first one considers the fuel initial composition, ^{232}Th, ^{235}U, and ^{238}U are classified in this topic. The second one considers the nuclides transmuted with high absorption cross sections ^{231}Pa, ^{233}U, ^{239}Pu, ^{241}Pu, ^{135}Xe, ^{149}Sm, ^{155}Eu, and ^{157}Gd are classified in this topic. The last consideration is about nuclides with high absorption cross section although they decay in a short amount of time to nuclides from the second consideration, these nuclides are ^{135}I and ^{149}Pm.

Analyzing the following graphs, all codes presented the same pattern for each nuclide, however, the intensity of production/consumption depended on the code used and nuclide analyzed. Indeed, these differences are main responsible for more divergent results over burnup.

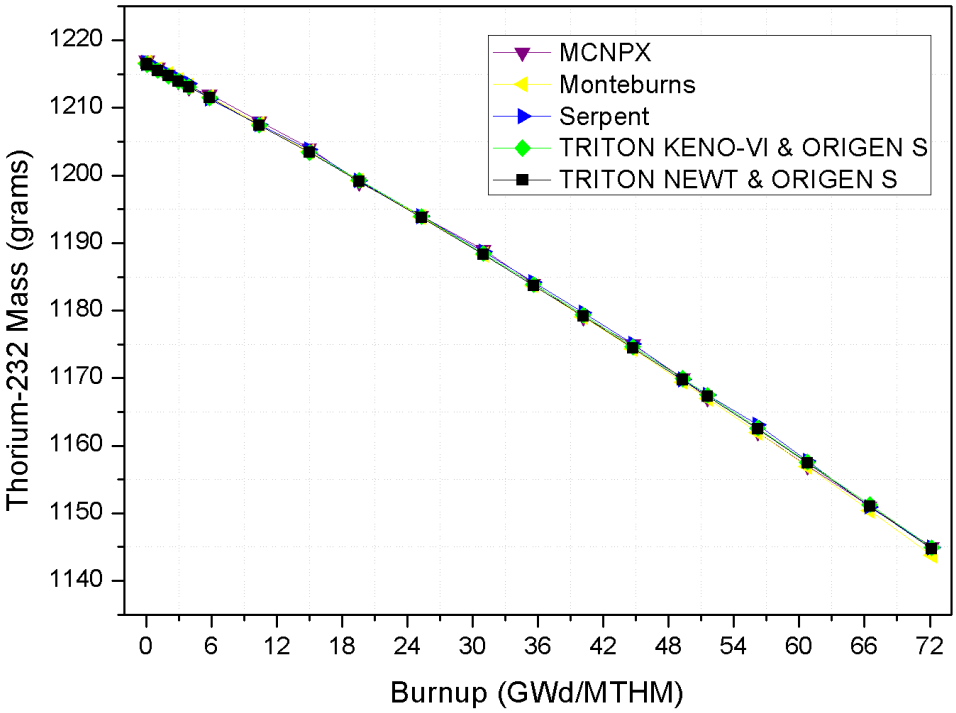

Figure 4: Thorium-232 mass modifications over burnup

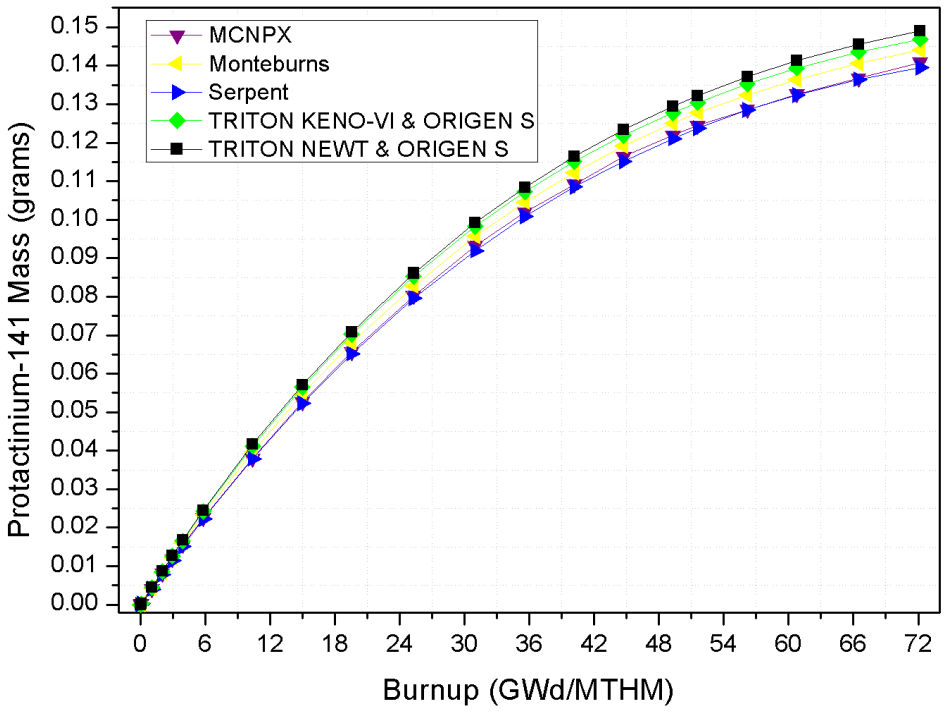

Figure 5: Protactinium-231 mass modifications over burnup

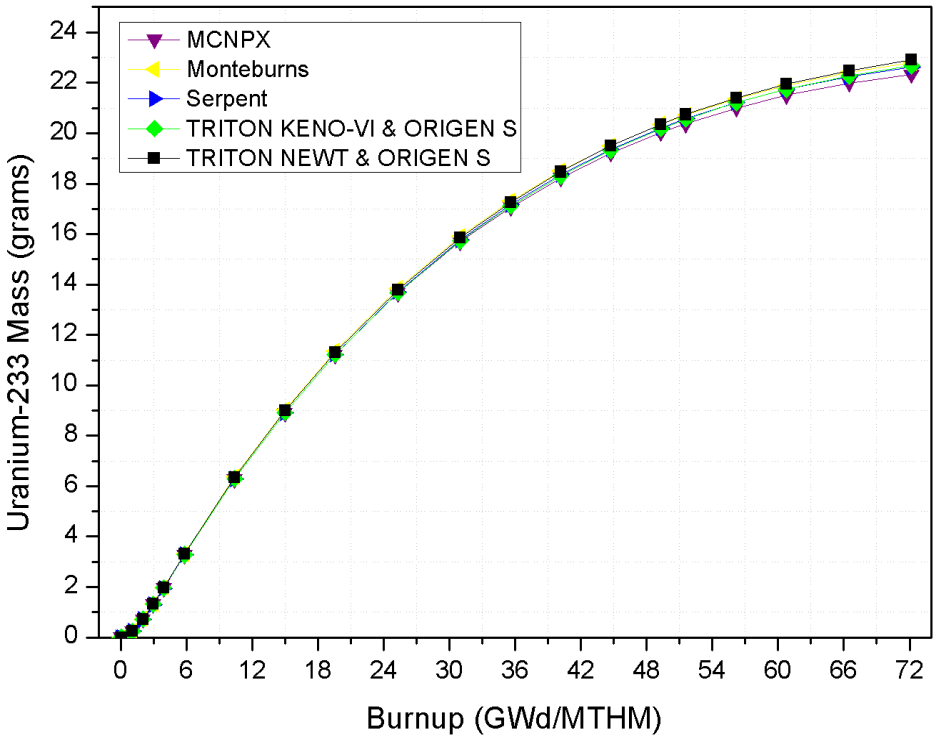

Figure 6: Uranium-233 mass modifications over burnup

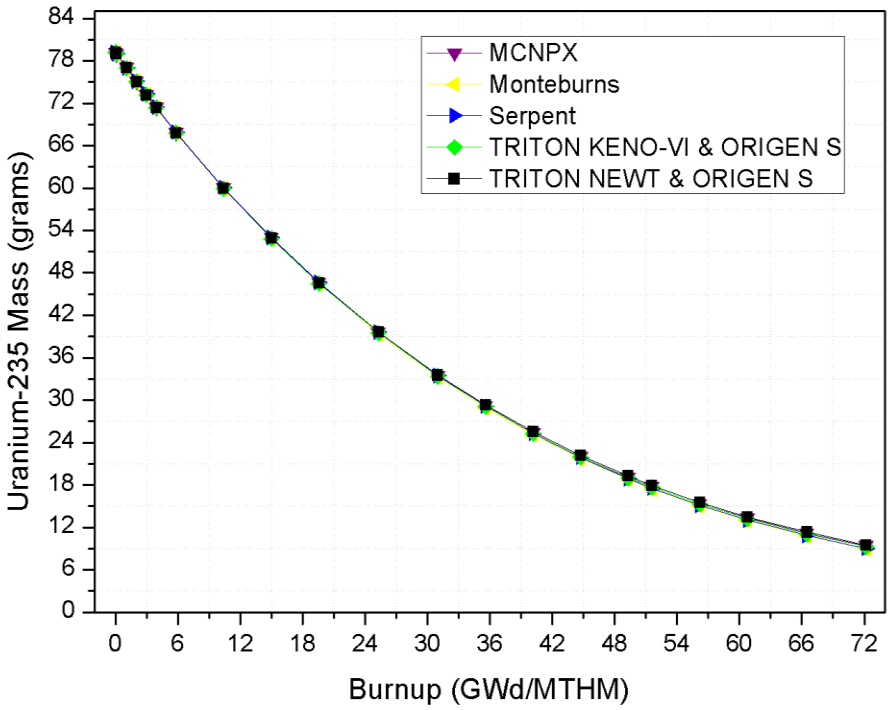

Figure 7: Uranium-235 mass modifications over burnup

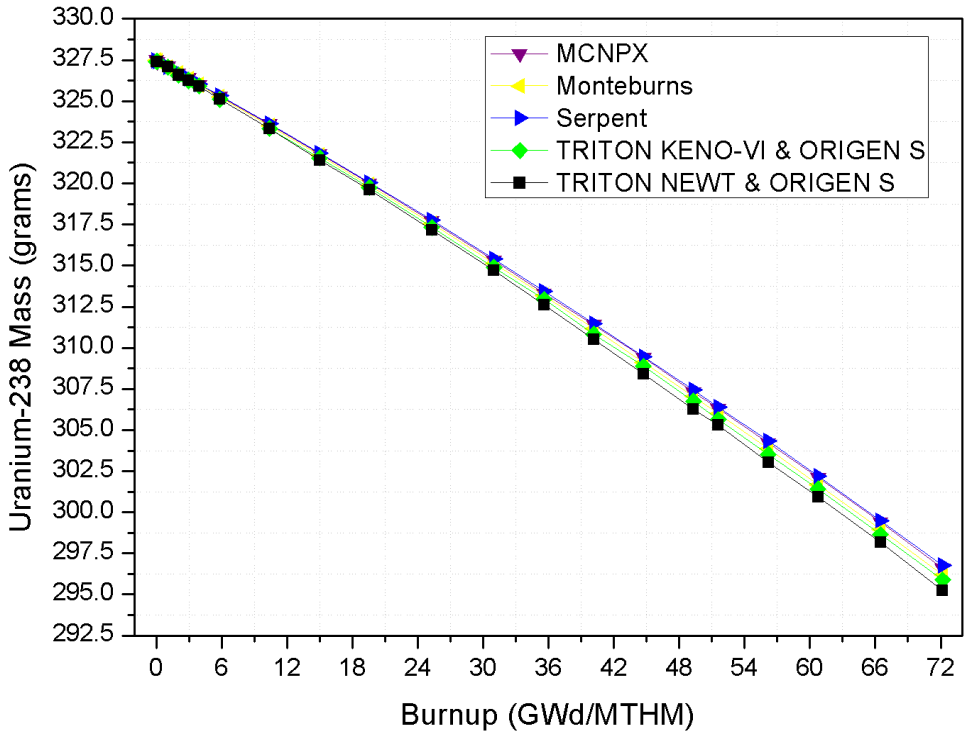

Figure 8: Uranium-238 mass modifications over burnup

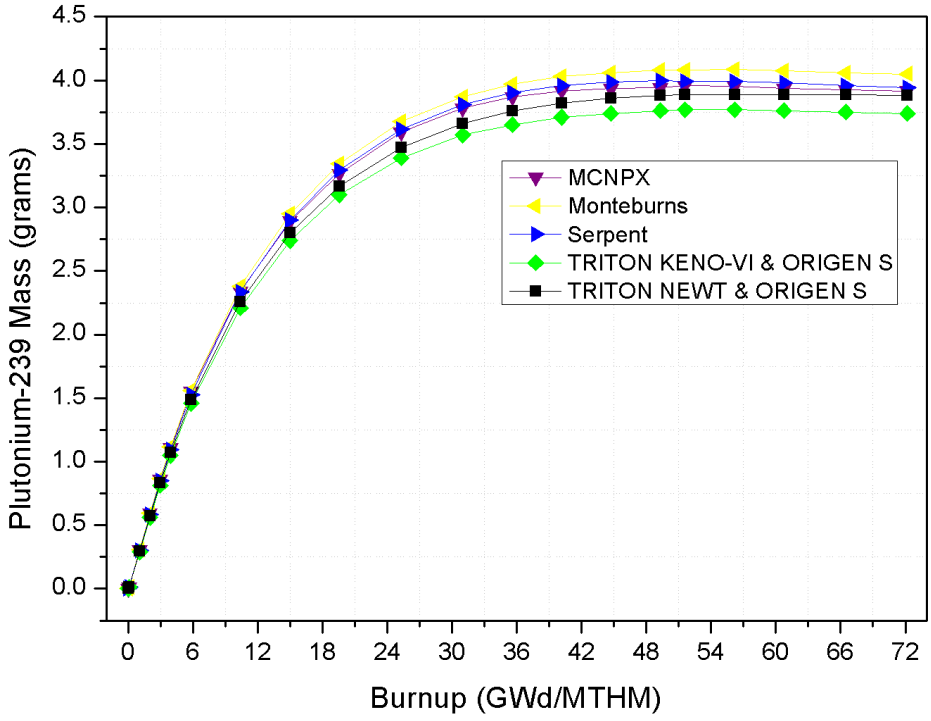

Figure 9: Plutonium-239 mass modifications over burnup

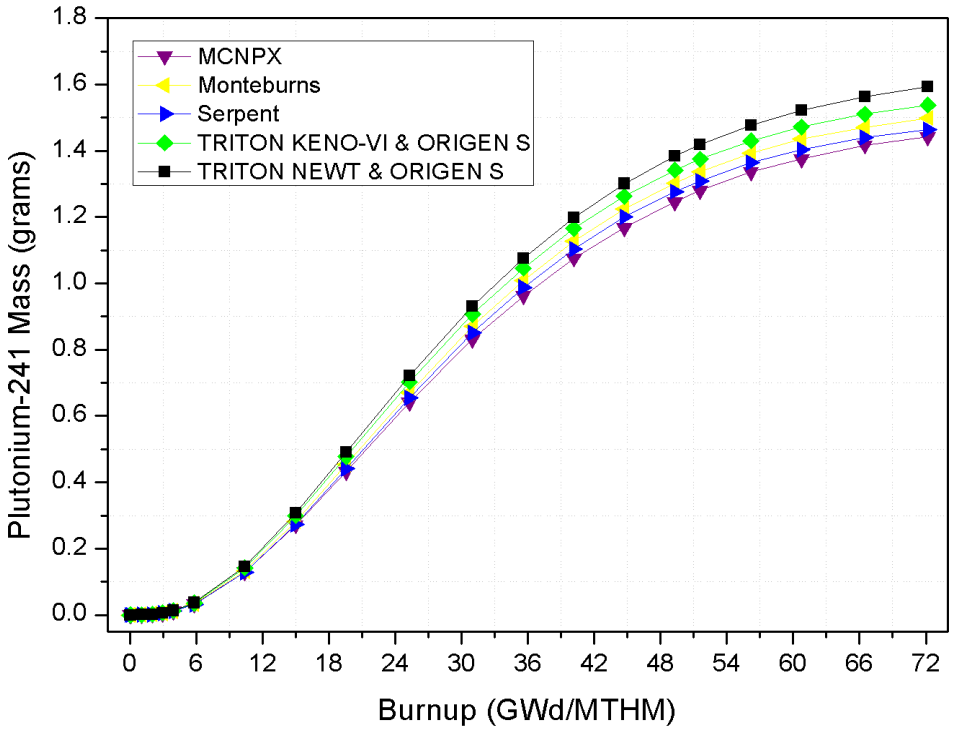

Figure 10: Plutonium-241 mass modifications over burnup

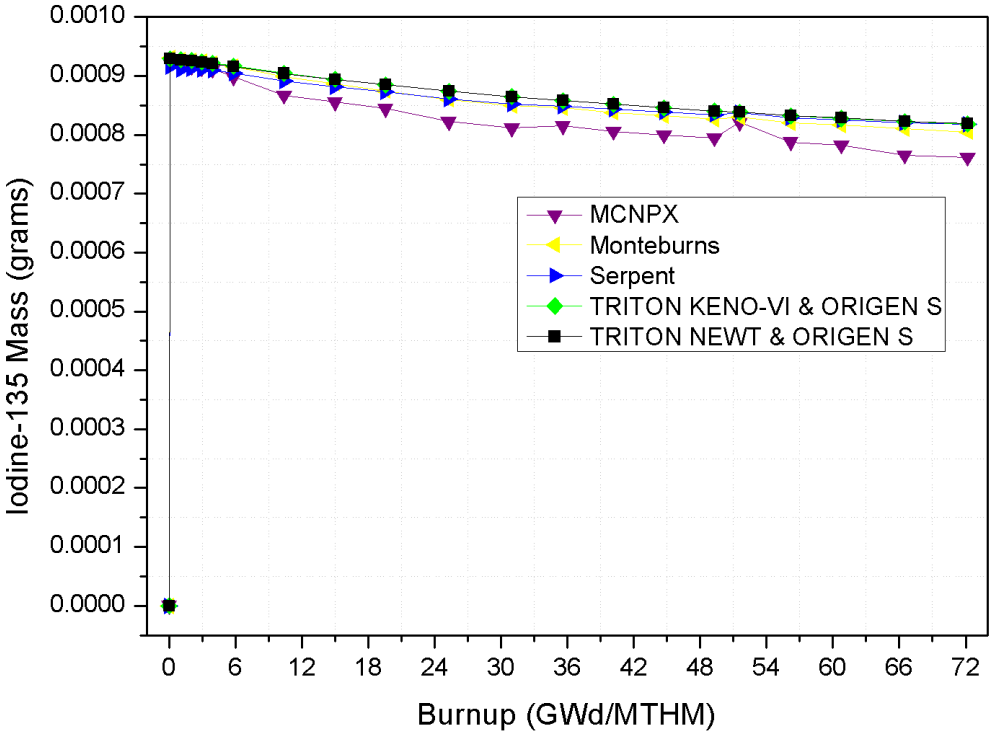

Figure 11: Iodine-135 mass modifications over burnup

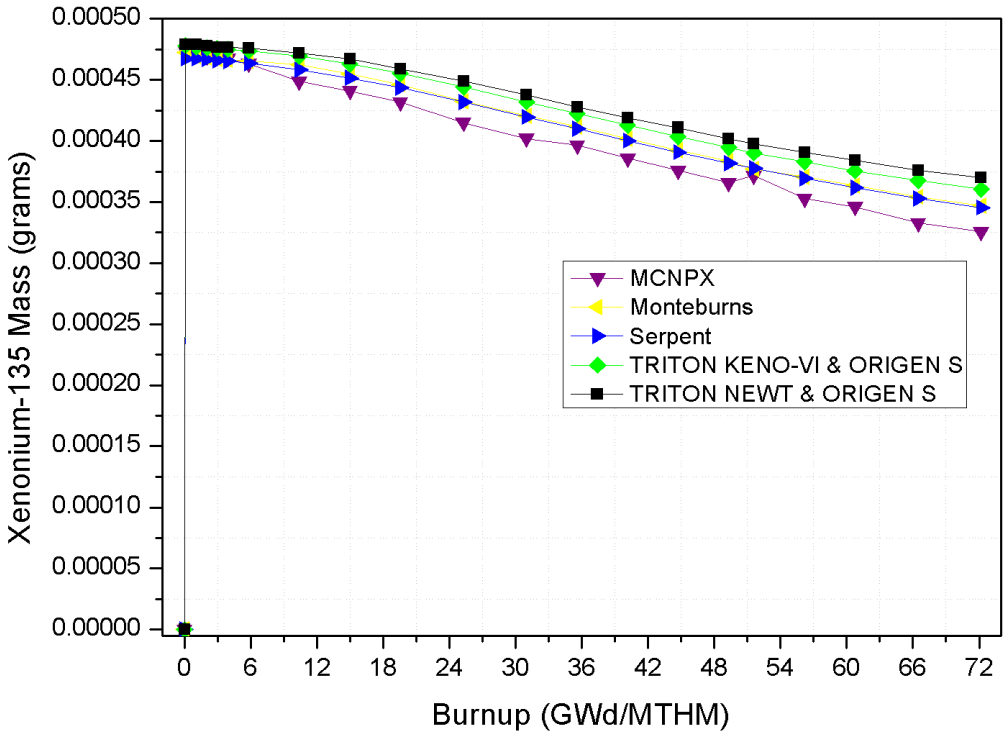

Figure 12: Xenonium-135 mass modifications over burnup

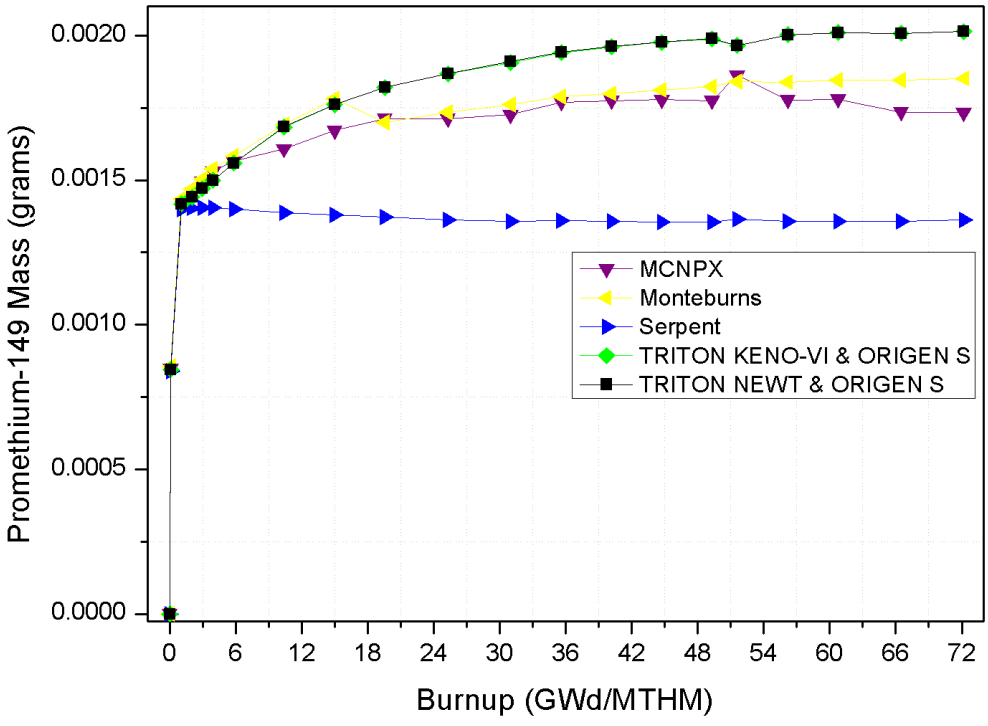

Figure 13: Promethium-149 mass modifications over burnup

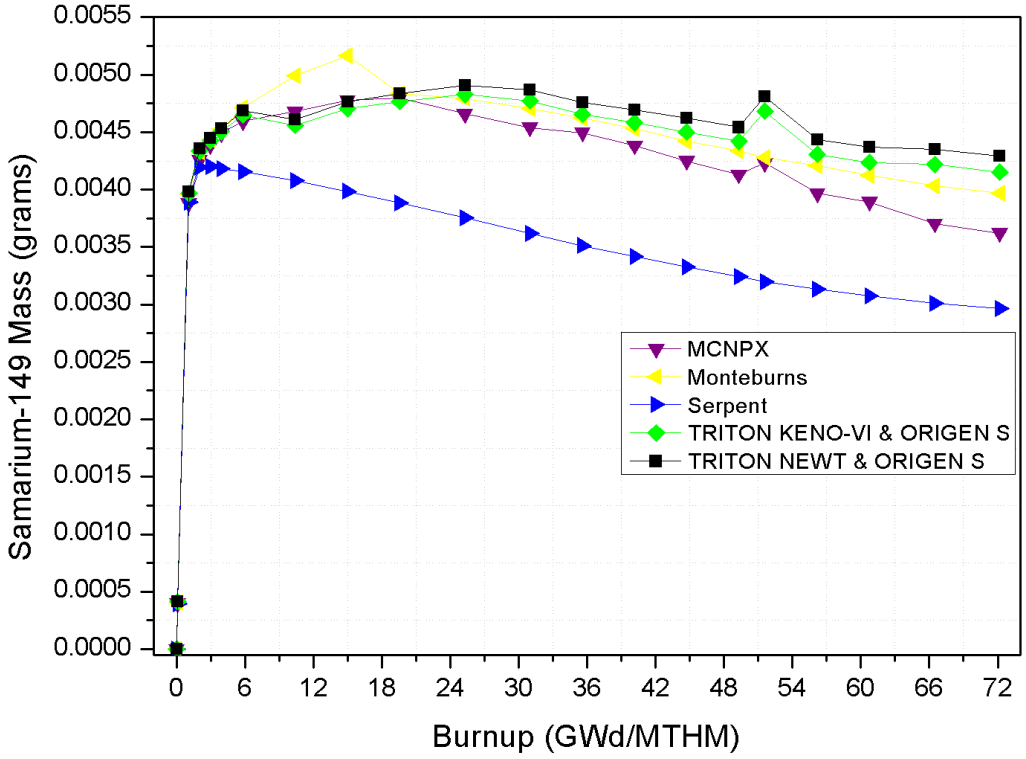

Figure 14: Samarium-149 mass modifications over burnup

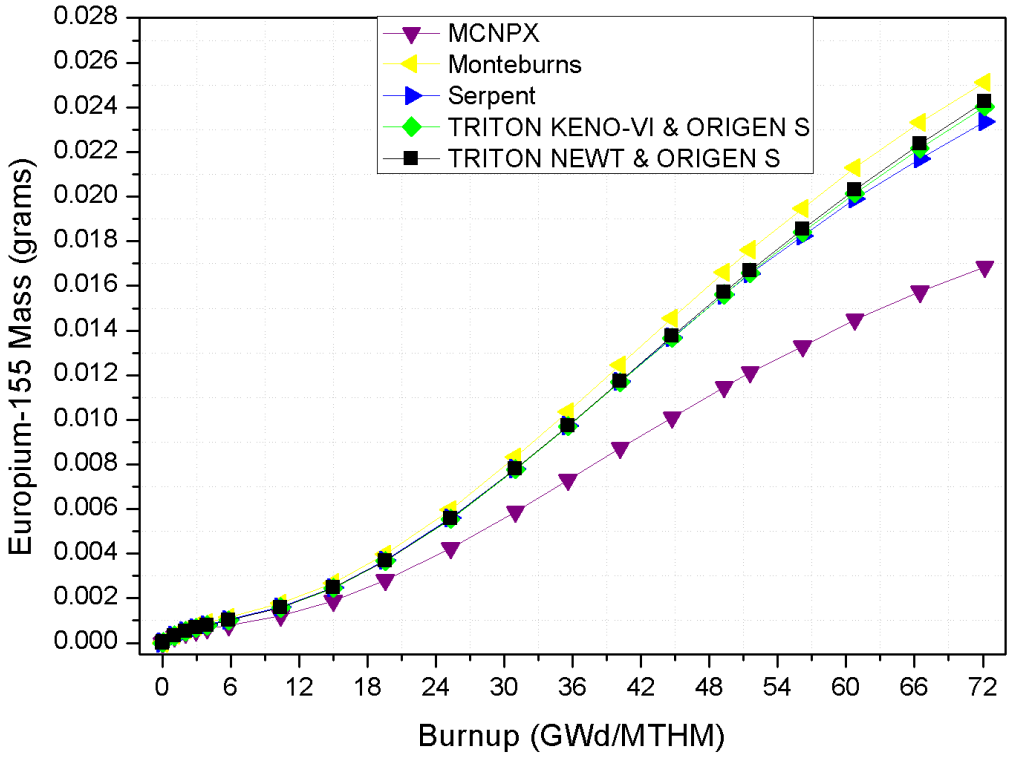

Figure 15: Europium-155 mass modifications over burnup

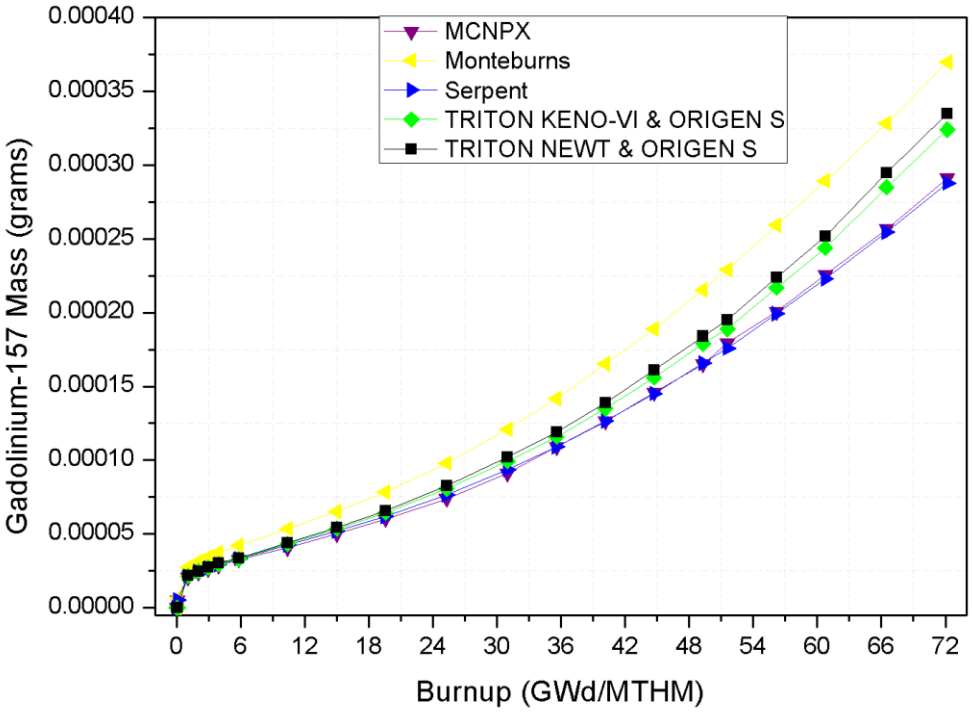

Figure 16: Gadolinium-157 mass modifications over burnup

In order to perform a second evaluation using the same data, the production/consumption graphs are presented for each of the selected nuclides. Using the data retrieved, the production and consumption rates for each nuclide.

Figures 17 to 29 presents the production and consumptions graphics for each nuclide selected in the previous evaluation. Downward graphics represent decreases in fuel initial mass, therefore upward graphics represent increases in fuel initial mass in grams.

Table 23 presents major and minor producer/consumers for each of nuclides analyzed. Production/consumption graphs provide overall results on burnup, different from the previous step by step analysis. The total production/consumption for each nuclide and code guarantees a trustworthy evaluation for designating major producers and consumers for each nuclide.

Table 23: Major and minor producer/consumer for each nuclide

NUCLIDE	MAJOR PRODUCER/ CONSUMERS	MINOR PRODUCER/ CONSUMERS
^{232}Th	Monteburns	TRITON – KENO-VI & ORIGEN-S
^{231}Pa	TRITON – NEWT & ORIGEN-S	Serpent
^{233}U	TRITON – NEWT & ORIGEN-S	MCNPX
^{235}U	Monteburns	TRITON – NEWT & ORIGEN-S
^{238}U	TRITON – NEWT & ORIGEN-S	Serpent
^{239}Pu	Monteburns	TRITON – KENO-VI & ORIGEN-S
^{241}Pu	TRITON – NEWT & ORIGEN-S	MCNPX
^{135}I	TRITON – NEWT & ORIGEN-S	MCNPX
^{135}Xe	TRITON – NEWT & ORIGEN-S	MCNPX
^{149}Pm	TRITON – NEWT & ORIGEN-S	Serpent
^{149}Sm	TRITON – NEWT & ORIGEN-S	Serpent
^{155}Eu	Monteburns	MCNPX
^{157}Gd	Monteburns	Serpent

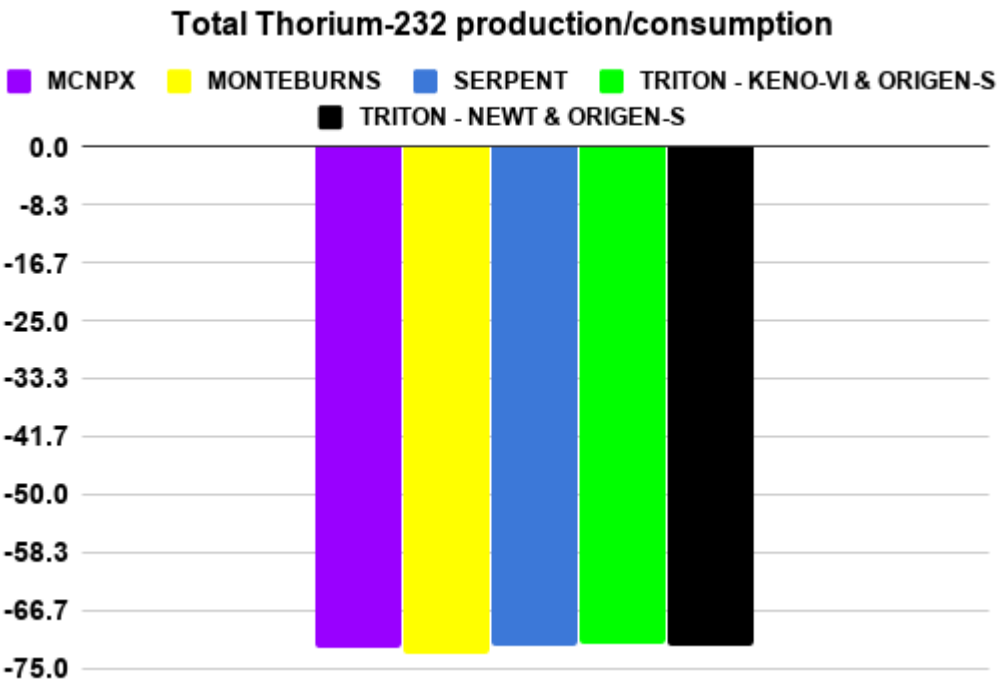

Figure 17: Total Thorium-232 mass (g) production/consumption for each code

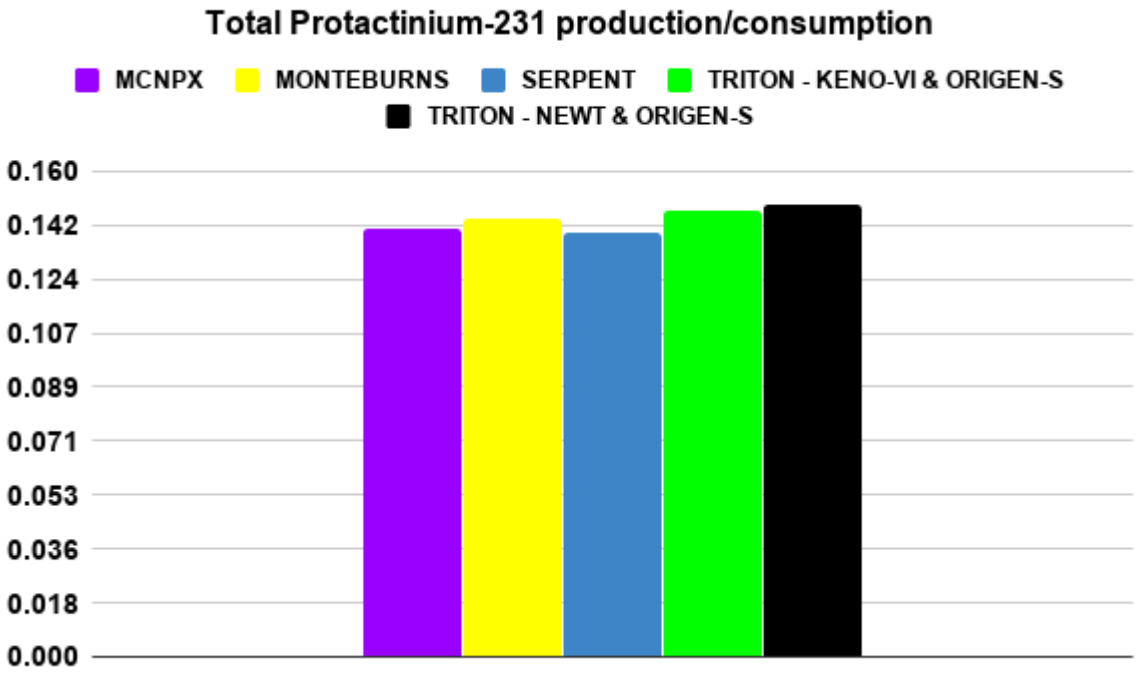

Figure 18: Total Protactinium-231 mass (g) production/consumption for each code

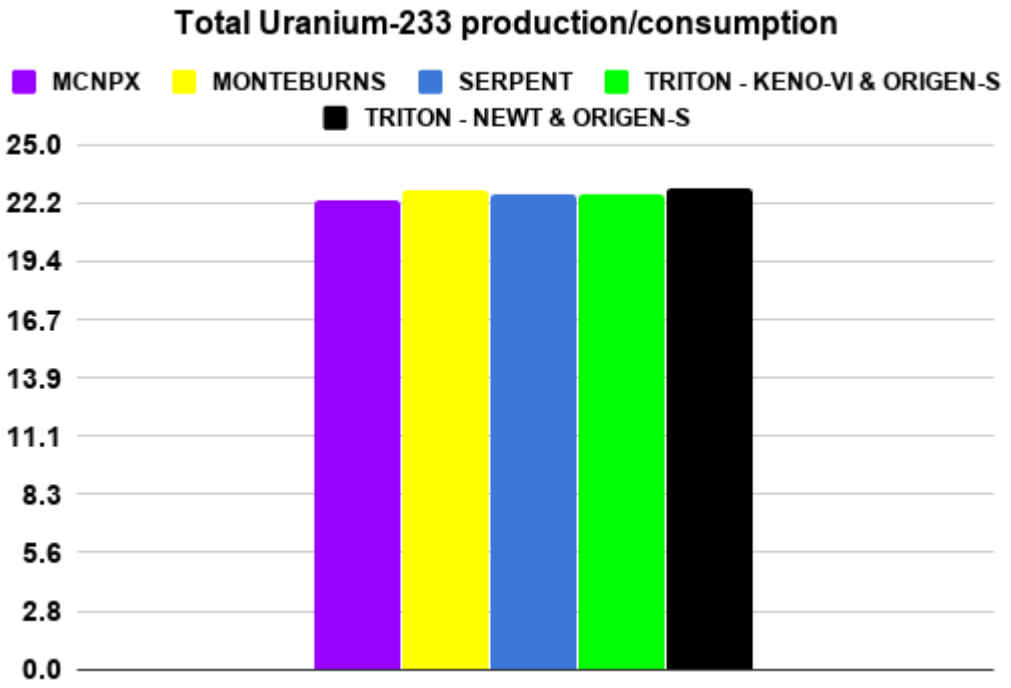

Figure 19: Total Uranium-233 mass (g) production/consumption for each code

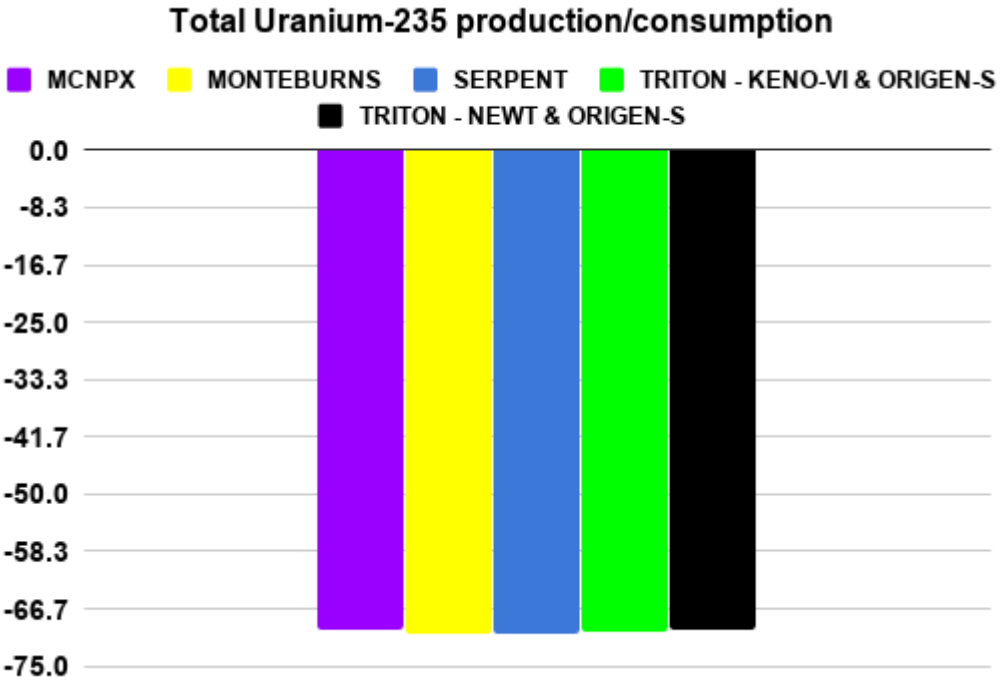

Figure 20: Total Uranium-235 mass (g) production/consumption for each code

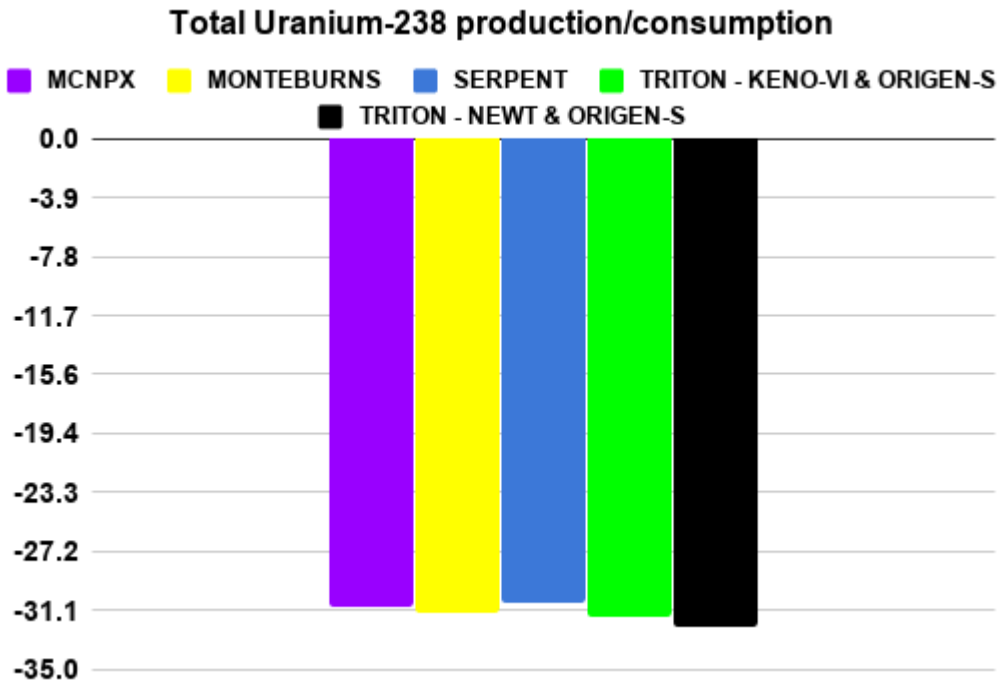

Figure 21: Total Uranium-238 mass (g) production/consumption for each code

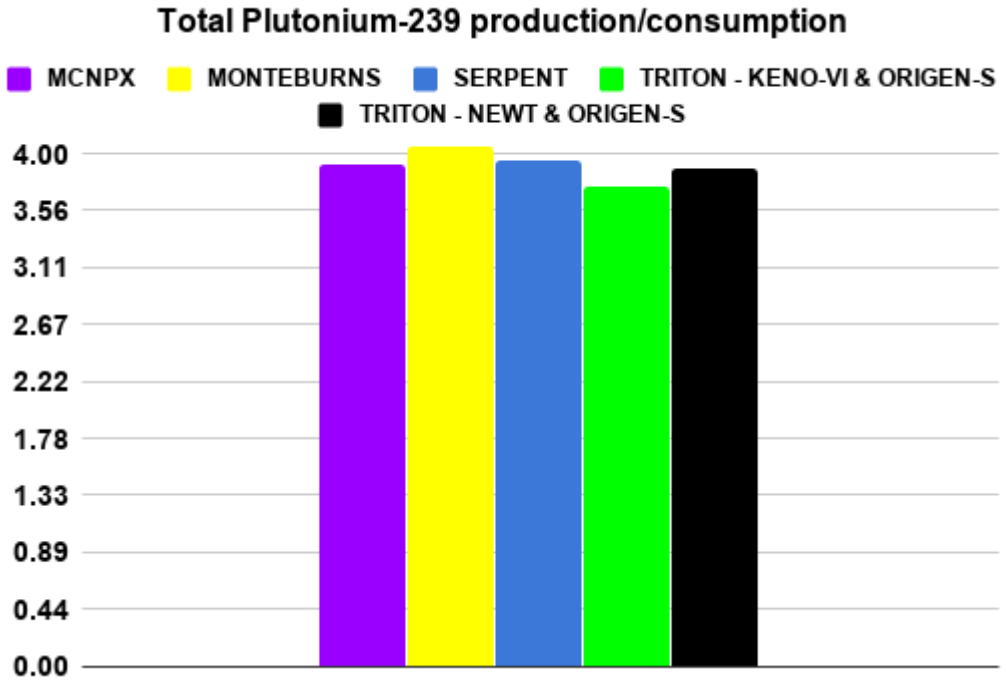

Figure 22: Total Plutonium-239 mass (g) production/consumption for each code

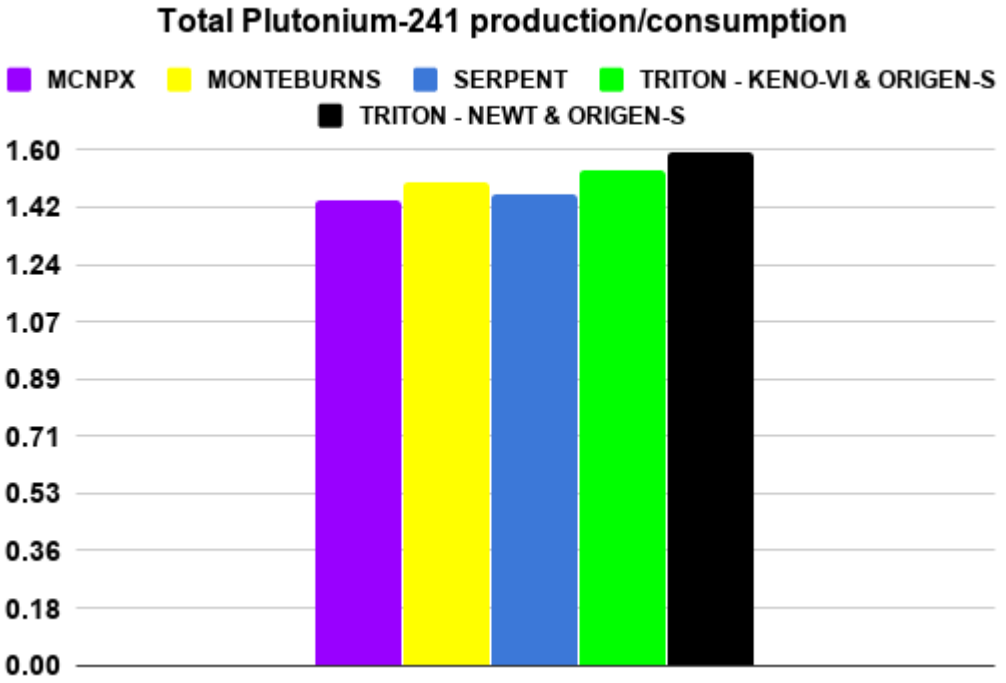

Figure 23: Total Plutonium-241 mass (g) production/consumption for each code

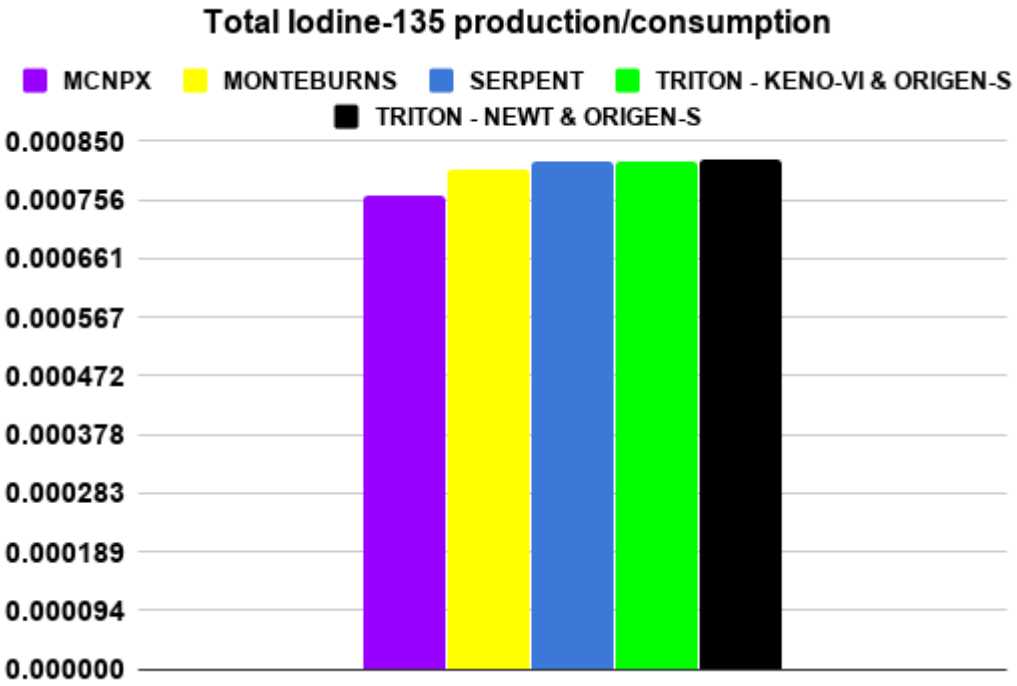

Figure 24: Total Iodine-135 mass (g) production/consumption for each code

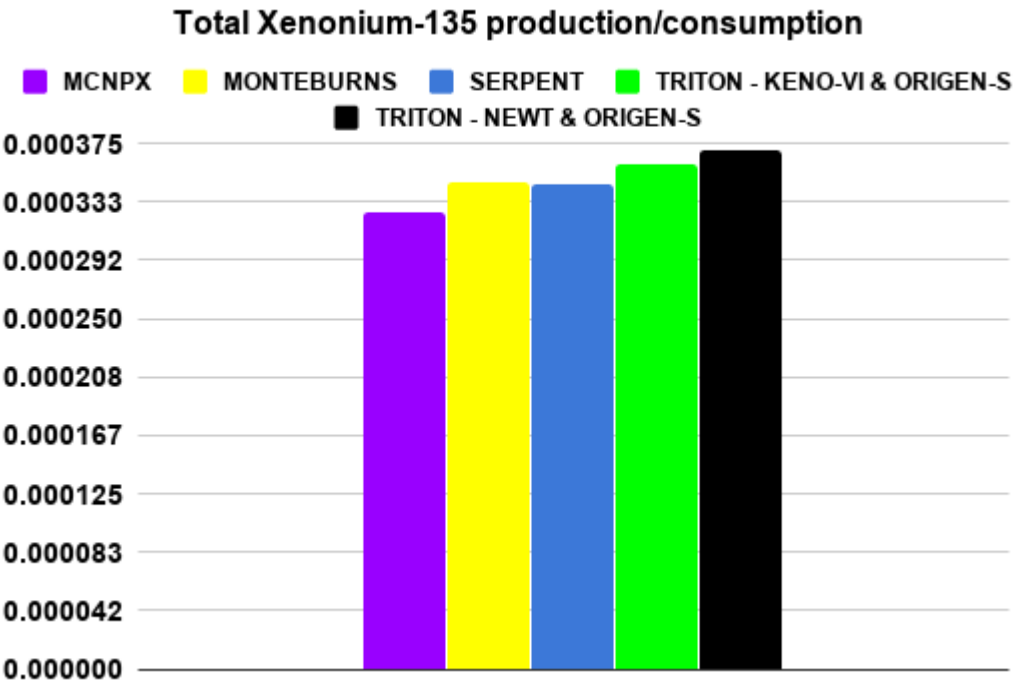

Figure 25: Total Xenonium-135 mass (g) production/consumption for each code

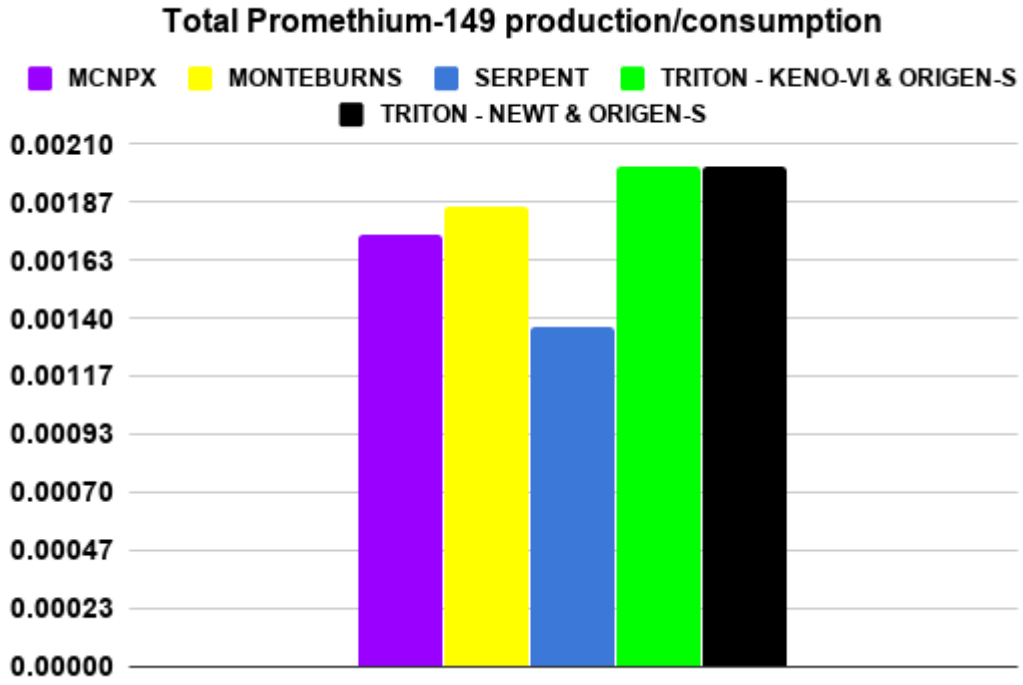

Figure 26: Total Promethium-149 mass (g) production/consumption for each code

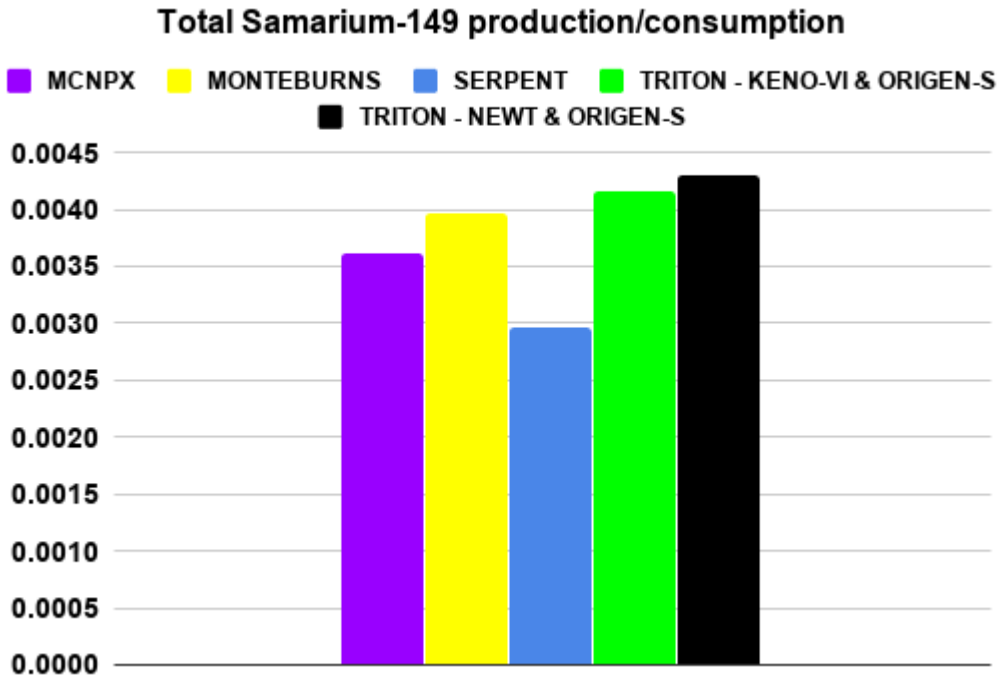

Figure 27: Total Samarium-149 mass (g) production/consumption for each code

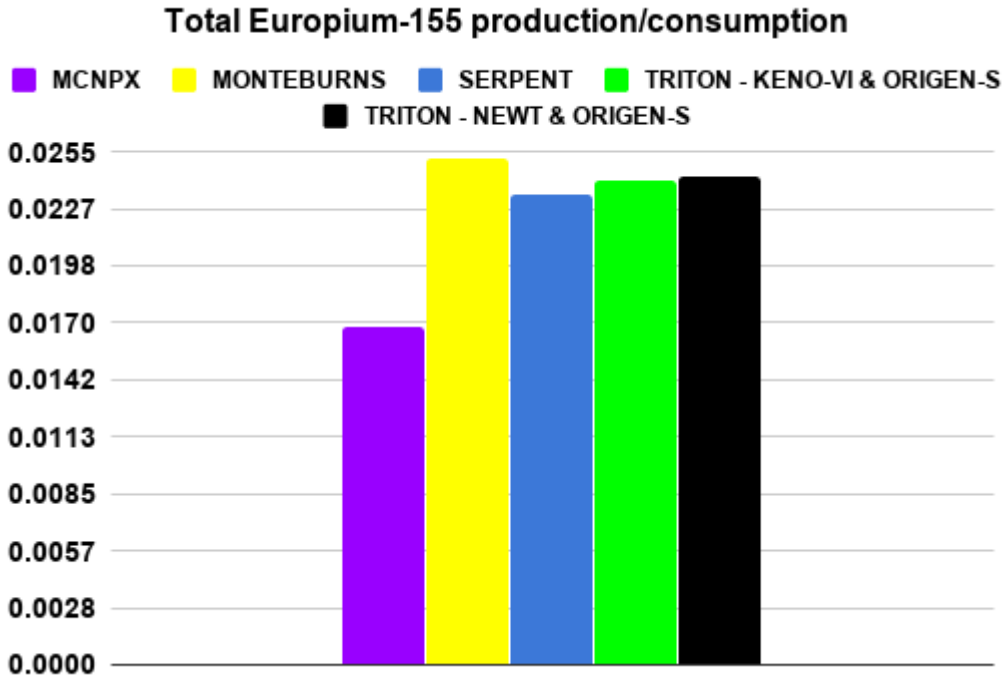

Figure 28: Total Europium-155 mass (g) production/consumption for each code

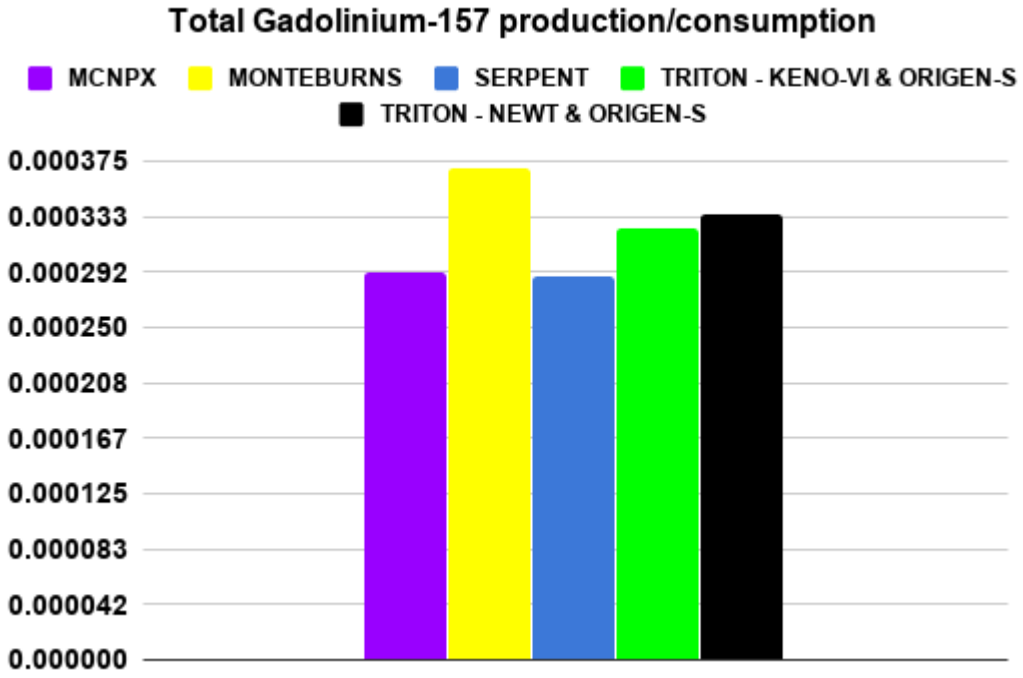

Figure 29: Total Gadolinium-157 mass (g) production/consumption for each code

4.4. CONCLUSION

4.4.1. Criticality

To perform the β_{eff} evaluation in this benchmark extension, the KENO-VI code could not be considered due to a malfunctioning in the prompt neutron parameter, already corrected in SCALE6.2 system.

Therefore, using the WT cross sections were performed in four different cases. In this evaluation, the fuel composition consisted of ^{232}Th, ^{234}U, ^{235}U, and ^{238}U. Thus, the only fissile nuclide is ^{235}U and it is expected β_{eff} results that correspond to the literature ones for this nuclide.

According to the adopted reference, the majority of results were in expected value range according to fuel composition and the standard deviation associated. The greater difference from results to the reference value was 28 pcm while the minor was 2 pcm. The mean β_{eff} was 0.00674 that range 9 pcm from reference value for ^{235}U.

The α_F evaluation was performed in two calculations. The first one consists in using 900 K and 870 K cross sections data, and the second calculation uses the 900 K and 600 K cross sections data.

The two evaluations were performed due to the low temperature absolute difference in the first evaluation. The low temperature absolute difference might lead to stochastics code to obtain superimposed results due to the standard deviation.

Indeed, the first evaluation resulted in 3 positives α_F, a null α_F, and a single negative α_F. On the other hand, all results from second α_F calculation resulted in negative values.

Although no references have been found using the same exact fuel composition, studies using uranium dioxide and a Th-MOX core considering different core arrangement are taken as reference, the results range from -1.37 pcm to -7.92 pcm.

Taking these values as a reference for comparison, only the SCALE6.0 system codes (KENO-VI and NEWT) working with collapsed 238 energy groups were in the reference range. The mean value from α_F results considering all cases was -4.52 pcm/K.

4.4.2. Depletion

The β_{eff} evaluation results from depletion analysis were more divergent than the ones from criticality analysis due to the relative lower number of particles. In addition, the dependence in the composition is observed when β_{eff} results decrease during the burnup.

The fuel initial composition consists of ^{232}Th,^{234}U, ^{235}U, and ^{238}U. As the fuel is depleted, new fissile nuclides appear from absorptions and decay. At the end of depletion, there are ^{233}U, ^{239}Pu, and ^{241}Pu besides the other actinides. Thus, responding to the changes in fuel composition, the effective delayed neutron fraction also changes it values.

It is presented then β_{eff} results ranging from higher values, corresponding to the ^{235}U β_{eff} values, and tending to lower values, corresponding the ^{233}U and ^{239}Pu β_{eff} reference values. The initial and final β_{eff} mean values were 0.00683 and 0.00371 respectively. In addition, it is observed that all stochastics β_{eff} results fall inside computational uncertainty, thus validating results.

Besides that, the analysis of isotopes masses resulted in relevant conclusions to the simulations in general. Using these data, it is noticed that TRITON - KENO-VI & ORIGEN-S and TRITON - NEWT & ORIGEN-S results are very similar in virtue of using the same cross sections for both neutron transport and fuel depletion.

Therefore, the major differences observed in all simulations, in this chapter and also in the previous chapter, come from differences in depletion code cross sections, since the neutron transport are all based on ENDF/B-VII.0 and uses the same temperatures.

In addition, the overall production and conversion bar graphics present the total amount of mass produced or consumed over the 72.189 GWd/MTHM burnup. Analyzing these data, the more substantial absolute deviation is presented by ^{238}U, and it refers to a 1.46 grams deviation. However, in percentage terms, other deviations are much higher than the ^{238}U variations.

Therefore, observing the total productions and conversions can be explained the k_∞ results from the previous chapter. The MCNPX code presented the highest k_∞ at depletion end in virtue of being one of the minor producers of fission products poison such as ^{135}Xe and ^{149}Sm and at the same time the case which more fissile material prevailed.

A similar analysis is performed for TRITON - KENO-VI & ORIGEN-S that presented the lowest k_∞ at burnups end and is observed that they are one of the major producers of fission products poison and the ones which less fissile material remained.

5. GENERAL CONCLUSIONS AND FUTURE PERSPECTIVES

The present chapter of this work is a compilation of all the achievements and conclusions that were obtained during their accomplishing, bringing explicitly the relevance of the academic study provided.

Being one of the first researches using the Serpent code by the DEN in UFMG, it showed necessary to try it and demonstrate the efficiency of this code that started with the specific purpose of reactor physics.

Among the Serpent functions, the Doppler broadening preprocessor routine for adjusting the processing temperatures of the cross-section data is chosen to be tested. Results from Table 9 showed that the use of the routine can be useful depending on the data or model to be simulated. Besides that, it is a tool that can save time for users. However, if precision is needed, dedicated cross section generation codes such as NJOY code system are appropriated.

The determinant factor for the results obtained, both in chapters three and four, are the cross sections data that are selected to perform the criticality calculation and the fuel depletion.

The β_{eff} values achieved showed themselves to correspond with the IAEA published data when a suitable number of particles are considered. The BOL mean value differed 2.6% from the IAEA published data for the ^{235}U.

Considering the fuel depletion, the β_{eff} results started around 0.00683 and ended near to 0.00371 according to fuel composition. Indeed, these values are expected since initial fuel composition is only based on ^{235}U and in final fuel composition ^{233}U and ^{239}Pu are majority responsible for fuels fissions.

The most significant differences all over the study are observed in the isotopic composition evaluation because of the different cross section data from different ENDL used by each fuel depletion code. Analyzing the masses along with burnup results it was possible to affirm the cross-sections severe dependence during fuel depletion. Apart from differences caused by cross sections, each fuel depletion code employed provided little divergent results, however, when

using the same fuel depletion code (KENO-VI & ORIGEN-S and NEWT & ORIGEN-S) the results were much more similar.

Thus, the main conclusion made as a result of this study is that the predominant influencer in all simulations is the ENDFs used for performing them, and erroneously choosing or processing the data that are used can lead to entirely unintended results. This observed difference in isotopic compositions also supports the evidence that overall average energy per fission plus capture differs slightly between the codes.

Therefore, the present work serves as support material for future research in the area, and also it ends up opening a great range of parameter prospection in nuclear reactors simulations using several nuclear codes and cross sections study.

Studies incorporating different geometries and fuels including reprocessed fuel containing a vast array of nuclides in their initial composition are examples of new opportunities in the area. According to the topics discussed in this study, the higher the number of nuclides in the fuel the more different results are obtained, especially if there are less common nuclides in the composition.

Besides that, this study there is still the possibility to extend this work into fuel assemblies and even cores, it also opens space to other concentration areas such as the thermohydraulic of the ThO_2-UO_2 fuel and expands it to the fuel assembly and posteriorly the nuclear core.

REFERENCES

1. Zhao, X., Pilat, E.E., Weaver, K.D., Hejzlar, P., 2000. A PWR thorium cell burnup benchmark. In: ANS Reactor Physics, Mathematics and Computation and Nuclear Criticality Safety, PHYSOR 2000 Topical Meeting, 7–12 May, Pittsburgh, USA.

2. L. S. Waters, Editor. "*MCNPX User's Manual Version 2.3.0*" LA-UR-02-2607, April 2002.

3. J. S. Hendricks, et al. "*MCNPX 2.6.0 EXTENSIONS*" LA-UR-08-2216, April 11, 2008.

4. H. R. Trellue, D. I. Poston. "*User's Manual, Version 2.0 for Monteburns, Version 5B*" LA-UR-99-4999, September 1999.

5. R. Brewer, Editor. "*Criticality Calculations with MCNP5: A Primer*" LA-UR-09-0380, January 2009.

6. Oak Ridge National Laboratory, Oak Ridge, Tennessee; Tennessee Valley Authority, Chattanooga, Tennessee; Office of Nuclear Waste Isolation, Battelle Project Management Division, Columbus, Ohio; Sargent and Lundy Engineers, Chicago, Illinois; Century Research Center Corporation, Tokyo, Japan; NUKEN GmbH, Alzenau, Federal Republic of Germany; Battelle Columbus, Columbus, Ohio, "*ORIGEN2.1 isotope generation and depletion code – matrix exponential method.*" August 1991.

7. J. Leppänen, et al. "*The Serpent Monte Carlo code: status, development and application in 2013.*" Annals of Nuclear Energy, Volume 82, 2015, Pages 142-150, ISSN 0306-4549.

8. Oak Ridge Laboratory "*SCALE: A Modular Code System for Performing Standardized Computer Analyses for Licensing Evaluations*" ORNL/TM-2005/39, Version 6, Vols. I–III, January 2009. Available from Radiation Safety Information Computational Center at Oak Ridge National Laboratory as CCC-750.

9. Goluoglu, S., Hollenbach, D. F., Petrie, L. M., "*CSAS6: Control Module for enhanced criticality safety analysis with Keno-VI*", Nuclear Science and Technology Division, Oak Ridge, Tennesse, USA, 2009.

10. M. D. DeHart "*TRITON: A two-dimensional transport and depletion module for characterization of spent nuclear fuel*" ORNL/TM-2005/39, Version 6, Volume I, Section T1, January 2009.

11. D. F. Hollenbach, et al. "*KENO-VI: A general quadratic version of the KENO program*" ORNL/TM-2005/39, Version 6, Volume II, Section F17, January 2009.

12. M. D. DeHart "*NEWT: A new transport algorithm for two-dimensional discrete ordinates analysis in non-orthogonal geometries*" ORNL/TM-2005/39, Version 6, Volume II, Section F21, January 2009.

13. I. C. Gauld, et al. "*ORIGEN-S: SCALE System module to calculate fuel depletion, actinide transmutation, fission product buildup and decay, and associated radiation source terms*" ORNL/TM-2005/39, Version 6, Volume II, Section F7, January 2009.

14. R. E. MacFarlane, et al. "*The NJOY Nuclear Data Processing System, Version 2012*" LA-UR-12-27079, December 20, 2012.

15. C.E. Velasquez, et al. "*Cross section evaluation for a LWR pin lattices with thorium applications*" Annals of Nuclear Energy, Volume 107, 2017, Pages 89-102, ISSN 0306-4549.

16. B. A. Fabiana, "*Proposta de Combustível Reprocessado Diluído em Tório para Sistemas PWR – Inserções homogênea e micro heterogênea*" Tese (Doutorado em Ciências e Técnicas Nucleares) – Escola de Engenharia, Departamento de Engenharia Nuclear, Pós-Graduação em Ciências e Técnicas Nucleares, Universidade Federal de Minas Gerais.

17. Monteiro F.B.A. et al. (2016) Thorium and Transuranic (TRU) Advanced Fuel Cycle: An Option for Brazilian Nuclear Plants. In: Revol JP., Bourquin M., Kadi Y., Lillestol E., de Mestral JC., Samec K. (eds) Thorium Energy for the World. Springer, Cham

18. M. B. Chadwick, et al. "*ENDF/B-VII.0: Next Generation Evaluated Nuclear Data Library for Nuclear Science and Technology*" UCRL-JRNL-225066, October 6, 2006.

19. Alejandro Núñez-Carrera, Juan Luis François, Gilberto Espinosa-Paredes, "*Comparison between HELIOS critical-depletion calculations and a PWR thorium cell burnup benchmark*", Annals of Nuclear Energy, Volume 31, Issue 7, 2004, Pages 713-722, ISSN 0306-4549

20. Anas Gul, K.S. Chaudri, R. Khan, M. Azeem. "*Development and verification of LOOP: A Linkage of ORIGEN2.2 and OpenMC*" Annals of Nuclear Energy, Volume 99, 2017, Pages 321-327, ISSN 0306-4549

21. F. Martins, C. E. Velasquez, V.F. Castro, C. Pereira, C. A. Mello da Silva. "*SENSIBILITY ANALYSIS OF FUEL DEPLETION USING DIFFERENT NUCLEAR FUEL DEPLETION CODES*" - International Nuclear Atlantic Conference 2017 – INAC 2017.

22. Felipe Martins, Carlos E. Velasquez, Cláubia Pereira. "*EVALUATION OF TEMPERATURE DEPENDENCE ON CROSS SECTIONS FOR A (Th-U)O_2 FUEL PIN*" – IV Semana de Engenharia Nuclear e Ciências da Radiação – IV SENCIR.

23. Felipe M. G. Pereira, Renato V. A. Marques, Carlos E. Velasquez, Márcia S. Santos, Claubia Pereira. "*A THORIUM CELL BENCHMARK COMPARISON USING DIFFERENT NUCLEAR CODES*" – International Conference on Emerging Nuclear Energy Systems – ICENES 2019

24. Michael L. F., John S. H., Gregg W. M., "*Monte Carlo Burnup Interactive Tutorial*" LA-UR-09-02051 Los Alamos National Laboratory, American Nuclear Society, 2009 Student Meeting, April 2009.

25. F. X. Gallmeier, et al. "*The CINDER '90 transmutation code package for use in accelerator application in combination with MCNPX*" ICANS XIX, 19th Meeting on Collaboration of Advanced Neutron Sources, March 8 – 12, 2010.

26. Nuclear Energy Agency, "JEFF Nuclear Data Library", http://www.oecd-nea.org/dbdata/jeff/ Web. June 15, 2019

27. Japan Atomic Energy Agency, "Nuclear Data Center" https://wwwndc.jaea.go.jp/jendl/jendl.html Web. June 15, 2019

28. I. C. Gauld, et al. "*ORIGEN-S data libraries*" ORNL/TM-2005/39, Version 6, Volume III, Section M6, January 2009.

29. R. E. MacFarlane, A. C. Kahler. "*Methods for Processing ENDF/B-VII with NJOY*" Nuclear Data Sheets, Volume 111, Pages 2739-2890, July 2010.

30. A. D. Caldeira. "*On processing material* $^{90232}Th$ *from ENDF/B-VII.0 with NJOY system*" Annals of Nuclear Energy, Volume 37, Issue 10, 2010, Pages 1420-1421, ISSN 0306-4549

31. Los Alamos National Laboratory – "*ENDF/B-VI Incident-Neutron Data*" - https://t2.lanl.gov/nis/data/endf/endfvi-n.html Web. June 15, 2019

32. Brookhaven Science Associates. "*Data Formats and Procedures for the Evaluated Nuclear Data Files ENDF/B-VI and ENDF/B-VII*" National Nuclear Data Center, Brookhaven National Laboratory, July 2010.

33. Edenius, M., Forssen, B., 1995. CASMO-4: A Fuel Assembly Burnup Program, User's Manual (Studsvik/SOA-95/1). Studsvik Energiteknik.

34. Moore, R.L., Schnitzler, B.G., Wemple, C.A., 1995. MOCUP, MCNP/ORIGEN Coupling Utility Program, User Manual (INEL-95/0523). Idaho National Engineering Laboratory.

35. Oak Ridge National Laboratory – Radiation Safety Information Computational Center. "*UTXS6: MCNP Continuous-Energy Neutron Cross Section Libraries for Temperatures from 300 to 1365 K.*" April 2001.

36. HELIOS, 1998. 1.5 Methods. Studsvik-Scandpower.

37. S.C. van der Marck, R. K. MeuleKamp. "*Calculating the effective delayed neutron fraction using Monte Carlo techniques*" PHYSOR 2004 – The physics of Fuel Cycles and Advanced Nuclear Systems: Global Developments, April 25-29, 2004.

38. M. A. Gonzales. "*Doppler Temperature Coefficient Calculations Using Adjoint-Weighted Tallies and Continuous Energy Cross Sections in MCNP6*" Dissertation submitted to The University of New Mexico, December 2016.

39. Oak Ridge National Laboratory. "*SCALE Newsletter*" Number 49, Fall 2016.

40. IAEA, "Delayed-neutron eight-group parameters", https://www-nds.iaea.org/sgnucdat/a7.htm Web. April, 25 2019.

41. Joint Evaluated Fission and Fusion File, Incident-neutron data, http://www-nds.iaea.org/exfor/endf00.htm, February 2006; see also A. Koning, R. Forrest, M. Kellett, R. Mills, H. Henriksson, Y. Rugama, The JEFF-3.1 Nuclear Data Library, JEFF Report 21, OECD/NEA, Paris, France, 2006, ISBN 92-64-02314-3.

42. L. Thilagam, C. Sunil Sunny and K.V. Subbaiah, "Doppler Coefficient of Reactivity — Benchmark Calculations for Different Enrichments of UO2" Joint International Topical Meeting on Mathematics & Computation and Supercomputing in Nuclear Applications (M&C + SNA 2007)

43. Cheuk Wah Lau, "*Improved PWR Core Characteristics with Thorium-containing Fuel*"- Division of Nuclear Engineering Department of Applied Physics Chalmers University of Technology S-412 96 Göteborg, Sweden 2014 ISBN 978-91-7385-990-5

APPENDIX – WORKS DEVELOPED RELATED TO THE ELABORATION OF THE DISSERTATION.

INTERNATIONAL NUCLEAR ATLANTIC CONFERENCE 2017 – INAC 2017

SENSIBILITY ANALYSIS OF FUEL DEPLETION USING DIFFERENT NUCLEAR FUEL DEPLETION CODES

F. Martins, C. E. Velasquez, V.F. Castro, C. Pereira, C. A. Mello da Silva

Departamento de Engenharia Nuclear - Universidade Federal de Minas Gerais
Av. Antonio Carlos, 6627 campus UFMG
31.270-901, Belo Horizonte, MG
felipmartins94@gmail.com, carlosvelcab@hotmail.com,victorfariascastro@gmail.com,
claubia@nuclear.ufmg.br, clarysson@nuclear.ufmg.br

ABSTRACT

Nowadays, the utilization of different nuclear codes to perform the depletion and criticality calculations has been used to simulated nuclear reactors problems. Therefore, the goal is to analyze the sensibility of the fuel depletion of a PWR assembly using three different nuclear fuel depletion codes. The burnup calculations are performed using the codes MCNP5/ORIGEN2.1 (Monteburns), KENO-VI/ORIGEN-S (TRITON- SCALE6.0) and MCNPX (MCNPX/CINDER90). Each nuclear code performs the burnup using different depletion codes. Each depletion code works with collapsed energies from a master library in 1, 3 and 63 groups, respectively. Besides, each code uses different ways to obtain neutron flux that influences the depletions calculation.

The results present a comparison of the neutronic parameters and isotopes composition such as criticality and nuclides build-up, the deviation in results are going to be assigned to features of the depletion code in use, such as the different radioactive decay internal libraries and the numerical method involved in solving the coupled differential depletion equations. It is also seen that the longer the period is and the more time steps are chosen, the larger the deviation become.

1. INTRODUCTION

There are computational codes that perform criticality analyses, nuclear fuel depletion and there are codes that couples both of them, such as MCNPX [1], Monteburns [2] and TRITON-SCALE6.0 [3]. They can simulate with more freedom the many geometries, fuels, assemblies and events that can occur to real reactors.

Even with the same function, the codes operate in different ways, using different numerical methods [4] to solve the coupled nuclide depletion (Equation 1) and neutron transport (Equation 2) differential equations. Beyond that, the number of energy groups for criticality calculation, depletion calculations, and the radioactive decay libraries changes from one to another code.

Both MCNPX and MCNP5 need the NJOY Nuclear Data Processing System [7] code package to retrieve continuous energy libraries at work temperature, for the steady-state flux calculations. KENO-VI could also use the continuous energy library for calculating the steady-state flux since the SCALE6.0 code package already does the needed corrections, but this SCALE version cannot

use these continuous libraries to perform the burnup. Therefore, KENO-VI uses collapsed libraries into 238 energy groups.

Each of these transport codes are coupled to a depletion code, MCNPX/CINDER90, MCNP5/ORIGEN2.1 and KENO-VI/ORIGEN-S. These depletion codes use the calculated fluxes, divided into 63, 1 and 3 energy groups, respectively, their internal radioactive decay and fission yield libraries to achieve the nuclide concentration inventory.

The updated nuclide inventory goes through transport calculations again, thus new fluxes are obtained and then new depletion calculations are done, this procedure occurs for every time step chosen for simulation.

$$\frac{dN_A(t)}{dt} = -(\sigma_A^a \phi + \lambda_A) N_A(t) + \sigma_C^\gamma \phi N_c(t) + \lambda_B N_B(t) \qquad (1)$$

$$\frac{1}{v}\frac{\partial \phi}{\partial t} + \Omega \cdot \nabla \phi(r,E,\Omega,t) + N_t \sigma_t(r,E)\phi(r,E,\Omega,t) = \frac{1}{4\pi} S_f(r,E,t) + \int_{\Omega'}\int_{E'} N_s \sigma_s(r,E' \to E, \Omega' \to \Omega)\phi(r,E',\Omega',t) dE' d\Omega' \qquad (2)$$

The multiplication factor, *k*, depends on the number of neutrons produced in the current generation and the number of neutrons absorbed in the last generation. These amounts vary according to fuel composition. In a fresh fuel element as modeled, it is expected to have the multiplication factor above 1, once there are no control rods or burnable poisons, and burnup increases, the value decreases until reaches the critical and then subcritical condition. This behavior occurs due to the fission products poisoning, some of them have enormous values of absorption cross-section and the reduction of fissile material inside the reactor. When these events affect reactor parameters too much, refuel process begin.

Each of criticality codes compute flux-weighted cross sections, simulating conditions within any given reactor fuel assembly. Then, they convert the data into a library that can be input to their respective depletion codes. This procedure is looped for all time steps in the operation period. The MCNPX 2.6.0 code is a Fortran90 Monte Carlo radiation transport code that can be used for nearly all particles at nearly all energies, used here for neutronic transportation, modeling their interaction with matter. It is the code responsible for the steady-state flux calculations using continuous energy libraries, the results are collapses into 63 energy groups, which will be used by CINDER90 for depletion process.

Already, the code MCNP is similar but does not include depletion calculation. Therefore, using Monteburns, which links with ORIGEN2.1 depletion code. Similarly, to MCNPX the criticality calculations are done but collapse the results into only one group to be used by ORIGEN2.1. The KENO-VI [11] is a 3D Monte Carlo code for nuclear criticality safety analyses that is responsible for criticality calculations in SCALE6.0 (Standardized Computer Analyses for Licensing Evaluation) code system. It uses 238 energy groups instead of continuous energy for flux calculations and collapses the results into 3 energy groups to be inserted as input in ORIGEN-S depletion code.

CINDER90 [13] is responsible for depletion in MCNPX, it is a code which calculates the time-dependent concentration of nuclides coupled in an arbitrary sequence of radioactive decay and neutron absorption in a specified neutron flux spectrum. The code seeks the solution solving 63 coupled differential equations, which considers all possible reactions with nuclides. CINDER90 has its own 63-group library that includes decay, cross section and fission products yield libraries, the data amount constantly rises along versions, and already describes over 3400 nuclides in the range $1 \leq Z \leq 103$.

ORIGEN2.1 [14] is a one group depletion and radioactive decay code developed by Oak Ridge National Laboratory (ORNL), it is the responsible for depletion in Monteburns taking the one neutron flux spectrum previous calculated by MCNP5 and using it to achieve nuclides concentration. It uses an exponential matrix method to solve a large system of coupled, linear, first-order ordinary differential equations with constant coefficients. It also includes its own one group data library, dividing the nuclides into three segments, the activation products, actinides and fission products, in each of these segments there are 3 libraries that may be read, the decay data library, cross section and fission products yield library and a photon yield library.

ORIGEN-S [15] obtain the nuclide concentration in the same way as the original ORIGEN. Essentially all features were retained, expanded or supplemented within new computations, the main difference is that calculations may utilize updated ENDF/B-VI fission products yields data libraries for most fissionable nuclides and the basis neutron cross-section have been replaced with collapsed three-group cross sections developed from ENDF/B-VI, Fusion Evaluated Nuclear Data Library (FENDL-2.0) and the European activation Library (EAF-99).

In this study, the goal is to analyze the sensibility of fuel depletion using the three different coupled codes, seeking distinctions on criticality calculations, fuel depletion, and other nuclides build-up. Deviations in results are going to be shown, analyzed and attributed to the code in use. Some discrepancy is expected due to the different methods of solution of both transport and depletion equations, and due to the different collapsing of energy groups by the depletion codes. The geometry consists of a fresh fuel assembly loaded with uranium dioxide enriched in 3.2% wt and is described in the Angra II Final Safety Analysis Report (FSAR) [5].

2. METHODOLOGY

2.1. Modelling

The specific power for the operation was 38 MW/MTU, as specified on FSAR. The operation period was selected as 800 days because it was the time needed for the multiplication factor to go from a supercritical to a subcritical condition. After, these definitions the given burnup is set as 30.4 GWd/MTU.

The chosen period has been split into 20 time intervals, with the first 5 having 10 days each and the 15 other with 50 days. This time step configuration was chosen to a better analysis of both multiplication factor behavior [6] and fuel composition, especially during the first days of operation.

First, before starting the modeling for simulations, it was necessary to retrieve the cross section from a master library (ENDF/B-VII), at desired temperatures, for each of nuclides involved somehow in depletion process such as fuel, coolants, moderators, cladding, fission products and actinides (Tables 2 and 3 show most of involved nuclides). This is required once neither MCNPX nor Monteburns have ways to evaluate the cross sections at the desired temperature for themselves and for this procedure was used the NJOY99 code [7].

The NJOY nuclear data processing system is a computer code package for producing pointwise and multigroup nuclear cross sections and related quantities from evaluated nuclear data in the ENDF6 format. It is used for converting evaluated nuclear data in the ENDF format into libraries useful for applications calculations, in this paper the Evaluated Nuclear Data File 7.0 [8] was chosen to be the master library.

ENDF/B is a data set that contains only complete, evaluated sets of nuclear data for all significant neutron-induced reactions in a range of 10^{-5}eV to 20MeV, therefore fits the purpose, the fact that ENDF/B data set is continually being reevaluated and updated as new cross section measurements become available turns it to a reliable data set.[9]

2.1.1. Criticality

The codes mentioned use Monte Carlo method [12] for solving the problem, in principle, the method can be used to solve any problem that has a probabilistic interpretation, and in a very simplified way to describe, it relies on repeated random sampling to obtain numerical results. In addition, they use the same master library (ENDF/B-VII) to steady-state flux calculations and, for the three codes the chosen number of neutrons histories was 10000, with 215 generations where the first 15 generations were skipped.

As previously stated, a fuel assembly based on the Angra II FSAR was used to carry out the analysis. This fuel element is composed of 16 x 16 positions, where 236 are fuel pins, and 20 are guide tubes, with zircaloy-4 clad and helium gap, operating in a pressurized water reactor (PWR) at a temperature of 873 K. Figure 1 and Table 1 shows further details such as dimensions, compositions and assembly distribution, the fuel used is fresh uranium dioxide (UO_2) with 3.2 of enrichment.

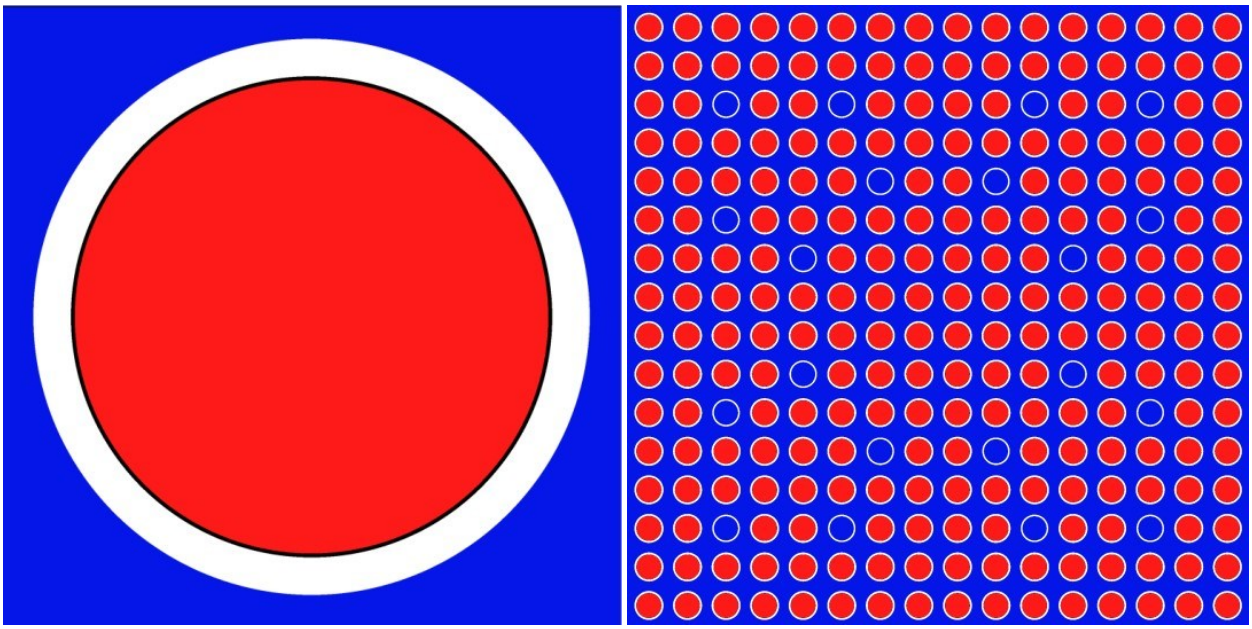

Figure 1: Pin and element geometries, media distribution, Red (UO_2), Black (Helium), White (Zirc-4), Blue (Water).

Table 1: Full power dimensions and physical data for modeling, according to FSAR

	Radius (cm)	Active Length (cm)	Media	Temperature (K)
Fuel	0.4583	391.6	UO_2	873
Gap	0.4659	391.6	Helium	873
Fuel Clad	0.5385	391.6	Zircaloy-4	618
Mod (half pitch)	0.7150	391.6	Unborated Water	582

2.1.2. Depletion

In the operation of a nuclear power plant is very important to determine the time evolution of the material composition and radionuclide inventory during the entire operation of it. It was considered in all simulations the same geometry and enrichment. Now its needed to be monitored the changes of neutron capture and radioactive decay in fuel due to the burnup. These nuclear reactions are responsible for fissile material reduction and fission products and actinides build up.

The condition for each code was created following same geometry and fuel parameters. Table 2 and Table 3 presents the nuclides followed during burnup. They were chosen based on other relevant PWR research [16].

Table 2: Followed actinides during burnup.

^{234}U ^{235}U ^{236}U ^{237}U ^{238}U ^{239}U	^{237}Np ^{238}Np ^{239}Np	^{238}Pu ^{239}Pu ^{240}Pu ^{241}Pu ^{242}Pu
^{241}Am ^{242}Am ^{243}Am	^{242}Cm ^{243}Cm ^{244}Cm ^{245}Cm	

Table 3: Followed fission products during burnup.

^{75}As	^{81}Br	^{82}Kr ^{83}Kr ^{84}Kr ^{86}Kr			^{85}Rb ^{87}Rb			^{89}Y	^{90}Zr ^{91}Zr ^{92}Zr ^{93}Zr ^{94}Zr ^{96}Zr		
^{95}Mo	^{99}Tc	^{101}Ru ^{103}Ru ^{105}Ru			^{104}Pd ^{105}Pd ^{106}Pd ^{108}Pd ^{110}Pd						
^{109}Ag	^{110}Cd ^{111}Cd ^{112}Cd ^{113}Cd				^{120}Sn	^{129}I ^{135}I		^{128}Xe ^{130}Xe ^{131}Xe ^{132}Xe ^{134}Xe ^{135}Xe ^{136}Xe			
^{133}Cs ^{134}Cs ^{135}Cs ^{136}Cs ^{137}Cs					^{138}Ba	^{141}Pr		^{143}Nd ^{145}Nd ^{147}Nd ^{148}Nd			
^{147}Pm ^{148}Pm ^{149}Pm			^{147}Sm ^{149}Sm ^{150}Sm ^{151}Sm ^{152}Sm					^{151}Eu ^{152}Eu ^{153}Eu ^{154}Eu ^{155}Eu			
^{152}Gd ^{154}Gd ^{155}Gd ^{156}Gd ^{157}Gd ^{158}Gd ^{160}Gd								^{165}Ho			

3. RESULTS

At beginning of cycle, the only fissile nuclide in the reactor is ^{235}U, Fig 3, but, as soon as, the burnup starts the nuclide concentrations inside reactor changes. In the second time step, the buildup of plutonium come out, Fig 5, along with others actinides and fission products Figs 6, 7 and 8.

It can be seen that most of the presented comparisons strongly agree with one to each other. Nevertheless, there is a slight deviation in plutonium graphic, and due to that, the actinide graphic, and the fission products buildup graphic.

The chosen period has a direct influence on results, the larger it is the larger the deviation will be. The mean values (Equation 3) for each of the parameters analyzed were taken, then, the standard deviation (Equation 4) is taken. Finally, Tables 4 and 5 show the relative standard deviations of the parameters with respect to their mean values during burnup, respectively.

$$\bar{\sigma} = \frac{1}{N}\sum_{i=1}^{N} \sigma_i \tag{3}$$

$$s = \sqrt{\frac{1}{N}\sum_{i=1}^{N} (\sigma_i - \bar{\sigma})^2} \tag{4}$$

$$RSD = \frac{100 * s}{\bar{\sigma}} \qquad (5)$$

Table 4: Relative standard deviation in Monteburns (I), SCALE (II) and MCNPX (III) between results and mean value.

Burnup (GWd/MTU)	K_{inf} (%)			^{235}U (%)			Plutonium (%)		
	I	II	III	I	II	III	I	II	III
0	0.05	0.19	0.14	0.009	0.001	0.006	0	0	0
7.6	0.04	0.09	0.13	0.15	0.19	0.03	1.74	3.11	1.36
15.2	0.30	0.14	0.16	0.60	0.95	0.35	2.95	5.42	2.47
22.4	0.27	0.07	0.20	1.29	2.20	0.91	3.56	6.83	3.27
30.4	0.39	0.05	0.34	2.19	3.93	1.75	3.99	7.76	3.76

Table 5: Relative standard deviation in Monteburns (I), SCALE (II) and MCNPX (III) between results and mean value.

Burnup (GWd/MTU)	Actinides Mass (%)			Fission Products (%)		
	I	II	III	I	II	III
0	0	0	0	0	0	0
7.6	0.37	0.72	0.35	0.66	1.14	1.80
15.2	0.48	1.66	1.18	0.63	1.16	1.79
22.4	0.98	2.17	1.19	0.78	1.08	1.86
30.4	1.09	2.36	1.27	0.85	1.02	1.87

As the fuel used is fresh uranium dioxide and it is very common and frequently studied fuel, libraries associated to it and others related nuclides coming either from fissions, absorptions or decay, are extremely similar. Therefore, even if the codes use different libraries the results are expected to be similar.

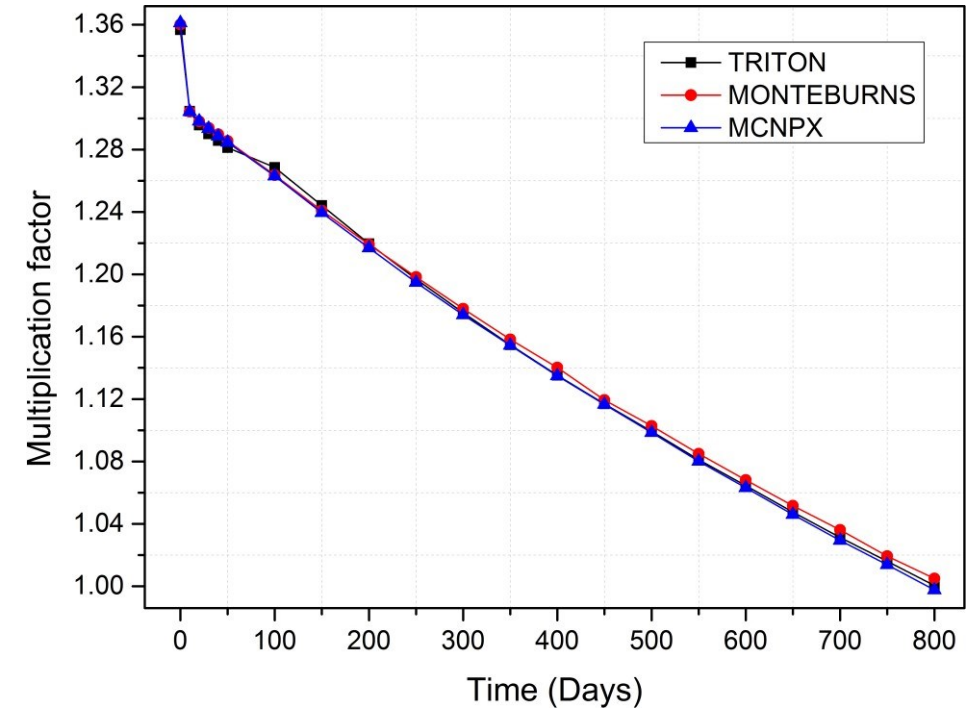

Figure 2: Multiplication factor during the time.

.

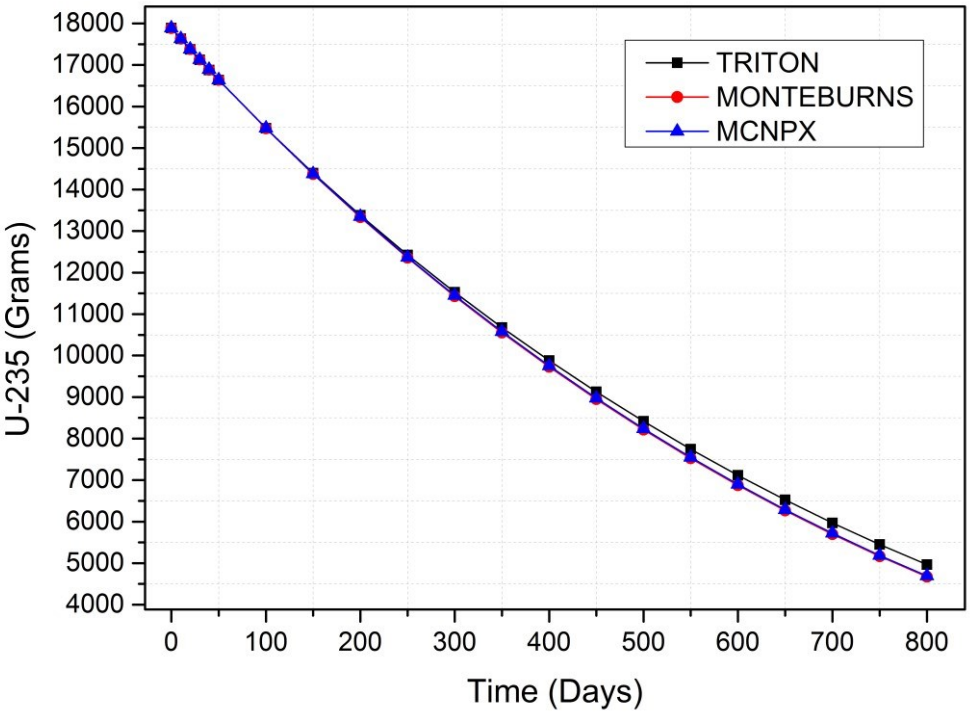

Figure 3: Fissile uranium (^{235}U) mass during the time.

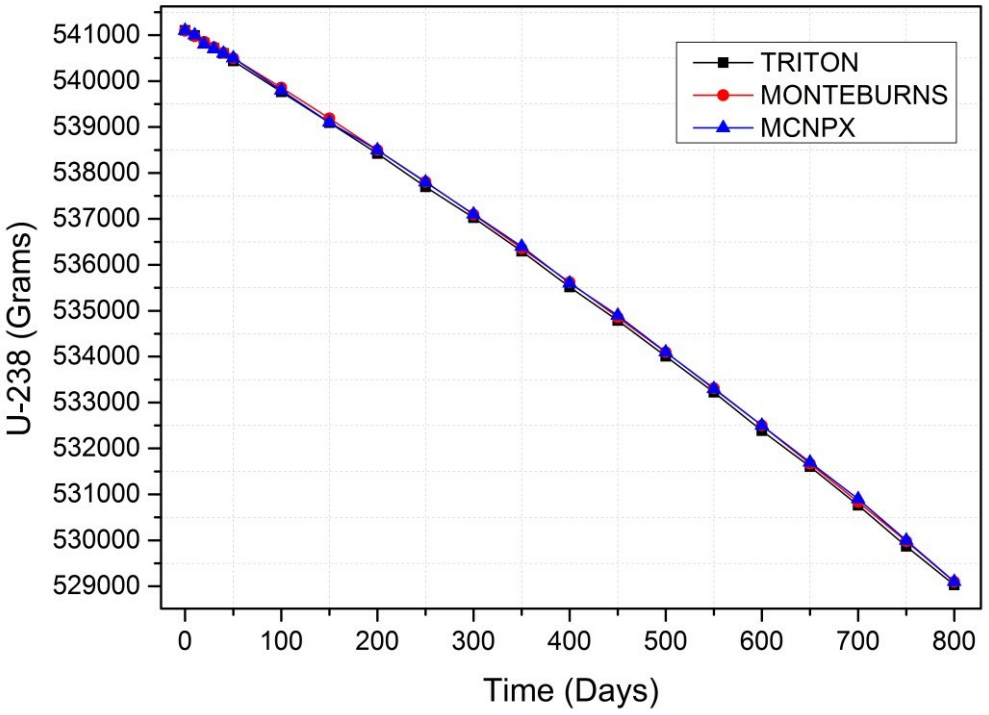

Figure 4: ^{238}U mass during the time.

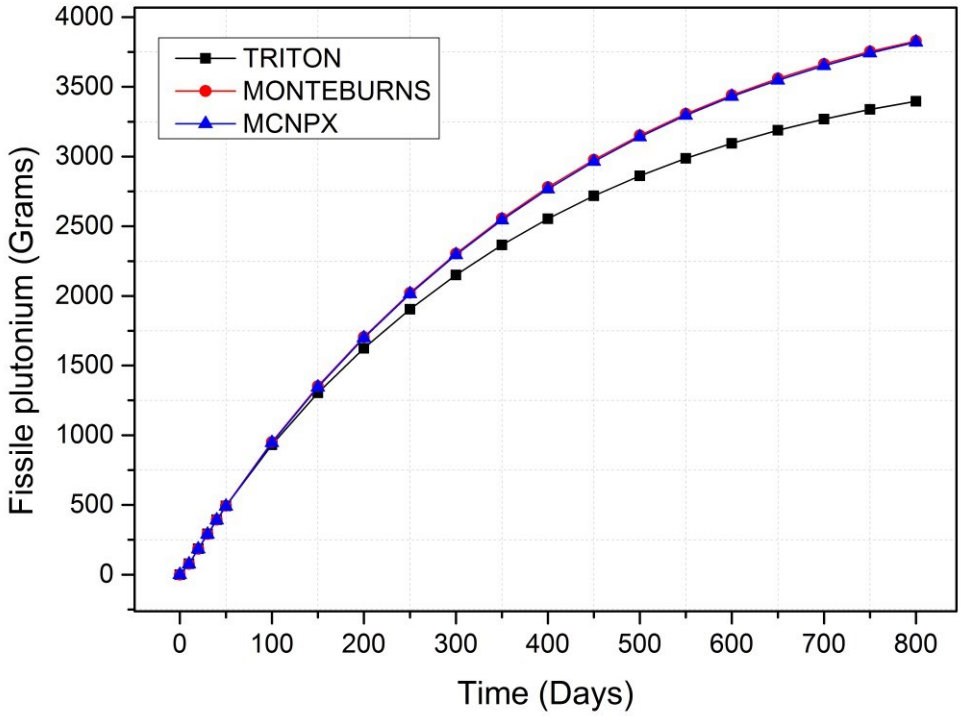

Figure 5: Fissile plutonium mass (^{239}Pu and ^{241}Pu) during the time.

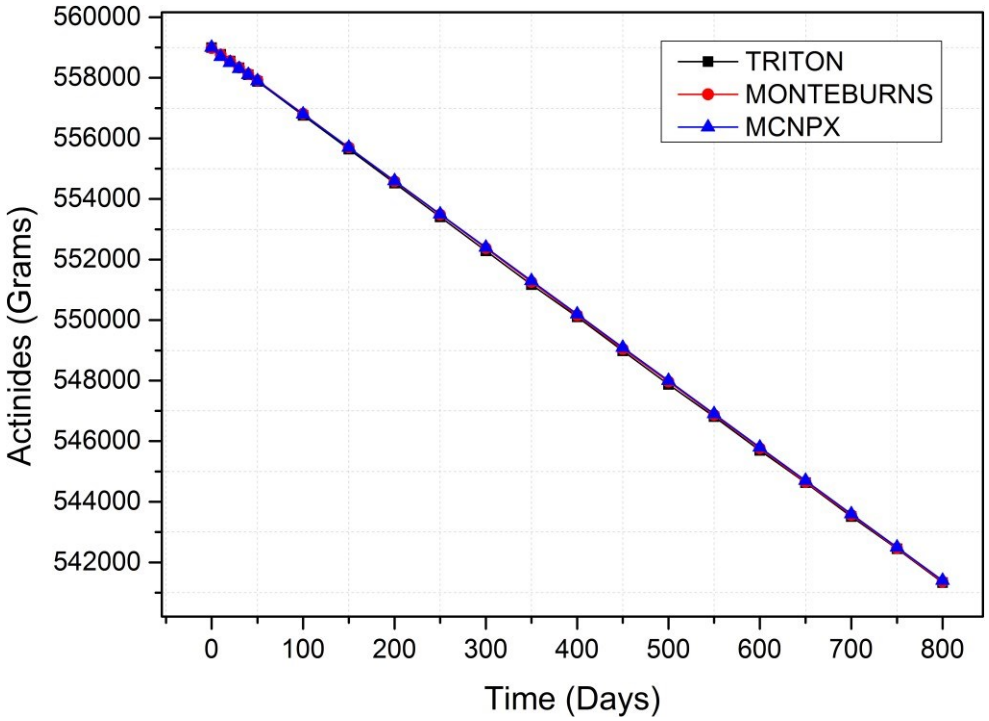

Figure 6: Total actinides mass during the time.

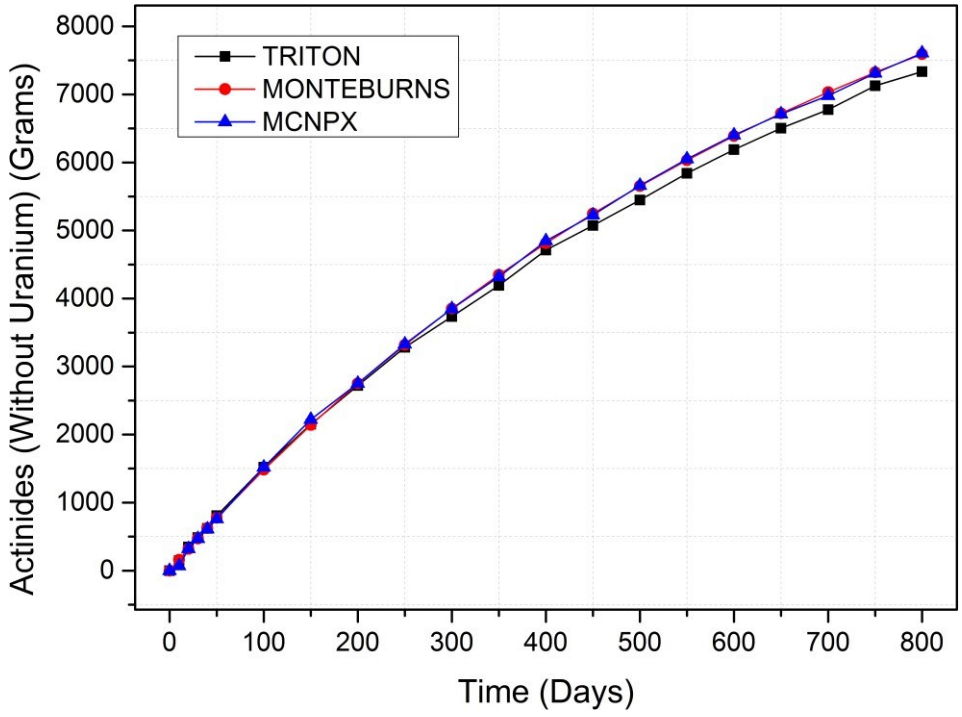

Figure 7: Actinide mass without uranium during the time.

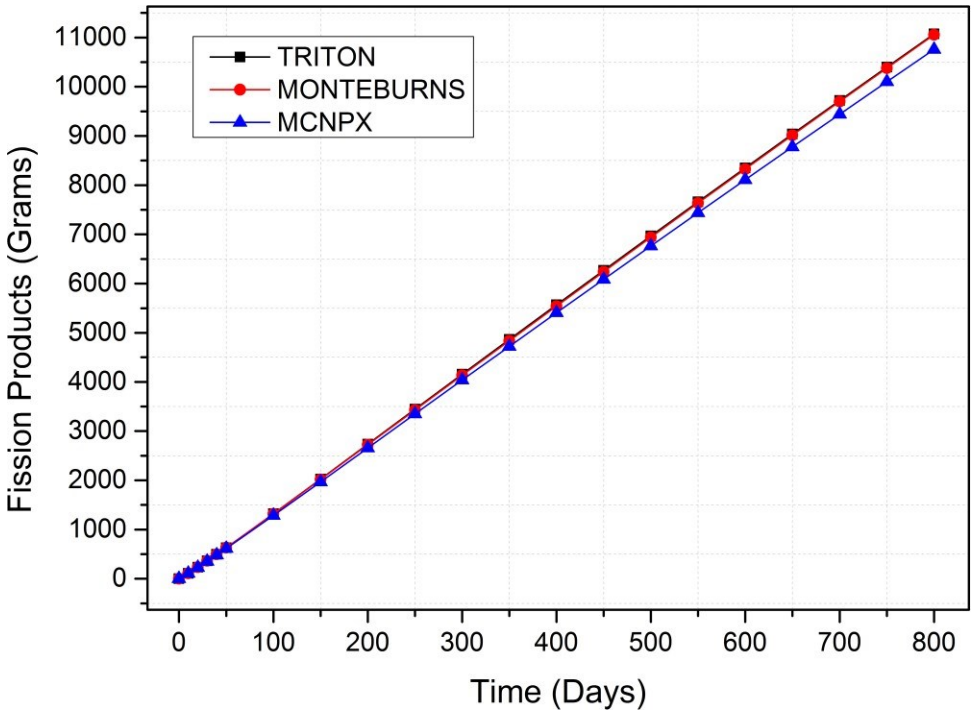

Figure 8: Fission products build up during the time.

4. CONCLUSION

According to the results, it can be concluded that numerical method involved solving criticality calculations, fuel depletion, plutonium production and fission products buildup has greater influence in results than the number of energy groups in depletion. In theory, the more energy groups the depletion code use, the closer to reality the results are. This is due to real reactors have neutrons in a long range of a continuous energy. However, this paper showed that for this type of fuel and geometry there is a fairly agreement between codes with different energy groups numbers and thus real reactors can be well represented by either 1, 3 or 63 energy groups.

As the difference in energy groups number was shown not to be the major responsible for divergence in results, it is attributed to the way the code solves the coupled differential equations involved in all the process, neutronic transport, fuel depletion, nuclides build-up and also nuclides radioactive decay.

This study was done with a modeled fresh fuel element with a period of 2.2 years for depletion. It is important to remember that the fuel composition directly affects the results. Because each code uses different libraries for the calculations, which was a minor effect in this paper due to the well knowledge of the data libraries involved in this process. For the nuclides of interest, most libraries agree on data collected.

Therefore, further researches are encouraged of how the use of different codes interferes in fuel depletion process when using different fuel composition. Different fuel composition includes mixed oxide fuel (MOX), thorium-uranium oxide fuel (Th-U)O_2 and other transuranics mixed oxides such as (TRU-U)O_2 and (TRU-Th)O_2.

Together with the changes in fuel composition an analysis with a greater number of time steps would show the deviations due to the greater number of communication between the neutronic transport code and burnup code. Each of these communications gives the burnup code an updated nuclide concentration inventory. Besides that, changing the burnup period would also ensure a good research subject.

ACKNOWLEDGMENTS

The authors are grateful to the Brazilian research funding agencies, CNEN – Comissão Nacional de Energia Nuclear (Brazil), CNPq – Conselho Nacional de Desenvolvimento Científico e Tecnológico (Brazil), CAPES – Coordenação de Aperfeiçoamento de Pessoal de Nível Superior (Brazil) and FAPEMIG – Fundação de Amparo à Pesquisa do Estado de Minas Gerais (MG/Brazil) for the support.

REFERENCES

1. J.S. Hendricks, et al., *"MCNPX 2.6.0 Extensions"*, LA-UR-08-2216 (2008).
2. Trellue, H. R. and Poston, D. I. Los Alamos National Laboratory *"User's Manual, Version 2.0 for Monteburns, Version 5B"*. LA-UR-99-4999 (1999).
3. Radiation Safety Information Computational Center at Oak Ridge National Laboratory, *"SCALE: A Modular Code System for Performing Standardized Computer Analyses for Licensing Evaluations, ORNL/TM-2005/39, Version 6, Vols. I–III, January"* Scale6.0 (2009).
4. P.P.Krüger, *"NUMERICAL METHODS TO SOLVE THE FUEL DEPLETION EQUATIONS FOR A NUCLEAR REACTOR", Dissertation submitted in partial fulfilment of the requirements for the degree Magister Scientiae in Physics at the Potchefstroomse Universiteit vir Christelike Hoer Onderwys, P.P.KRUGER* (2004).
5. Eletrobrás eletronuclear, *"Final Safety Analysis Report – Central Nuclear Almirante Álvaro Alberto UNIT 2"* (2013).
6. Rochkhudson B. de Faria, Patrícia A.L. Reis, Carlos E. Velasquez, Javier G. Mantecon, Adolfo R. Hamers, Antonella L. Costa, Cláubia Pereira, *"Sensitivity analysis of a PWR fuel element using zircaloy and silicon carbide claddings, Nuclear Engineering and Design*", Volume 320, Pages 103-111, ISSN 0029-5493, http://dx.doi.org/10.1016/j.nucengdes.2017.05.006 (2017).
7. A.C. Kahler, *"NJOY99 Tutorial"*, presented at the ANS Annual Meeting, June 2008, LA- UR-08-2149 (2008).
8. M.B. Chadwick, P. Obložinský, M. Herman, N.M. Greene, R.D. McKnight,

D.L. Smith,P.G. Young, R.E. MacFarlane, G.M. Hale, S.C. Frankle, A.C. Kahler, T. Kawano, R.C. Little, D.G. Madland, P. Moller, R.D. Mosteller, P.R. Page, P. Talou, H. Trellue, M.C. White, W.B. Wilson, R. Arcilla, C.L. Dunford, S.F. Mughabghab, B. Pritychenko, D. Rochman, A.A. Sonzogni, C.R. Lubitz, T.H. Trumbull, J.P. Weinman, D.A. Brown, D.E. Cullen, D.P. Heinrichs, D.P. McNabb, H. Derrien, M.E. Dunn, N.M. Larson, L.C. Leal, A.D. Carlson, R.C. Block, J.B. Briggs, E.T. Cheng, H.C. Huria, M.L. Zerkle, K.S. Kozier,A. Courcelle, V. Pronyaev, S.C. van der Marck, *"ENDF/B-VII.0: Next Generation Evaluated Nuclear Data Library for Nuclear Science and Technology"*, Nuclear Data Sheets, Volume 107, Issue 12, Pages 2931-3060, ISSN 0090-3752, http://dx.doi.org/10.1016/j.nds.2006.11.001 (2006).

9. Duderstadt, James J. and Hamilton, Louis J. "*Nuclear reactor analysis / James J. Duderstadt, Louis J. Hamilton"* Wiley, New York USA (1976).
10. R. Brewer, Editor, *"Criticality Calculations with MCNP5: A Primer",* LA-UR-09- 0380 (2009).
11. Bowman, Stephen M. *"KENO-VI Primer: A Primer for Criticality Calculations with SCALE/KENO-VI Using GeeWiz."* United States: N. p., 2008. Web. doi:10.2172/992515.
12. YU.A. SHREIDER, N.P. BUSLENKO, , D.I. GOLENKO, I.M. SOBOL', and V.G. SRAGOVICH *"CHAPTER I - PRINCIPLES OF THE MONTE CARLO METHOD, In The Monte Carlo Method"*, Pages 1-90, ISBN 9780080110882, Pergamon, 1966 https://doi.org/10.1016/B978-0-08-011088-2.50005-5
13. England, T. R. *"CINDER--A ONE-POINT DEPLETION AND FISSION PRODUCT PROGRAM."* United States: N. p., 1962. Web. doi:10.2172/4765256. https://www.osti.gov/scitech/biblio/4765256
14. "MIT", "Massachusetts Institute of Technology" "*22.251 Systems Analysis of the Nuclear Fuel Cycle"*, 2009 MIT_ORIGEN2.1
15. Hermann, O.W., & Westfall, R.M. *"ORIGEN-S: SCALE system module to calculate fuel depletion, actinide transmutation, fission product buildup and decay, and associated radiation source terms (NUREG/CR--0200-Vol2)."* United States (1984).
16. Raghava R. Kommalapati, Fiifi Asah-Opoku, Hongbo Du and Ziaul Huque *"Monte Carlo Simulations of Nuclear Fuel Burnup"*, Nuclear Material Performance, Prof. Rehab Abdel Rahman (Ed.), InTech, DOI: 10.5772/62572. Available from: https://www.intechopen.com/books/nuclear-material-performance/monte-carlo- simulations-of-nuclear-fuel-burnup (2016).

IV SEMANA DE ENGENHARIA NUCLEAR E CIÊNCIAS DA RADIAÇÃO – IV SENCIR

EVALUATION OF TEMPERATURE DEPENDENCE ON CROSS SECTIONS FOR A (Th-U)O_2 FUEL PIN

Felipe Martins, Carlos E. Velasquez, Cláubia Pereira

Departamento de Engenharia Nuclear - Universidade Federal de Minas Gerais
Av. Antônio Carlos, 6627 campus UFMG
31.270-901, Belo Horizonte, MG
claubia@nuclear.ufmg.br

Keywords: MCNP5, Serpent, NJOY99, Cross Section, Doppler Broadening.

ABSTRACT

A (Th-U)O_2 fuel pin benchmark, consisting of 75w/o Th and 25w/o U, was used to analyze the effects of the temperature on the nuclear cross-sections obtained from the libraries on criticality calculations. In this case, the multiplication factor and the effective delayed neutron factor have been compared for different corrections, libraries and nuclear codes. The MCNP5 and Serpent codes were used to criticality calculations and the NJOY99 code was used to obtain the cross-section at working temperature. The results demonstrated that the use of temperature correction on cross sections is fundamental to reach more precise neutronic calculations.

1. INTRODUCTION

There are many nuclear codes to evaluate the nuclear reactor physics. Some of them use continue nuclear data libraries, which contains important information about the cross section of each nuclide for few temperatures. Due to the temperature dependence effects, the use of an approximated temperature may cause differences in the criticality and depletion calculations. This effect is more important to absorbers nuclides in fuels that are composed by ^{238}U and ^{232}Th. To obtain nuclear data in the working temperature (WT), the NJOY99 [1] could be used. Another possibility is by interpolation using the temperature-dependent data available in the nuclear code data libraries.

In this work, the codes MCNP [2] and Serpent [3] were used to the criticality calculations. Each one has its own cross-section data package. Most of the data libraries on MCNP5 are at room temperature and if not indicated the correction card, it assumes room temperature for the simulation. On the other hand, Serpent has data libraries at specific temperatures e.g. 300K, 600K, 900K, and 1200K. Also, in this case, if the specific temperature is not indicated, it uses in the simulation nuclear data at room temperature. So, there are many ways to model and simulate the temperature effects in a fuel pin, assembly or core and it can influence the results related to.

For the analysis, it was used a thorium unitary cell benchmark [4] to compare the criticality calculations using different temperatures modeled by MCNP5 and Serpent codes. The first criticality evaluation is based on the utilization of the cross sections data package on the Serpent at specific temperatures (300K, 600K, 900K and 1200K) and the

cross sections generated with NJOY99 at work temperature, both using the library ENDF/B-VII [5]. The second evaluation was done for both codes using the temperature correction leading to the working temperature (WT), which for the coolant material, the cladding and the fuel are 583K, 621K, and 900K, respectively.

2. METHODOLOGY

The methodology follows the benchmark calculations as a reference, using the same nuclear fuel based on thorium. The evaluation was performed using the codes temperature correction and the cross-section data at work temperature.

2.1. CRITICALITY EVALUATION BENCHMARK

Fig. 1. shows the fuel pin cell modeled on Serpent and MCNP5 based on the benchmark [4]. Table 1 presents the parameters used in the benchmark and in the Table 2 it is shown the composition.

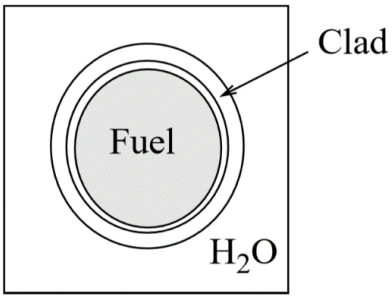

Figure 1. Thorium pin cell model extracted from benchmark [4]

Table 1. Full power operation parameters [4].

Parameters	Full Power
Fuel Density (g/cm³)	9.424
Fuel Temperature (K)	900
Cladding Density (g/cm³)	6.505
Cladding Temperature (K)	621.1
Coolant Density (g/cm³)	0.705
Coolant Temperature (K)	583.1
Fuel Pellet Radius (mm)	4.1274
Cladding Inner Radius (mm)	4.1896
Cladding Outer Radius (mm)	4.7609
Pin Pitch (mm)	12.626

Table 2. Nuclides Weight Percentage. [4]

	Nuclide	Weight Percent (%)
Fuel	Th-232	65.909
	U-234	0.034
	U-235	4.291
	U-238	17.740
	O-16	12.026
Cladding	Zr-4 (Zircaloy-4)	100
Coolant	H-1	11.19
	O-16	88.81

Table 3 shows nine different cases using the codes temperature correction and then the cross-section generated at work temperature (WT). In the first case, it was used the codes temperature correction, which uses the data package from the Serpent ENDF/B-VII with cross-sections at

300K, 600K, 900K, and 1200K and room temperature for MCNP5. In the second case, it takes into consideration the cross-sections at working temperature (WT) using the library ENDF/B-VII, generated at 583K, 621K, and 900K.

In the Serpent code, the temperature correction can only be used if the given temperature is above the original. Thus, to use the temperature correction on coolant and cladding, the 900K and 1200K datasets could not be used.

Table. 3. Data sets temperature definitions

Data Set	Material	Temperatures
Working Temperature (WT) ENDF/B-VII NJOY99	Fuel	900K
	Cladding	621K
	Coolant	583K
300K (03c) Serpent ENDF/B-VII	Fuel	300K
	Cladding	300K
	Coolant	300K
600K (06c) Serpent ENDF/B-VII	Fuel	600K
	Cladding	600K
	Coolant	600K
900K (09c) Serpent ENDF/B-VII	Fuel	900K
	Cladding	900K
	Coolant	900K
1200K (12c) Serpent ENDF/B-VII	Fuel	1200K
	Cladding	1200K
	Coolant	1200K
300K corrected to WT (03c→WT) Serpent ENDF/B-VII	Fuel	300K→900K
	Cladding	300K→621K
	Coolant	300K→583K
600K corrected to WT (06c→WT) Serpent ENDF/B-VII	Fuel	600K→900K
	Cladding	600K→621K
	Coolant	300K→583K
900K corrected to WT (09c→WT) Serpent ENDF/B-VII	Fuel	900K→900K
	Cladding	600K→621K
	Coolant	300K→583K
1200K corrected to WT (12c→WT) Serpent ENDF/B-VII	Fuel	1200K→1200K
	Cladding	600K→621K
	Coolant	300K→583K

→ it indicates the use of temperature correction.

3. RESULTS

The total number of neutrons used in each case was 100 million, 2000 generations with 50000 neutrons per generation. This large number of neutrons allowed the standard deviation of the codes to be around 6 pcm. The results present the differences in multiplication factor using a different type of correction, the Serpent correction, the MCNP5 correction and both codes using working temperature data (WT) library generated with NJOY.

3.1. CRITICALITY

Table 4 shows the multiplication factor calculation for the Serpent and MCNP5 using the codes correction (third and fourth column) at different temperature compared to the mean value (first column) obtained from the benchmark [4]. The last columns present the absolute differences of the multiplication factor between the codes used at DEN/UFMG and the MIT CASMO-4 case.

The case that presents the lowest absolute difference for Serpent and MCNP5 was the (12c→WT). On the other hand, when the temperature corrections are not used, the results indicate that the MCNP5 using the 09c has a low absolute difference of the multiplication factor. Besides, the cases using the working temperature (WT) have the second lower absolute difference of the multiplication factor values for both codes.

Table 4. Multiplication factors and their respective maximum absolute difference. [4]

Reference Value	Cases	$k_{Serpent}$	k_{MCNP5}	Absolute Differences (pcm)	Serpent	MCNP5
1.23161*	WT	1.23389	1.23517	MIT CASMO4 – WT	228	356
	03c	1.29379	1.24774	MIT CASMO4 - 03c	6218	1613
	06c	1.26342	1.23841	MIT CASMO4 - 06c	3181	680
	09c	1.24194	1.23009	MIT CASMO4 - 09c	1033	152
	12c	1.22506	1.22499	MIT CASMO4 - 12c	655	662
	03c→ WT	1.24469	1.25153	MIT CASMO4 - (03c→WT)	1308	1992
	06c→ WT	1.24475	1.24218	MIT CASMO4 - (06c→WT)	1314	1057
	09c→ WT	1.24504	1.23476	MIT CASMO4 - (09c→WT)	1343	315
	12c→ WT	1.22942	1.22857	MIT CASMO4 - (12c→WT)	219	304

→ it indicates the use of temperature correction.

To identify the impact of different nuclear data in the criticality calculations, the mean value, standard deviation and the relative standard deviations are applied to the multiplication factor

values obtained with different codes/institutions. “Before” are the data just for the MIT case (benchmark) and “Updated” includes the MIT data and DEN/UFMG data.

Table 5. Statistics parameter for the chosen cases [4]

Country	Institute	Code	Library	k
USA	MIT[1]	CASMO-4	ENDF/B-VI	1.23782
USA	MIT	MOCUP	UTXS	1.23354
USA	INEEL[2]	MOCUP	UTXS	1.22347
BRAZIL	DEN[3]	MCNP5	ENDF/B-VII 09c	1.23009
BRAZIL	DEN	Serpent	ENDF/B-VII 09c	1.24194
BRAZIL	DEN	MCNP5	ENDF/B-VII 12c→WT	1.22857
BRAZIL	DEN	Serpent	ENDF/B-VII 12c→WT	1.22942
BRAZIL	DEN	MCNP5	ENDF/B-VII NJOY99	1.23517
BRAZIL	DEN	Serpent	ENDF/B-VII NJOY99	1.23404
Multiplication Factor Mean Value			Before	1.23161
			Updated	1.23267
Multiplication Factor Standard Deviation			Before	0.00602
			Updated	0.00516
Multiplication Factor Relative Standard Deviation			Before	0.49%
			Updated	0.42%

→ it indicates the use of temperature correction.
1-Massachusetts Institute of Technology – MIT [4]
2-Idaho National Engineering and Environmental Laboratory – INEEL [4]
3-Departamento de Engenharia Nuclear – DEN - UFMG

3.2. DELAYED NEUTRON AND FUEL TEMPERATURE COEFFICIENT

The benchmark [4], uses the ^{235}U as a fissile material spiked with thorium as a nuclear fuel. Therefore, it is considered the delayed neutrons for the ^{235}U. According to the International Atomic Energy Agency (IAEA) publication [7], the delayed neutron data for ^{235}U is $\beta_{235U} = 0.00665 \pm 0.00021$, which is like the ones obtained by MCNP5 and Serpent for the three temperatures evaluated.

Table 6 provides the effective neutron delayed factor for the chosen cases in the analysis of Table 4 for MCNP5 and Serpent codes. A similar statistics analysis is done for the effective delayed neutron factor, including the mean value, the standard deviation, and the relative standard deviation.

Table 6. Effective delayed neutron factors and statistics parameters.

$\beta_{235U(IAEA)}$	Cases	$\beta_{Serpent}$	β_{MCNP5}		$\beta_{Serpent}$	β_{MCNP5}

0.00665	WT	0.00669	0.00674	Relative differences	0.6%	1.33%
	09c	0.00668	0.00672		0.44%	1.04%
	12c→WT	0.00669	0.00677		0.6%	1.77%

→it indicates the use of temperature correction.

4. CONCLUSION

The k_{inf} absolute differences for Serpent present six out of eight values above 1000 pcm in contrast to the MIT and INEEL mean value. Although, MCNP5 only has three out of eight results above 1000pcm.The optimal scenario for neutronic simulations involves the use of appropriate cross-section data. The corrections done by Serpent and MCNP5 approximate the results to the MIT CASMO-4 reference case. Nevertheless, the results still varying with an average of 1046 pcm and 917 pcm from reference.

The results obtained at WT with cross sections generated using NJOY had an average absolute difference of 300 pcm in relation to reference case. Therefore, the results obtained depends strongly on cross-section generated temperatures. This observation is supported by the differences were lower at WT using NJOY. In fact, using the temperature correction without the corresponding cross-section, the results diverge from the expected value, contributing to the lack of accuracy.

The effective delayed neutron fraction obtained had very similar values when compared to theory. The maximum absolute difference from values obtained was 9pcm. The calculated fuel temperature coefficients values were -5.15492 and -0.08740 pcm/K for Serpent and MCNP5, respectively. Therefore, the use of appropriate cross sections data was equally significant on all calculation performed.

ACKNOWLEDGMENT

The authors are grateful to Vitor Vasconcelos, from CDTN – Centro de Desenvolvimento de Tecnologia Nuclear (Brazil), the holder of Serpent license, for executing all cases needed to this paper. The authors are also grateful to Brazilian research funding agencies, CNEN – Comissão Nacional de Energia Nuclear (Brazil), CNPq – Conselho Nacional de Desenvolvimento Científico e Tecnológico (Brazil), CAPES – Coordenação de Aperfeiçoamento de Pessoal de Nível Superior (Brazil) and FAPEMIG – Fundação de Amparo à Pesquisa do Estado de Minas Gerais (MG/Brazil) for the support. Furthermore, we are also grateful to sponsors and donor volunteers for their support of this event.

REFERENCES

[1] A. C. Kahler, *"NJOY99 Tutorial"*, presented at the ANS Annual Meeting, June 2008, LA-UR-08-2149 (2008).

[2] R. Brewer, Editor, "Criticality Calculations with MCNP5: A Primer", LA-UR-09-0380 (2009).

[3] J. Leppänen et al. (2015) *"The Serpent Monte Carlo code: Status, development and applications in 2013."* Ann. Nucl. Energy, 82 (2015) 142-150.

[4] K. D. Weaver et al., A PWR Thorium Pin Cell Burnup Benchmark Advances in Reactor Physics and Mathematics and Computation into the Next Millennium (PHYSOR 2000), 2000.

[5] M. B Chadwick et al., "ENDF/B-VII.0: Next generation evaluated nuclear data library for nuclear science and technology", Nucl. Data Sheets 107(2016)2931.

[6] R. K. Meulekamp, S. C. van der Marck (2006) Calculating the Effective Delayed Neutron Fraction with Monte Carlo, Nuclear Science and Engineering, 152:2, 142-148, DOI: 10.13182/NSE03-107

[7] IAEA, "Delayed-neutron eight-group parameters", https://www-nds.iaea.org/sgnucdat/a7.htm

ICENES 2019: INTERNATIONAL CONFERENCE ON EMERGING NUCLEAR ENERGY SYSTEMS*

***Under revision**

A THORIUM CELL BENCHMARK COMPARISON USING DIFFERENT NUCLEAR CODES

Felipe M. G. Pereira, Renato V. A. Marques, Carlos. E. Velasquez, Márcia S. Santos, Claubia Pereira

Abstract

Over the past years thorium attractiveness as subject of study have grown due to the positive qualities it contributes to the reactor. This fact jointly with the expanding use of criticality and depletion nuclear codes lead to the purpose of this paper.

This paper aim to use three different coupled codes MCNP5/ORIGEN2.1 (Monteburns), KENO-VI/ORIGEN-S (TRITON-SCALE6.0) and MCNPX (MCNPX/CINDER90) to perform a thorium cell evaluation. All these codes use data coming out of the same library (ENDF/B VII), the criticality results will be compared to a benchmark obtained from a thesis submitted to the Departamento de Engenharia Nuclear da Universidade de Minas Gerais (DEN – UFMG). Each depletion code works with collapsed energies from a master library in different energy groups and different embedded cross section data. Furthermore, the β factor that indicates the fraction of fission neutrons that are delayed will also be analyzed.

Also, this paper intends to find out the dependence of the analyzed parameters, such as multiplication factor, nuclides build-up and delayed neutrons fraction (β_{eff}) to the employed code. The results present a comparison and discussion of these parameters simultaneously to the benchmark values.

Keywords: Thorium, Nuclear codes, benchmark

1. Introduction

The nuclear engineering department (DEN) at UFMG uses different codes for researching. The SCALE6.0 (KENO-VI/ORIGEN-S) [1] [2], MCNPX/CINDER90 [3] [4] and MCNP5/ORIGEN2.1 [5] [6] are some of the coupled codes used in the department. Each of these codes have particularities such as the considered number of energy groups used to criticality and burnup calculations.

A thorium pin cell model benchmark [7] is used to evaluate the burnup using the three mentioned coupled codes. The results present two sections, the first presenting criticality results for the fresh fuel situation. The second section presents the burnup situation, in this section the criticality results, the effective delayed neutron factor and some isotope concentrations are compared to MIT and INEEL reference.

The criticality cases are performed using the continuous energy master library ENDF/B-VII [8], besides that, the collapsed 238 groups of energy are evaluated for KENO-VI. The burnup cases use the same master library although depletion codes collapse to different numbers of energy groups, one group for ORIGEN2.1, three energy groups for ORIGEN-S and sixty-three

energy groups for MCNPX. The KENO-VI code uses collapsed 238 energy groups instead of continuous energy in burnup cases due to the inability to use continuous energy during burnup.

2. Methodology

2.1 Criticality

The modelled cell was performed for all three coupled codes and it represents a PWR pin from a standard 17x17 pin assembly. The fuel is a mixture of ThO_2-UO_2 consisting of 75 w/o Th and 25 w/o U on a heavy metal basis. The total fissile amount (^{235}U) using this configuration is 4.869 w/o of the total heavy metal.

Table 1 shows fuel composition and full power operation parameters used in pin cell model. For all cases the same parameters and fuel composition were utilized. The number of neutrons generations was set as 2000 and for each 50000 neutrons were used. The total amount of neutrons was 100 million. Using this neutronic parameters allowed the codes standard deviation to be lower than 10 pcm.

Table 1: Full power operation parameters and nuclides weight percentage.

PARAMETERS	FULL POWER	FUEL COMPOSITION		
Fuel Density (g/cm³)	9.424		Nuclide	Weigh Percent (%)
Fuel Temperature (K)	900			
Cladding Density (g/cm³)	6.505	Fuel	Th-232	65.909
Cladding Temperature (K)	621.1		U-234	0.034
Coolant Density (g/cm³)	0.705		U-235	4.291
Coolant Temperature (K)	583.1		U-238	17.740
Fuel Pellet Radius (mm)	4.1274		O-016	12.026
Cladding Inner Radius (mm)	4.1896	Cladding	Zr-4 (Zircaloy-4)	100
Cladding Outer Radius (mm)	4.7609	Coolant	H-001	11.19
Pin Pitch (mm)	12.626		O-016	88.81

Figure 1 illustrates the modelled pin cell and shows material placement in it. The employed master library was ENDF/B-VII. This was the same library used in the reference thesis. The NJOY99 [9] data processing system was used to generate the proper cross section at work temperatures.

In order to evaluate the results, all criticality codes use the same master library (ENDF/B-VII) and energy treatment (continuous). The results present the comparison to multiplication factors obtained for all three coupled codes and the values from the references results. In addition, due to delayed neutron importance to safety in a reactor, the effective delayed neutron factor (β_{eff}) obtained is evaluated for each code.

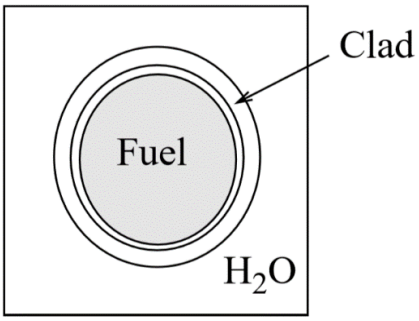

Figure 2. Thorium pin cell model extracted from benchmark

Equation 1 [10] is the relation used to obtain the effective delayed neutron fraction. For achieve these calculations two different multiplication factor were obtained. The first considering only prompt neutrons (k_p) and the second multiplication factor taking into account the prompt and the delayed neutrons (k).

$$\beta_{eff} = 1 - \frac{k_p}{k}$$

Equation 1. Effective delayed neutron fraction equation.

2.2 Burnup

The number of generations used was lowered to 315 generations and the amount neutrons per generations was set as 10000 neutrons. The complete time interval was divided into 20 steps, the first one with 5 days and the remnant as 94.5 days. The power density was specified as 38.1347 MW/THM.

Table 3 shows depletion parameters used to study the multiplication factor and isotopic composition differences along burnup. Further, it shows the number of energy groups that each criticality and depletion code use. To perform burnup calculation KENO-VI is unable to use continuous energy instead it used 238 collapsed cross sections data sets.

Table 3: Number of energy groups for each coupled code and burnup parameters.

CODES	ENERGY GROUPS	BURNUP PARAMETERS	
		Power Density (MW/THM)	38.1347
MCNP5/ORIGEN2.1	Continuous / 1	Burnup (GWd/THM)	72.2
KENO-VI/ORIGEN-S	238 / 3	Time (Days)	1895
MCNPX/CINDER90	Continuous / 63	Fuel Temperature (K)	900

Furthermore, the effects of burnup in effective delayed neutron fraction is evaluated using the same described methodology. Moreover, the results are compared to the International Atomic Energy Agency (IAEA) publication of delayed neutron data [11].

According to Equation 2 the fractional difference in isotope concentration during burnup is calculated. Therefore, this fractional difference represents the difference correlated to MIT CASMO-4 case.

$$Fractional\ Diff. = \frac{N - N_{Ref}}{N_{Ref}}$$

Equation 2. Fractional difference in isotope concentration.

All burnup cases are performed until 72.2 GWd/THM, although the referenced results are presented in a particular burnup step 60.749 GWd/THM that refers to the upper limit of discharge burnup if a 3-batch core refueling scheme is considered. Therefore, DEN results are equally presented at this burnup step.

3. Results

3.1 Criticality

Table 4 shows the multiplication factor results, their respective standard deviation and effective delayed neutron fraction for each code. The KENO-VI effective delayed neutron fraction could not be properly calculated using the owned version.

Table 4: Multiplication factor and effective delayed neutron factor for each criticality code.

Codes	Energy groups	k_{inf}	Standard deviation	Effective Delayed Neutron Fraction (β)
MCNP5	Continuous Energy	1.23537	0.00006	0.00672
KENO-VI	Continuous Energy	1.24418	0.00005	n.a.*
KENO-VI	238 collapsed energy groups	1.23601	0.00006	n.a.*
MCNPX	Continuous Energy	1.23537	0.00006	0.00667

* Value could not be properly calculated using the owned version.

So as to evaluate data above, the absolute differences between the multiplication factors for all three codes are calculated. The maximum and minimum absolute difference were 363 pcm, for KENO-VI Continuous energy and MCNPX/MCNP5 and 0 pcm, for MCNP5 and MCNPX, respectively. The results for fresh fuel effective delayed neutron fraction are justified by nuclear source fission to be primarily ^{235}U, $\beta_{235U} = 0.00665 \pm 0.00021$.

As the values from MIT and INEEL are from burnup calculations, the comparison to the fresh fuel calculations is not valid and it is not performed. Furthermore, in burnup results section the comparison along burnup is performed. The comparison is done at 60.749 GWd/THM that refers to the upper limit of discharge in a 3-batch core refueling scheme.

Figures 3 show the results for multiplication factor for the three coupled codes and reference values along burnup. All DEN performed cases are very similar at beginning, middle and end of simulation, diverging 0.6% one from another. Although MIT and INEEL have some divergent behavior in its own results (1.24%), DEN results have percentage difference of 0.3% from MIT MOCUP case at burnup end.

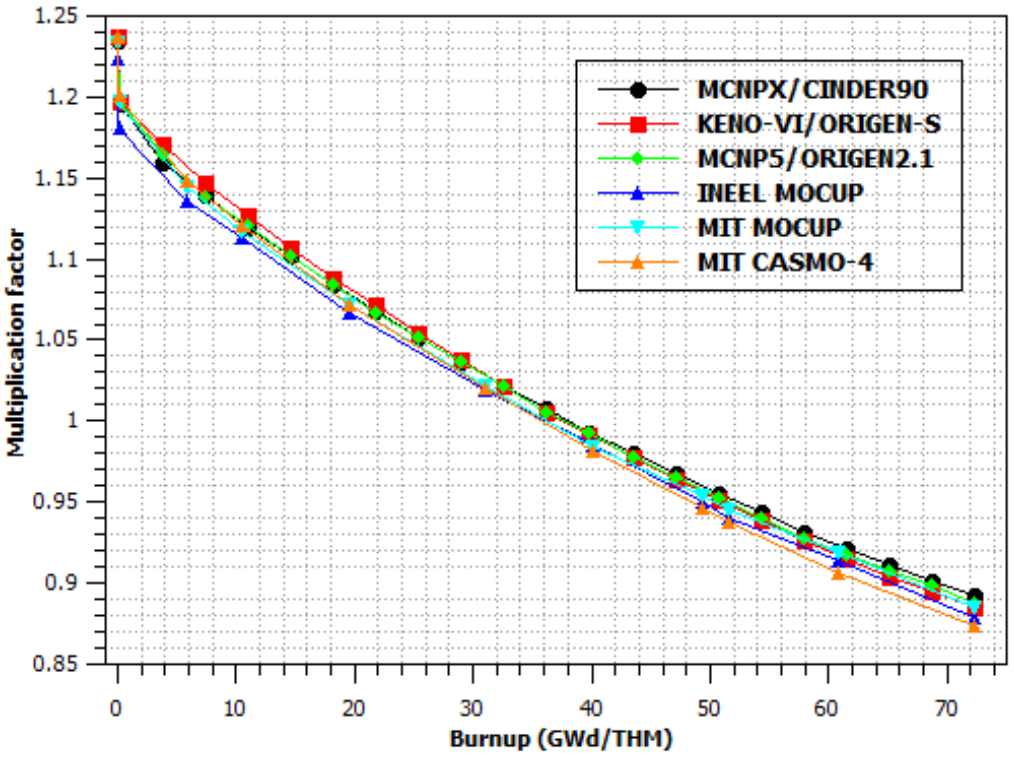

Figure 3. Multiplication factor along burnup.

Table 5 exhibits the name of institution, code used, the step 0 multiplication factor value followed by the standard deviation presented by code. The maximum percentage difference from at step 0 multiplication factor of MIT CASMO-4 case from DEN results is 0.2% while the minimum is 0.04%.

Moreover, in addition to data above, table 6 presents the absolute differences between each of DEN codes to the MIT and INEEL codes. The maximum absolute difference was 1174pcm obtained from MCNPX/CINDER90 – INEEL MOCUP and the minimum absolute difference was 74 obtained from KENO-VI/ORIGEN-S – MIT MOCUP.

Table 5: Step 0 Multiplication factors and their respectively standard deviation.

Institution	Codes	Step 0 Multiplication Factor	Standard Deviation
MIT[1]	CASMO-4	1.23782	n.a.
MIT	MOCUP	1.23354	n.a.
INEEL[2]	MOCUP	1.22347	n.a.
DEN[3]	MCNP5/ORIGEN2.1	1.23514	0.00034
DEN	KENO-VI/ORIGEN-S	1.23728	0.00033
DEN	MCNPX/CINDER90	1.23521	0.00033

Table 6: Absolute differences between step 0 multiplication factor.

Codes	Absolute Differences (pcm)
MCNP5/ORIGEN2.1 – CASMO-4	268
MCNP5/ORIGEN2.1 – MIT MOCUP	160
MCNP5/ORIGEN2.1 – INEEL MOCUP	1167
KENO-VI/ORIGEN-S – CASMO-4	54
KENO-VI/ORIGEN-S – MIT MOCUP	374
KENO-VI/ORIGEN-S – INEEL MOCUP	1381
MCNPX/CINDER90 – CASMO-4	261
MCNPX/CINDER90 – MIT MOCUP	167
MCNPX/CINDER90 – INEEL MOCUP	1174

Figure 4 show the effective delayed neutron fraction along burnup calculated to MCNP5 and MCNPX. The initial value of β starts as expected values for LWR fueled with ^{235}U. On the other hand, as fuel composition changes the β values starts decreasing as nuclides other than ^{235}U contributes to fissions inside reactor. Thorium fertile aspects contributes to ^{233}U build up inside the reactor. As a result of this, the β value decreases due to the higher contribution in effective delayed neutrons fraction for ^{233}U than to ^{235}U.

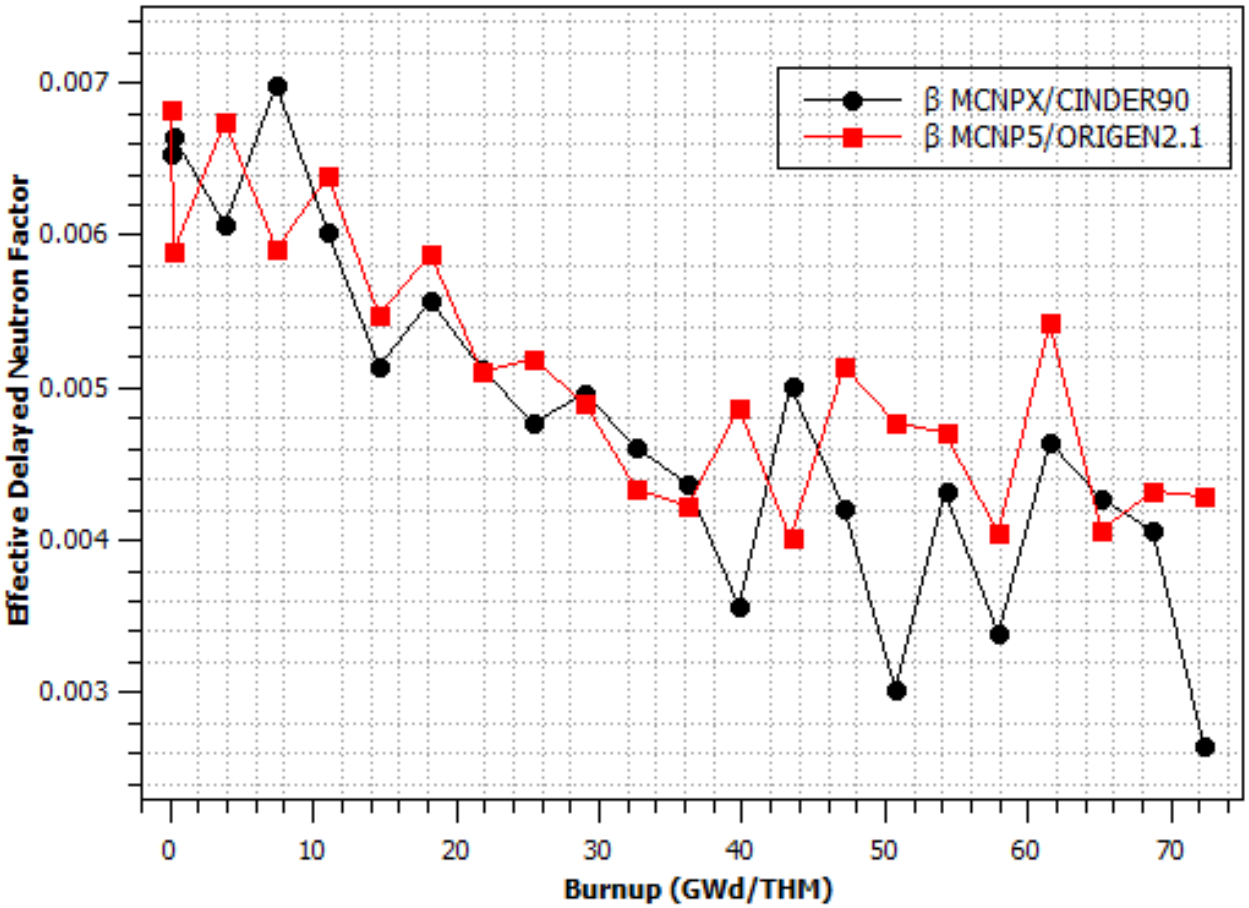

Figure 4. β_{eff} along burnup using MCNP5 and MCNPX.

Figure 5 show the ^{233}U and ^{235}U masses along burnup. The decrease of ^{235}U and the increase of ^{233}U justifies the β results. According to IAEA effective delayed neutron fraction for ^{233}U and ^{235}U are 0.00268 ± 0.00013 and 0.00665 ± 0.00021, respectively.

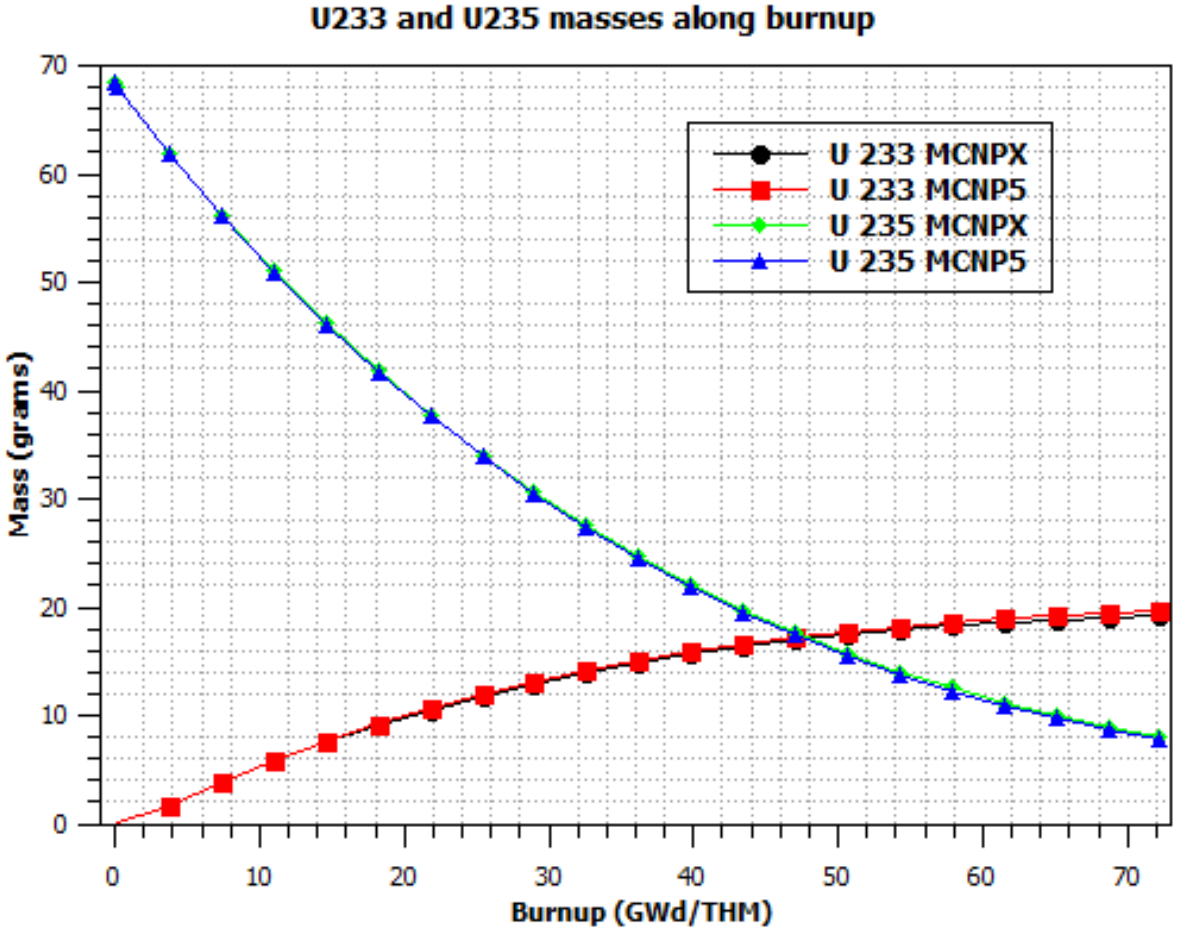

Figure 5. U233 and U235 masses along burnup for MCNP5 and MCNPX.

Table 7 presents the fractional differences between reference results and DEN results. In brief, these data indicate the difference between MIT CASMO-4 case and all other cases in the table at 60.749 GWd/THM.

Table 7 show fractional difference* between obtained results and data presented in reference results at 60.749GWd/THM.

Isotopes	MIT CASMO-4	MIT MOCUP	INEEL MOCUP	MCNP5	KENO-VI	MCNPX
Th-232	1.53769e+22	-0.003	-0.003	-0.0037	-0.0031	-0.0037
U-233	2.74202e+20	0.040	0.044	0.0552	0.05496	0.0361
U-234	5.15172e+19	0.176	0.174	0.0891	0.0744	0.0950
U-235	1.78104e+20	-0.021	-0.033	-0.0724	-0.0495	-0.0477
U-238	3.88419e+21	0.004	0.003	0.0024	0.0016	0.0031

*Fractional difference in isotope concentration $(N - N_{CASMO-4})/N_{CASMO-4}$

Figures 5A, B, C, D and E, illustrate the isotopes concentration for ^{232}Th, ^{233}U, ^{234}U, ^{235}U and ^{238}U respectively. Overall, DEN results were very similar to MIT and INEEL MOCUP results. In summary, for all codes, including MOCUP results, the differences observed have similar values from MIT CASMO-4 case. These narrow divergences observed in DEN coupled codes, supports the idea of slightly different overall average energy per fission plus capture for the different codes, presented by WEAVER, K. D., et al. In other words, each code has different nuclear chains for the same burnup.

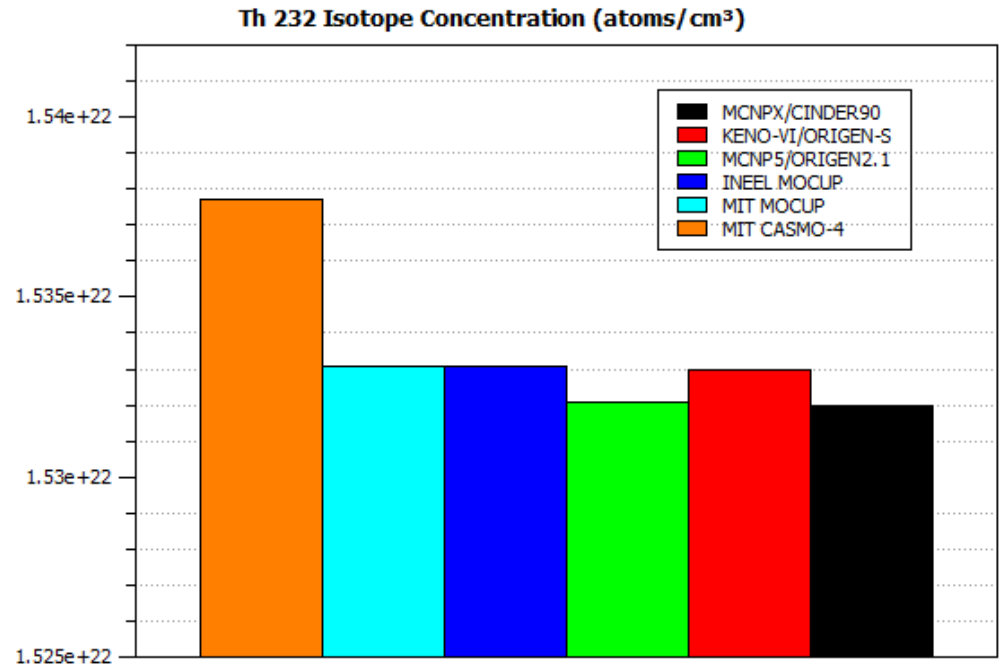
Th 232 Isotope Concentration (atoms/cm³)
1.54e+22
1.535e+22
1.53e+22
1.525e+22
MCNPX/CINDER90
KENO-VI/ORIGEN-S
MCNP5/ORIGEN2.1
INEEL MOCUP
MIT MOCUP
MIT CASMO-4

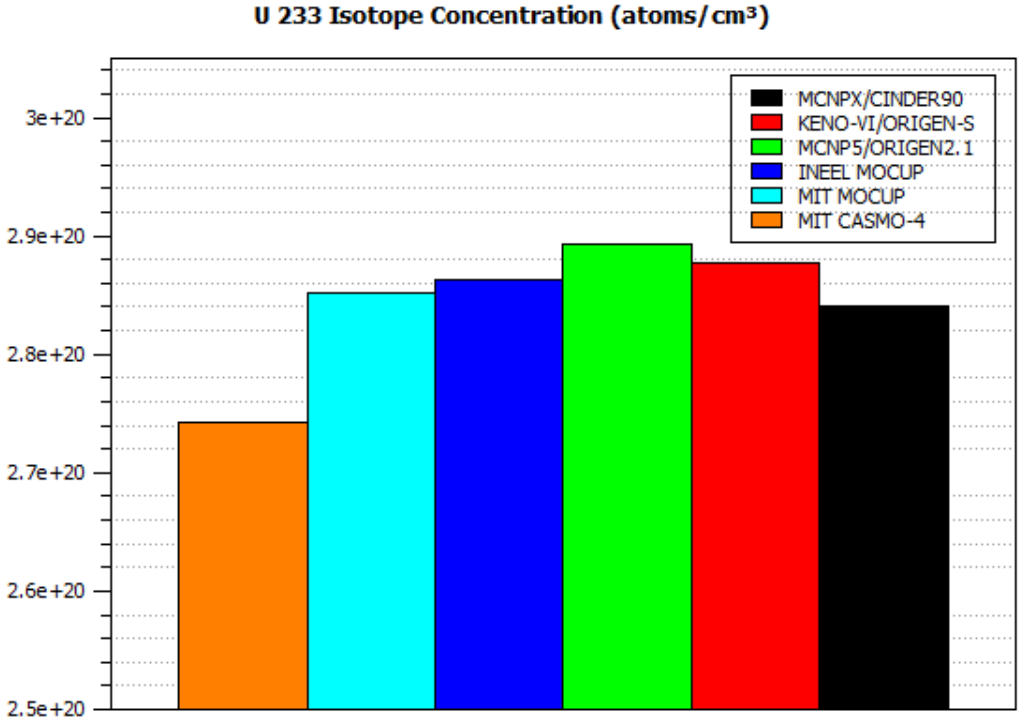
U 233 Isotope Concentration (atoms/cm³)
3e+20
2.9e+20
2.8e+20
2.7e+20
2.6e+20
2.5e+20
MCNPX/CINDER90
KENO-VI/ORIGEN-S
MCNP5/ORIGEN2.1
INEEL MOCUP
MIT MOCUP
MIT CASMO-4

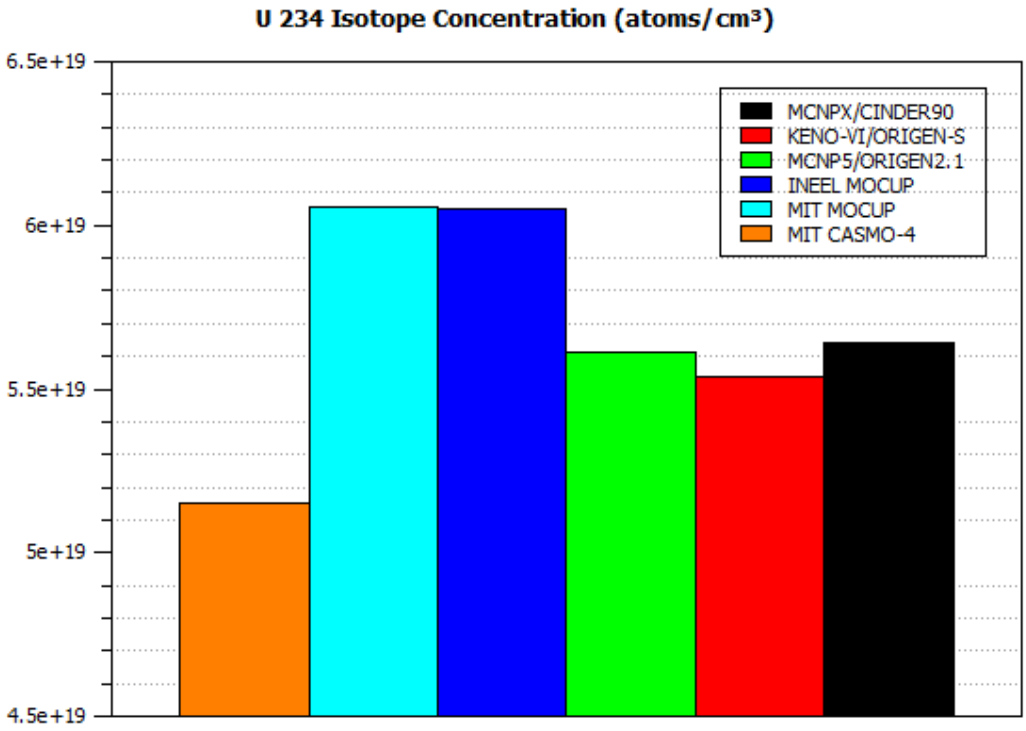
U 234 Isotope Concentration (atoms/cm³)
6.5e+19
6e+19
5.5e+19
5e+19
4.5e+19
MCNPX/CINDER90
KENO-VI/ORIGEN-S
MCNP5/ORIGEN2.1
INEEL MOCUP
MIT MOCUP
MIT CASMO-4

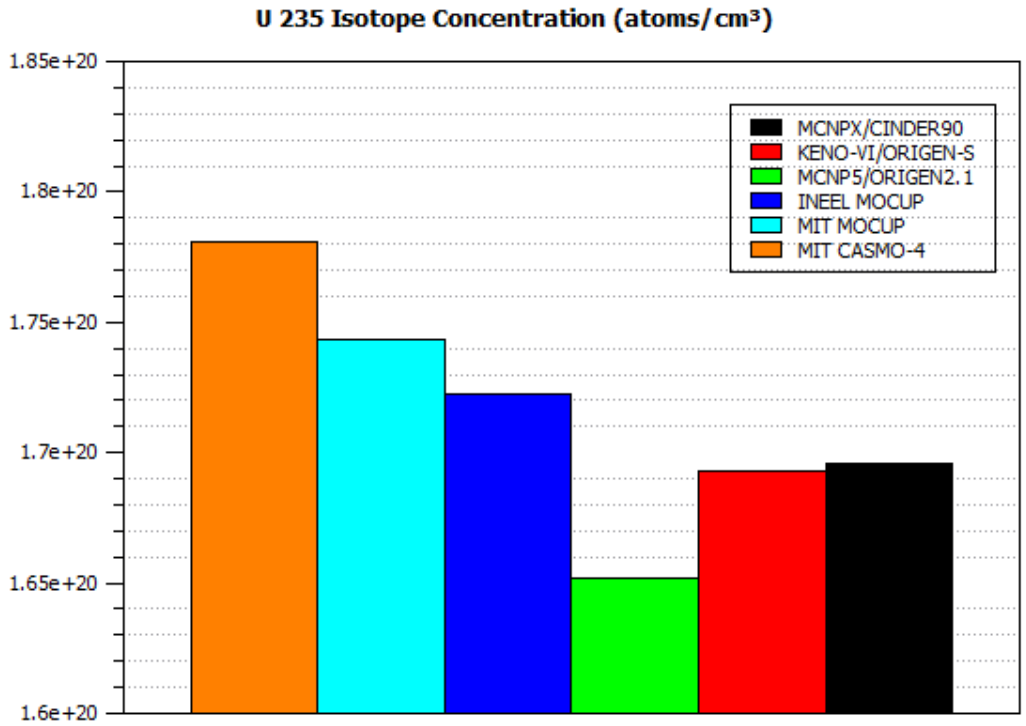
U 235 Isotope Concentration (atoms/cm³)
1.85e+20
1.8e+20
1.75e+20
1.7e+20
1.65e+20
1.6e+20
MCNPX/CINDER90
KENO-VI/ORIGEN-S
MCNP5/ORIGEN2.1
INEEL MOCUP
MIT MOCUP
MIT CASMO-4

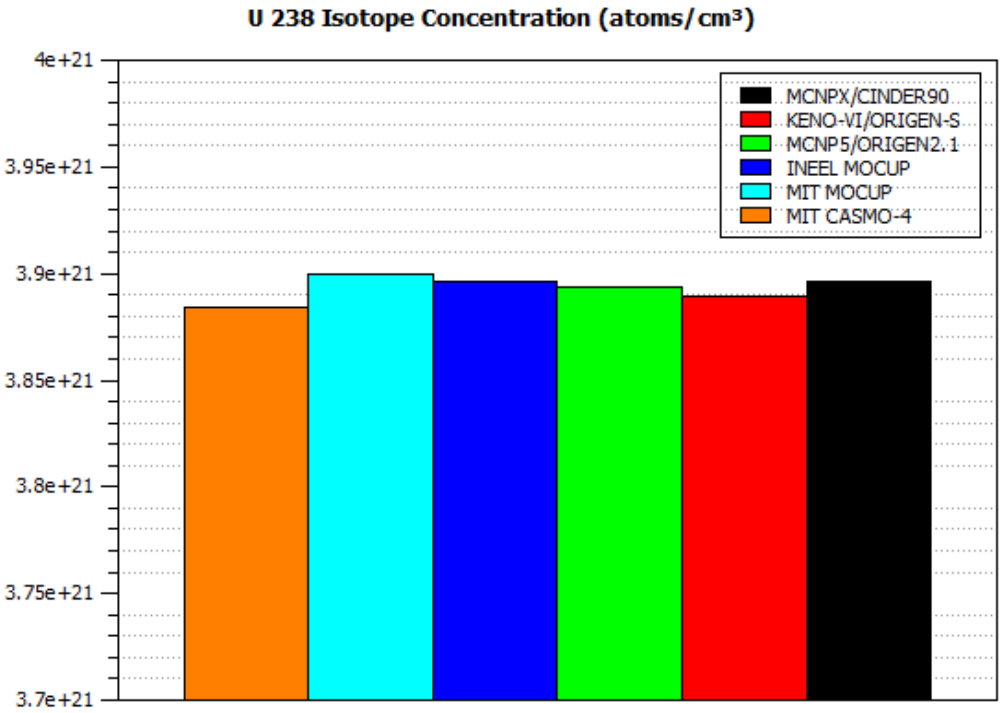

Figures 5A, B, C, D and E. Isotopes concentration (atoms/cm³) in 60.749GWd/THM.

4. Conclusion

In brief, DEN results were similar to MIT and INEEL results. All cases used the same master library ENDF/B-VII. DEN criticality results presented dependency on code energy treatment, the difference in multiplication factor for KENO-VI using continuous energy and the collapsed 238 energy groups was up to 817pcm, while for MCNP5 and MCNPX the multiplication factor was exactly the same. The effective delayed neutron fraction for the beginning of life was close to the IAEA published values for delayed neutrons.

To sum up, multiplication factor results at end of burnup diverged less than 1% from MIT and INEEL reference values, validating the further results. For all DEN codes and all observed nuclides, the fractional differences results were similar to MIT and INEEL MOCUP results. Some may argue that results might depend on depletion cross section, that slightly changes due to different number of energy groups considered in each depletion code. Although the results obtained still support the idea of the disagreement of capture contribution in depletion codes, that is, each code grind for different nuclide chains for same burnup.

Similarly to criticality situation, the effective delayed neutron fraction along burnup was very similar to delayed neutron published values by IAEA, since from beginning where fission source was mostly ^{235}U until the end where other fission sources were considered i.e. ^{233}U which the theoretical value for effective delayed neutron fraction is 0.00268 ± 0.00013.

Acknowledgments

The authors are grateful to the Brazilian research funding agencies, CNEN – Comissão Nacional de Energia Nuclear (Brazil), CNPq – Conselho Nacional de Desenvolvimento Científico e Tecnológico (Brazil), CAPES – Coordenação de Aperfeiçoamento de Pessoal de

Nível Superior (Brazil) and FAPEMIG – Fundação de Amparo à Pesquisa do Estado de Minas Gerais (MG/Brazil) for the support.

References

[1] S. M. Bowman, *KENO-VI Primer: A Primer for Criticality Calculations with SCALE/KENO-VI Using GeeWiz,*ORNL/TM-2008/069, Oak Ridge National Laboratory, Oak Ridge, Tenn., September 2008.

[2] Hermann, O.W., & Westfall, R.M. (1984). *ORIGEN-S: SCALE system module to calculate fuel depletion, actinide transmutation, fission product buildup and decay, and associated radiation source terms* (NUREG/CR--0200-Vol2). United States

[3] L.S. Waters, Ed., "MCNPX User's Manual, Version 2.3.0", LA-UR-02-2607 (2002).

[4] W. B. Wilson, S. T. Cowell, T. R. England, A. C. Hayes & P. Moller, “A Manual for CINDER'90 Version 07.4 Codes and Data,” LA-UR-07-8412 (December 2007, Version 07.4.2 updated March 2008).

[5] R. Brewer, Editor, "Criticality Calculations with MCNP5: A Primer", LA-UR-09-0380 (2009).

[6] A. G. Croff, "A User's Manual for the ORIGEN2 Computer Code," ORNL/TM-7175 (July 1980).

[7] WEAVER, K. D., et al., A PWR Thorium Pin Cell Burnup Benchmark Advances in Reactor Physics and Mathematics and Computation into the Next Millennium (PHYSOR 2000), 2000.

[8] M.B Chadwick et al., “ENDF/B-VII.0: Next generation evaluated nuclear data library for nuclear science and technology”, Nucl. Data Sheets 107(2016)2931.

[9] A.C. Kahler, *"NJOY99 Tutorial"*, presented at the ANS Annual Meeting, June 2008, LA-UR-08-2149 (2008).

[10] Robin Klein Meulekamp & Steven C. van der Marck (2006) Calculating the Effective Delayed Neutron Fraction with Monte Carlo, Nuclear Science and Engineering, 152:2, 142-148, DOI: 10.13182/NSE03-107

[11] https://www-nds.iaea.org/sgnucdat/a7.htm